ABSTRACT

Title of Dissertation: CHARACTERIZATION OF HEME ACQUISITION IN *LEISHMANIA*

Rebecca Lynn Renberg, Doctor of Philosophy, 2014

Directed By: Dr. Norma W. Andrews,
Department of Cell Biology and Molecular Genetics

Heme is an essential co-factor for many critical cellular processes. The protozoan parasite *Leishmania amazonensis* is a heme auxotroph and must acquire heme from the environment. One pathway of heme acquisition is through *Leishmania* Heme Response 1 (LHR1), a heme transporter localized to the plasma membrane and acidic intracellular compartments. In this work we further characterize LHR1 and the mechanism by which it promotes heme uptake. We show that overexpression of LHR1 in *L. amazonensis* increases the total parasite intracellular heme pool, and that expression in *S. cerevisiae* promotes uptake of the heme analog Zinc Mesoporphyrin IX (ZnMP). Our results indicate that heme binding to LHR1 is pH independent, whereas heme transport by the parasites is more efficient under acidic conditions. To examine the molecular mechanisms responsible for LHR1 heme transport, we performed a mutagenesis analysis of LHR1. We show that three key tyrosines residues, Tyr-18, Tyr-80, and Tyr-129, located in predicted transmembrane domains near the cytoplasmic leaflet of the plasma membrane, are important for heme transport. Although the mutant proteins appear to not affect promastigote growth,

they have a profound inhibitory effect on intracellular amastigote replication in macrophages, and are necessary for virulence *in vivo*. Finally, we also examine the differential regulation of LHR1 expression in a visceralizing species, *L. chagasi*, compared to *L. amazonensis*, a species that causes cutaneous lesions. *L. chagasi* has higher amounts of LHR1 transcripts than *L. amazonensis* under heme-depleted conditions, and uptakes ZnMP faster and to a greater extent than *L. amazonensis*. This differential regulation of LHR1 may be due to differences in the gene 3′ Untranslated Regions (UTRs) between the two species. This works adds to our understanding of the critical process of heme transport and its role in *Leishmania* virulence.

CHARACTERIZATION OF HEME ACQUISITION IN *LEISHMANIA*

By

Rebecca Lynn Renberg

Dissertation submitted to the Faculty of the Graduate School of the
University of Maryland, College Park, in partial fulfillment
of the requirements for the degree of
Doctor of Philosophy
2014

Advisory Committee:
Professor Norma Andrews, Chair
Professor Najib El-Sayed
Professor Iqbal Hamza
Professor Stephen Wolniak
Professor Louisa Wu

Dedication

I would like to dedicate this work to my family, Chris, Owen and Rhys, and my parents, Dickie and Denise White, for their unfailing support and many sacrifices on my behalf.

I would also like to dedicate this work to my high school science teacher Mr. Jeff Miller who initially helped me develop a scientific curiosity for things microscopic and the many professors that encouraged me to pursue research: Dr. Kim L. O'Neill, Dr. Byron K. Murray, and Dr. F. Brent Johnson.

Acknowledgements

I would like to acknowledge present and past members of the Andrews Lab.

I would like to thank Dr. Chau Huynh and Dr. Andrew R. Flannery for their guidance, direction, advice, and mentoring.

I would like to thank Dr. Tamika K Samuel, Dr. Xiaojing Yuan, and Dr. Iqbal Hamza for their advice and extensive assistance in experimental design and performance.

I also acknowledge and thank all the members of my dissertation committee Dr. Najib El-Sayed, Dr. Iqbal Hamza, Dr. Louisa Wu and Dr. Stephen Wolniak, and also Dr. Dr. Wenxia Song for their time, insights, and encouragement.

Finally, I would also like to sincerely thank my mentor, Dr. Norma Andrews, for support, guidance, understanding, and advice.

Table of Contents

List of Abbreviations

LHR1 – *Leishmania* Heme Response 1

ZnMP – Zinc Mesoporphyrin IX

UTR – Untranslated Region

PV – Parasitophorous Vacuole

Fe - Iron

NRAMP1 – Natural resistance-associated macrophage protein 1

Slc11a1 – Solute Carrier 11a1

HRG1 – Heme Response Gene1 (SLC48A1) - human

HO-1 – Heme Oxygenase

LFR1 – *Leishmania* Ferric Reductase 1

LIT1 – *Leishmania* Iron Transporter 1

ROS – Reactive Oxygen Species

ABC- ATP-binding cassette

LABCG5 – *Leishmania* ATP-Binding Cassette G5

ATP – adenosine triphosphate

HCP1/Slc46A1/PCFT – Heme Carrier Protein 1/Solute Carrier 46A1/Proton Coupled Folate Transporter

CeHRG-1 – *C. elegans* Heme Response Gene 1

CeHRG-4 – *C. elegans* Heme Response Gene 4

FLVCR2 – Feline Leukemia Virus Subgroup C Receptor 2

FLVCR1a – Feline Leukemia Virus Subgroup C Receptor 1a

FLVCR1b – Feline Leukemia Virus Subgroup C Receptor 1b

ABCG2/BCRP – ATP-Binding Cassette G2/Breast Cancer Resistance Protein

ABCB6 – ATP-Binding Cassette B6

MgPP - Magnesium Protoporphyrin IX

SKO – *L. amazonensis* Δ*lhr1/LHR1*

HYG - *hygromycin B phosphotransferase*

NEO - *neomycin phosphotransferase*

SL – Splice Leader

RT-qPCR – Reverse Transcription Quantitative Polymerase Chair Reaction

PGM – Promastigote Growth Media

ALAS – δ-aminolevulinic acid synthase

ALA - δ-aminolevulinic acid

V-ATPase - vacuolar H^+-ATPase proton pump

List of Figures

Chapter 1: An Introduction to *Leishmania*, Leishmaniasis, Heme, Iron, and Heme Transporters

The goal of this dissertation is to characterize the protozoan heme transporter, *Leishmania* Heme Response 1 (LHR1), and examine the potential role of differential heme acquisition and LHR1 regulation in two species of *Leishmania*. In this chapter the necessary background information will be given. First, an overview of the protozoan parasite *Leishmania* and the disease it causes, leishmaniasis, will be given. Then the role of iron and heme in the parasite biology and leishmaniasis will be outlined, followed by a brief overview of the known heme transporters. Finally, the current understanding of heme transport in *Leishmania* will be discussed.

Leishmania

Leishmania parasites were first described in the late 1800s in skin lesions, called Delhi Sores, by Peter F. Borovsky, David Cunningham, and James Homer Wright (3-5). A few years later in the early 1900s, William Leishman and Charles Donovan independently described *Leishmania* parasites in the spleens of patients with kala azar (6-8). *Leishmania spp*. are protozoan parasites that belong to the Trypanosomatidae family that have a bimodal life cycle alternating between a sand fly vector and a vertebrate host. When a sand fly ingests a blood meal containing amastigote forms of *Leishmania*, the parasites transform into extracellular procyclic promastigotes and replicate within the digestive tract of the sand fly. After a few days, the procyclic promastigotes differentiate into infective metacyclic promastigotes and migrate to the proboscis of the sand fly. When the sand fly takes another blood meal the metacyclic promastigotes are inoculated

into the skin of another vertebrate host. The metacyclic promastigotes are phagocytosed by macrophages, where they transform into the intracellular amastigotes and replicate inside a parasitophorous vacuole (PV) that shares many properties of phagolysosomes (9). The cycle is completed when another sand fly takes a blood meal from an infected host that contains amastigote forms (Figure 1).

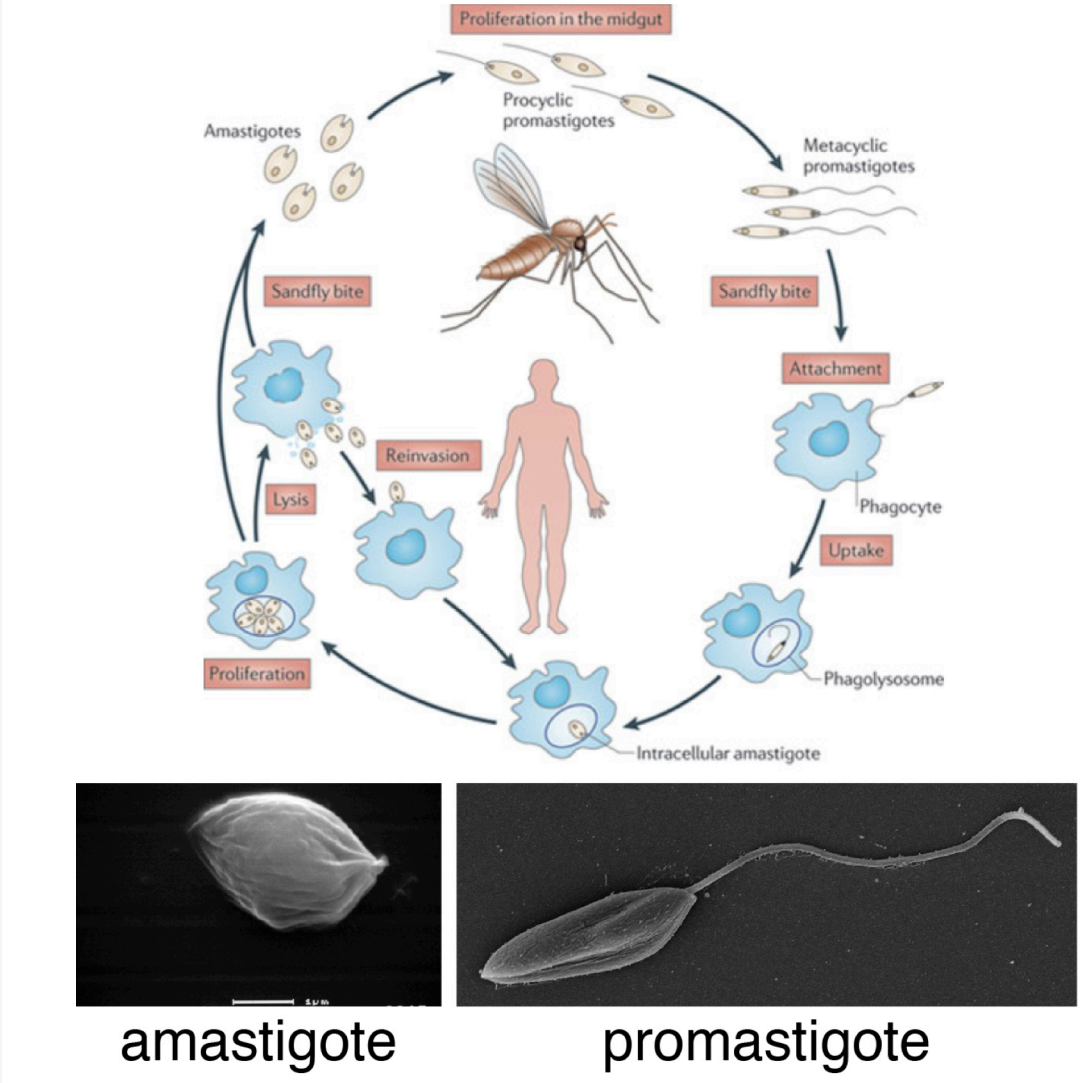

Figure 1 – Life Cycle of *Leishmania*. Illustration depicting the different life cycle stages of *L. amazonensis* from Kaye & Scott 2011 (1). Below the life cycle are scanning electron micrographs of an amastigote and a promastigote form. Images courtesy of A. Flannery, B. Mittra and the Laboratory for Biological Ultrastructure at UMD College Park; scale bar = 1 μM.

Leishmaniasis

Leishmania spp. cause a spectrum of human disease called leishmaniasis. The clinical manifestations of leishmaniasis vary, and depending upon the infecting species and the host, range from self-healing cutaneous lesions to severely disfiguring mucocutaneous disease, or serious visceralizing disease that can be fatal if not treated. There are more than twenty known species of *Leishmania* that can cause disease in vertebrate animals, with approximately a dozen species known to infect humans. The World Health Organization estimates that leishmaniasis is the ninth largest disease burden attributed to an individual infectious disease and the second largest human parasitic infection after malaria (10). Approximately 310 million people living in countries where 90% of reported leishmaniasis cases occur are at risk for infection, and there are approximately 1.3 million new cases occurring annually with more than 20,000 deaths (11). *Leishmania* transmission is currently endemic in more than eighty tropical and subtropical countries. In 2012, India, Brazil, South Sudan, Sudan, and Ethiopia reported the greatest number of visceral leishmaniasis cases, and Afghanistan, Syria, Brazil, and Iran reported the greatest number of cutaneous leishmaniasis cases (12) (Figure 2). Current treatments are expensive and quite toxic, and drug resistance has arisen in highly endemic areas (13-15). Consequently there is a great need for development of new drugs that are more affordable and less toxic.

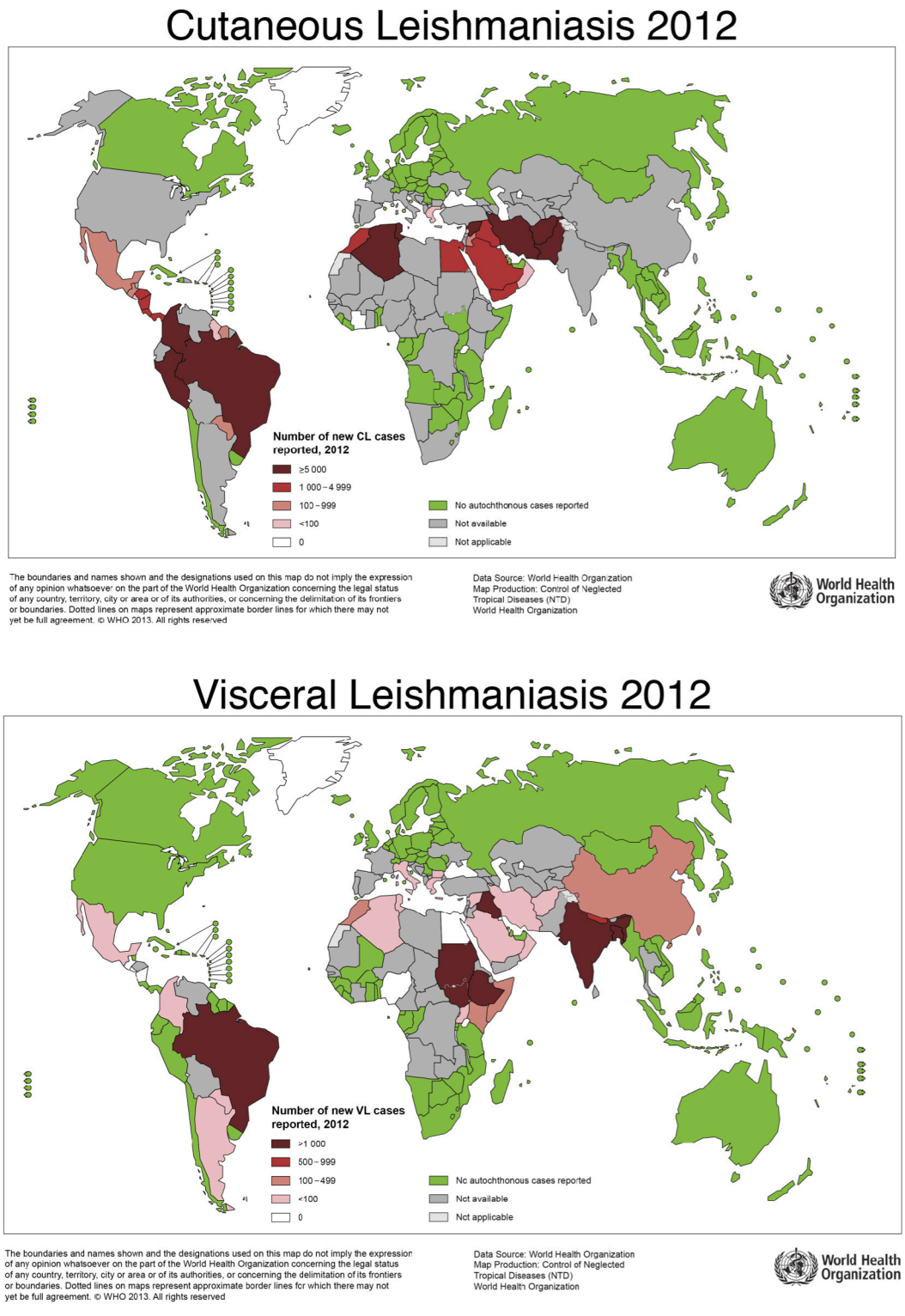

Figure 2 – Global Distribution of Leishmaniasis 2012. The World Health Organization (WHO) tracks reported cases of cutaneous and visceral leishmaniasis. Images adapted from WHO website (http://www.who.int/neglected_diseases/ ntddata/leishmaniasis/leishmaniasis.html).

Iron and Heme at the Host-Parasite Interface

In leishmaniasis the availability of nutrients for parasite growth is known to have a drastic effect on disease outcome (16). Two of those key nutrients are iron (Fe) and heme. Iron is an essential element for many biological processes because its oxidation-reduction (redox) potential can facilitate multiple types of electron transfer reactions. In biological systems iron normally exists in either of two oxidation states, Fe^{2+} or Fe^{3+}. This inherent characteristic of iron to undergo redox reactions also makes it toxic because it can serve as a catalyst in generating reactive oxygen species via the Fenton reaction (17). During an infection, both the host and the parasite require iron to perform normal biological functions, but in addition, the host must limit a pathogen's access to iron in order to prevent pathogen replication (18). This battle for iron within the host is illustrated well by the divalent cation transporter Natural Resistance-Associated Macrophage Protein 1 (NRAMP1), also called Solute Carrier (Slc11a1), which is specifically expressed in professional phagocytes such as macrophages. NRAMP1 removes iron and other divalent cations from late endocytic compartments, consequently depriving intracellular pathogens like *Leishmania* of these important factors. NRAMP1 was identified as a host susceptibility gene for *Leishmania* infection; thus providing the first evidence that *Leishmania* is acutely dependent on the availability of iron for intracellular growth and replication (19,20). NRAMP1 normally resides in the late endosome/lysosome of resting macrophages and is recruited to mature phagosomes (21). *Leishmania* is an intracellular parasite of macrophages, and its mechanisms to gain access to iron have been shown to influence the host cell's ability to regulate iron pools by stimulating iron uptake and inhibiting iron export (22,23).

Heme also plays a central role in iron availability at the host-parasite interface via recycling of iron during erythrophagocytosis. Erythrophagocytosis occurs in reticuloendothelial macrophages located mainly in the spleen and to a lesser extent in the liver and bone marrow (24). In humans, approximately 5 million red blood cells are recycled each second via erythrophagocytosis, which provides twenty-fold more iron than absorption from the diet (25-27). Senescent red blood cells are phagocytosed by macrophages and degraded in phagolysosomes releasing heme. Heme is then translocated to the cytosol via Heme Response Gene 1 (HRG1) (25) where it is degraded via heme oxygenase (HO-1) to release iron from the porphyrin ring. Iron is then available to be stored in ferritin in the cytosol of the macrophage or it can be transported out of the cell via ferroportin (Figure 3). At a critical junction in this iron and heme recycling pathway sits *Leishmania,* which replicates inside PVs, phagosomal-like compartments that are found in macrophages. *L. amazonensis* has been shown to posses a ferric iron reductase (LFR1) and a ferrous iron transporter (LIT1) that work in concert to allow the parasite to reduce extracellular ferric iron (Fe^{3+}) to ferrous iron (Fe^{2+}) and then transport that ferrous iron across the plasma membrane (28-31) (Figure 3). In addition to the ability to acquire iron directly from the environment, *Leishmania* can also acquire iron from heme, via LHR1, and other heme sources such as hemoglobin (32-35).

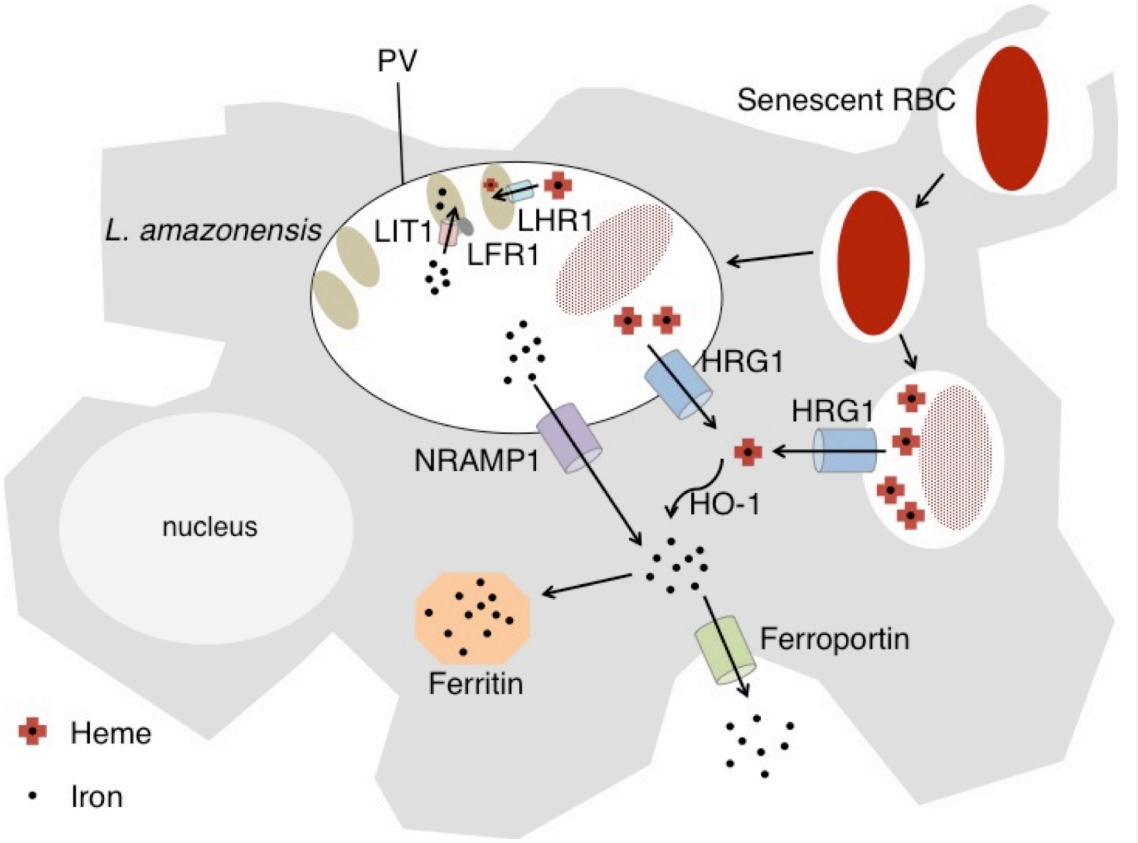

Figure 3 – Macrophages Recycle Iron via Erythrophagocytosis. Hemoglobin is degraded in the phagolysosome releasing heme, which is translocated into the cytosol by HRG1 where it can be broken down by HO-1. This iron can be exported by ferroportin or stored in ferritin. Within the PV, *L. amazonensis* utilizes LFR1 and LIT1 to acquire iron and LHR1 to obtain heme.

Heme

Heme is an iron-containing porphyrin that acts as an important prosthetic group for many enzymes involved in a variety of cellular functions (Figure 4) (36). The heme biosynthesis pathway in eukaryotes consists of eight enzymes located in the cytoplasm and in the mitochondria and has been well characterized (37). However, not all eukaryotes have the ability to synthesize heme, generally because they are lacking one or more of the enzymes in the biosynthetic pathway. Heme is a large amphipathic

porphyrin that is toxic in its free form because of its ability to intercalate into lipid membranes and catalyze the formation of reactive oxygen species (ROS) causing oxidative stress that can damage proteins, lipid membranes, and nucleic acids (38,39). Consequently, in biological systems, heme is usually maintained in a protein-bound form to protect the cell from its toxic effects (40). In order to supply heme to the compartments where it is needed as a cofactor in hemoproteins and maintain iron homeostasis, cells use heme importers and exporters to facilitate movement of heme within the cell.

Leishmania are heme auxotrophs that lack the first five enzymes in the heme biosynthetic pathway but possess the final three, which have been annotated in the genome and shown to be enzymatically active (32,41-52). *L. amazonensis* has been shown to bind heme specifically (53), and *L. donovani* was shown to have a transporter, *Leishmania* ATP-Binding Cassette G5 (LABCG5), proposed to be involved in salvage of heme after breakdown of hemoglobin. LABCG5 was proposed to function in a mechanistically different manner, when compared to direct heme uptake (54). Heme plays an essential role in the replication and survival of *Leishmania,* and a better understanding of how these species acquire, traffic, and store heme is needed.

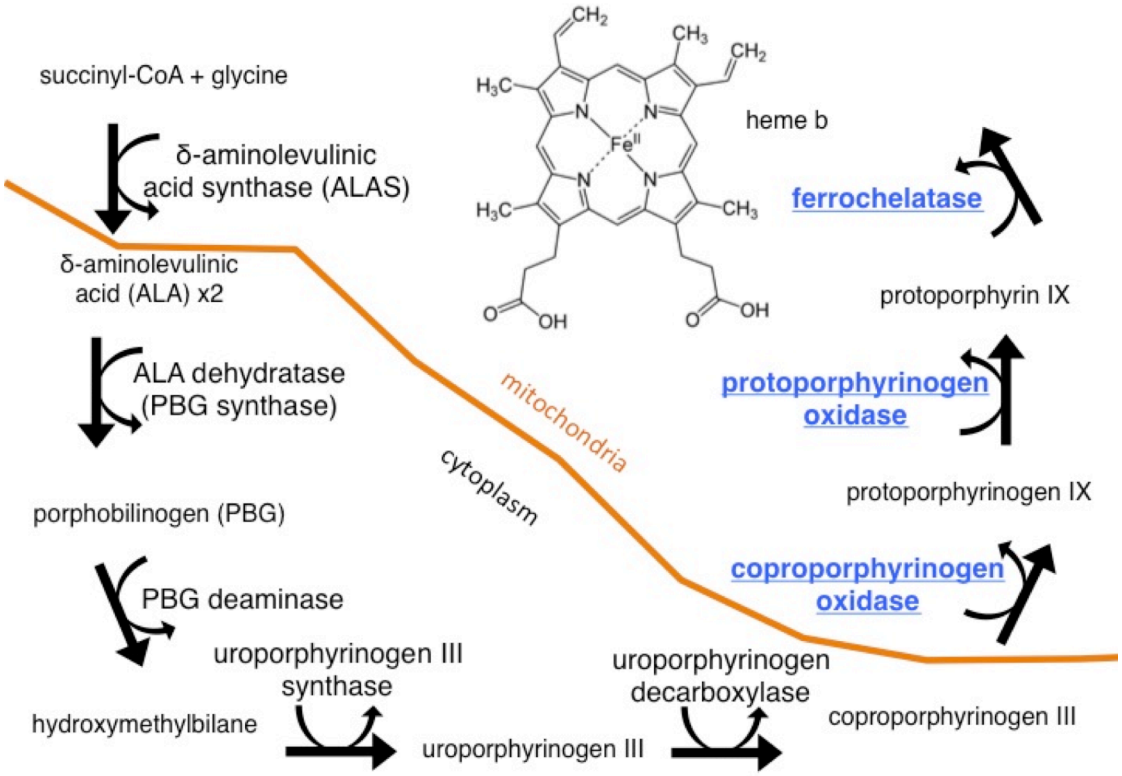

Figure 4 – Heme Biosynthesis Pathway. *Leishmania* only possesses the last three enzymes of the heme biosynthesis pathway (noted in blue).

Heme Transporters

The existence of human heme transporters was first observed in intestinal and hepatocyte cells lines (55), but only a few proteins have been fully characterized as dedicated heme transporters (38,39,56). Two classes of heme transporters, heme importers and heme exporters, are described below using the heme tranport proteins that have been characterized.

Heme Importers

Heme Carrier Protein 1 (HCP1) (also known as Solute Carrier Family 46A1 (*SLC46A1*) / Proton Coupled Folate Transporter (PCFT)), which is located on the plasma

membrane in mammalian cells, was initially thought to import heme (57). However, HCP1 was later shown to be primarily a folate transporter with lower affinity for heme (58-60). The best characterized heme importers, Heme-Responsive Gene 1 (CeHRG-1) and Heme-Responsive Gene 4 (CeHRG-4) were discovered using a genetic screen in the heme auxotrophic organism *C. elegans* (61). CeHRG-1 localizes to endosomes and lysosomes, binds heme better at low pH values, and utilizes a histidine in the predicted transmembrane domain 2 as well as the C-terminal FARKY motif (a potential heme interacting cluster of basic and aromatic amino acids) to transport heme. CeHRG-4 localizes to the plasma membrane, binds heme over a broad pH range, and utilizes a histidine in extracellular loop 2 as well as the FARKY motif to transport heme (61,62). Of all the heme responsive genes identified in the *C. elegans* genetic screen, only CeHRG-1 has a human homologue, hHRG-1 (also known as Solute Carrier Protein 48A1 (*SLC48A1*), which has been shown to localize to the plasma membrane and endosomal membranes, transports heme from the endosome into the cytoplasm, and is involved in heme salvage during erythrophagocytosis (25,61-65). Feline Leukemia Virus Subgroup C Receptor 2 (FLVCR2) is a heme importer located on the plasma membrane in mammalian cells that is associated with a vascular disease of the brain, Fowler Syndrome. However, there is mixed evidence about the ability of this protein to import heme (38,62,66-68)

Heme Exporters

Feline Leukemia Virus Subgroup C Receptor 1a (FLVCR1a) is a heme exporter located at the plasma membrane in mammalian cells that is required for erythroid maturation, depends upon extracellular hemopexin for efficient export, and is linked to

posterior column ataxia and retinitis pigmentosa syndrome and Blackfan anemia (38,67,69,70). Feline Leukemia Virus Subgroup C Receptor 1b (FLVCR1b), another isoform of FLVCR1a, is a mitochondrial heme exporter that is involved in erythroid differentiation (71). The ATP-binding cassette G2/breast cancer resistance protein (ABCG2/BCRP) is a heme exporter located on the plasma membrane that is involved in hypoxic cell survival (72) and transfers heme to albumin via an extracellular loop (73), and may be involved in porphyrin homeostasis. ATP-Binding cassette B6 (ABCB6) may play a role in heme transport, but there is mixed evidence as to its physiological role (74-81).

Leishmania Heme Transporters

This characterization of heme transporters in animals has facilitated the identification of heme transporters in *Leishmania* (31,82,83). The first heme transporter characterized was LABCG5 in *L. donovani*. LABCG5 is a putative heme importer located in the flagellar pocket and on internal vesicles of the parasites proposed to mediate intracellular trafficking of heme to the mitochondria after breakdown of hemoglobin (54). The second heme transporter characterized was LHR1 in *L. amazonensis*. LHR1 localizes to the plasma membrane and acidic intracellular compartments, functions in the direct transport of heme from the environment into the cytoplasm (35), and was shown to be essential for virulence during macrophage and mouse infections (84).

Heme Transport in *Leishmania*

A few studies have been performed involving heme and *Leishmania* that provided guidance for our examinations of heme acquisition in *L. amazonensis*. Galbraith *et al*. showed that heme binds specifically to the surface of *L. amazonensis* promastigotes with a K_d of ~ 0.03 nM^{-1} (53), and Carvalho *et al*. showed that *L. infantum* amastigotes have a ligand for heme on their surface with a K_d of ~ 0.044 nM^{-1} (34). Campos-Salinas *et al*. used a fluorescent heme analog, Magnesium Protoporphyrin IX (MgPP) in *L. donovani* to show, for the first time, that heme and hemoglobin uptake follow different pathways with different kinetics, and that direct heme uptake is temperature dependent (54). In order to verify that *L. amazonensis* behaves in a manner similar to what had been described in other species, we collaborated with Dr. Tamika Samuel and Dr. Iqbal Hamza at the University of Maryland to demonstrate kinetic [^{55}Fe]-heme uptake in *L. amazonensis* promastigotes over 120 minutes. We were able to confirm previous observations that were made using other *Leishmania* species and heme analogs. *L. amazonensis* takes up [^{55}Fe]-heme with a kinetic curve that is indicative of a transporter at the plasma membrane (Figure 5).

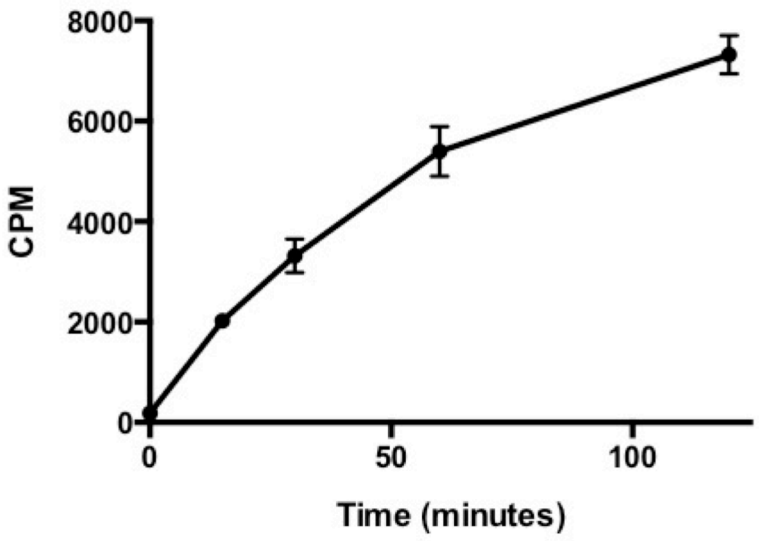

Figure 5 - [^{55}Fe]-heme Uptake in *L. amazonensis*. Mid-log promastigotes were grown in heme-depleted conditions O/N before uptake assay was performed. CPM from 0° C for parallel time points was subtracted from the CPM obtained at 26° C incubation. Assays were performed in triplicate and data is representative of two independent experiments. Data represents the mean +/- SD of triplicates. (T. Samuel, unpublished data).

Chapter 2: *Leishmania* Heme Response 1 (LHR1) is a Heme Transporter

Partially adapted from Huynh et al. PLoS Pathog 2012 (35)

Introduction

Leishmania are known to be heme auxotrophs (32,41,46) and consequently completely dependent upon heme acquisition from the environment. Because of this unique dependence on exogenous heme, *Leishmania* have multiple pathways of heme acquisition. It has been proposed that *Leishmania* can acquire heme via hemoglobin receptor-mediated endocytosis followed by heme salvage (54,85-89) and via direct transmembrane transport (34,35,53,54). Direct transmembrane transport of heme has also been observed in *Trypanosoma cruzi*, another member of the Trypanosomatidae family (90,91). LHR1 is a heme transporter that is involved in direct transmembrane heme transport that was discovered and characterized by the Andrews laboratory. During the course of characterizing LHR1 we were able to show that LHR1 is a small 20 kDa protein, with four predicted transmembrane domains, that localizes to acidic intracellular compartments and the plasma membrane of promastigotes and amastigote stages of the parasite. Importantly, LHR1 transcript levels increase when the parasites are grown under heme depleted conditions, a property that is expected of heme transporters. LHR1 is involved in the control of intracellular heme pools, can rescue the growth of a yeast strain defective in heme biosynthesis, and can directly transport radioactive heme when expressed in a yeast system (35).

Results

LHR1 Increases Total Intracellular Heme Concentrations

In order to verify that LHR1 was contributing to the total intracellular heme pools, two different tagged versions of LHR1 were created and episomally expressed in *L. amazonensis*. The expression of either GFP-LHR1 or LHR1-3xFLAG increased the overall intracellular heme content (Figure 6). The modulation of total intracellular heme pools upon over expression of the tagged constructs was moderate, but because of the inherent toxicity of heme, it is conceivable that intracellular concentrations would be tightly controlled to avoid large changes in intracellular heme concentrations.

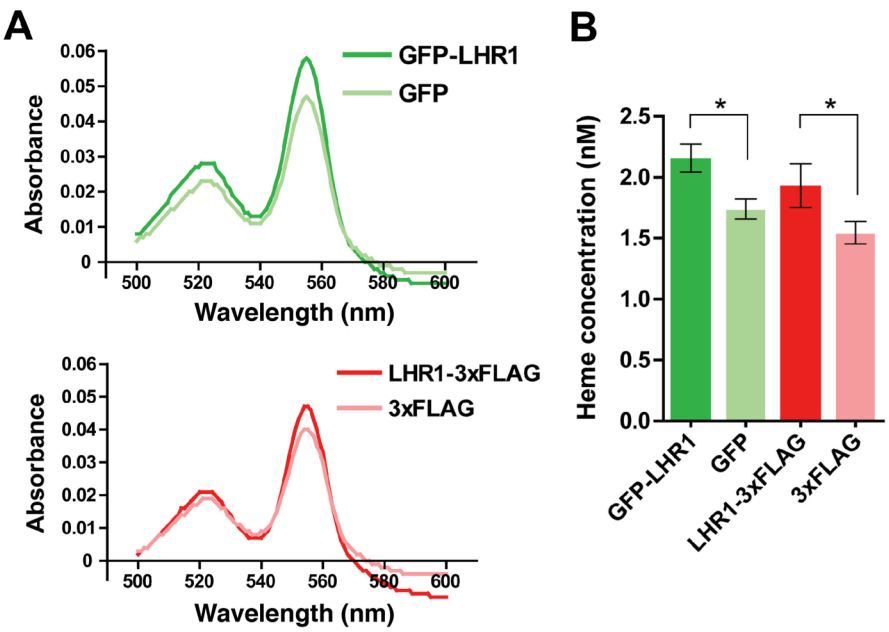

Figure 6 – Overexpression of GFP-LHR1 and LHR1-3xFLAG Increases the Intracellular Heme Content in *L. amazonensis*. Promastigotes overexpressing two different tagged version of LHR1 both showed an increase in intracellular heme content. **A)** Representative absorption spectra of hemochrome content of *L. amazonensis* promastigote lysates ($4x10^9$ parasites) transfected with vectors only (GFP and 3xFLAG) or LHR1 (GFP-LHR1 and LHR1-3xFLAG) grown in regular growth media. **B)** Calculated heme concentrations from (A) based on heme millimolar extinction coefficient of 20.7. Data represented is the mean ± standard error of three independent experiments. * p = 0.020 (GFP-LHR1 vs. GFP) and p = 0.031 (LHR1-3xFLAG vs. 3xFLAG) (two-tailed Student's *t*-test).

Zinc Mesoporphyrin (ZnMP) Uptake Assays in the Yeast *Saccharomyces cerevisiae*

To characterize LHR1 as a heme transporter, we sought a kinetic assay that would reflect direct uptake of heme or a heme analog. In order to do this, we took advantage of the *S. cerevisiae* yeast strain Δ*hem1* (6D) (62,92,93) because it utilizes exogenous heme poorly and is deficient in the biosynthetic pathway of heme. Δ*hem1* (6D) cells expressing LHR1 were incubated with the fluorescent heme analog ZnMP at 30°C over 90 minutes. There was clear uptake of ZnMP in cells expressing LHR1 when compared

to cells with empty vector, and this uptake could be significantly reduced when incubated with 10-fold excess hemin indicating hemin can compete with ZnMP for uptake via LHR1 (Figure 7).

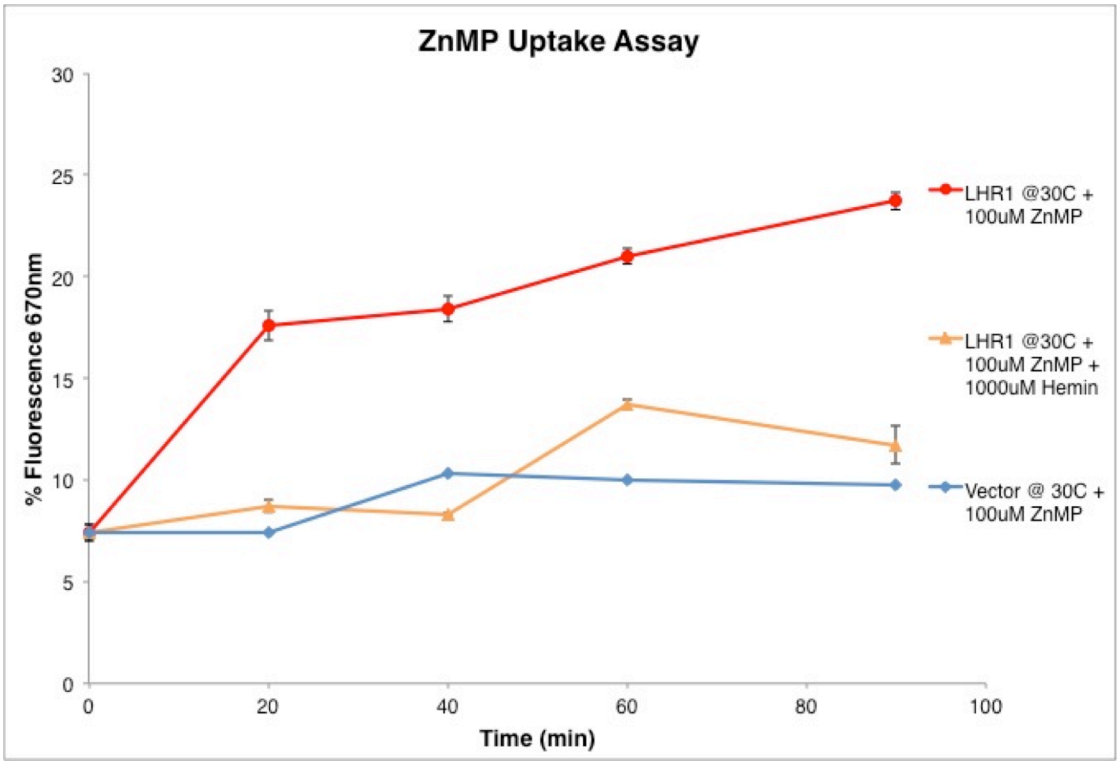

Figure 7 – LHR1 Promotes ZnMP Uptake in Yeast Δ*hem1* (6D). Yeast transformed with LHR1-HA or empty vector were incubated with 100 µM ZnMP or 100 µM ZnMP + 1000 µM hemin at 30°C for varying lengths of time. Fluorescence was measured using FACS. Error bars are the standard deviation of technical replicates and graph is representative of two biological replicates.

Efforts to Generate *L. amazonensis* Δ*lhr1*/Δ*lhr1*

We were able to generate a heterozygous knockout of *LHR1* in *L. amazonensis* (Δ*lhr1/LHR1*; referred to as SKO) via homologous recombination using a *hygromycin B phosphotransferase* (*HYG*) replacement construct where the *HYG* gene was flanked on

the 3′ end with 1000-bp region upstream of *LHR1* and on the 5′ end with a 2,500-bp region downstream of *LHR1* (Figure 8) (35). After extensive attempts to

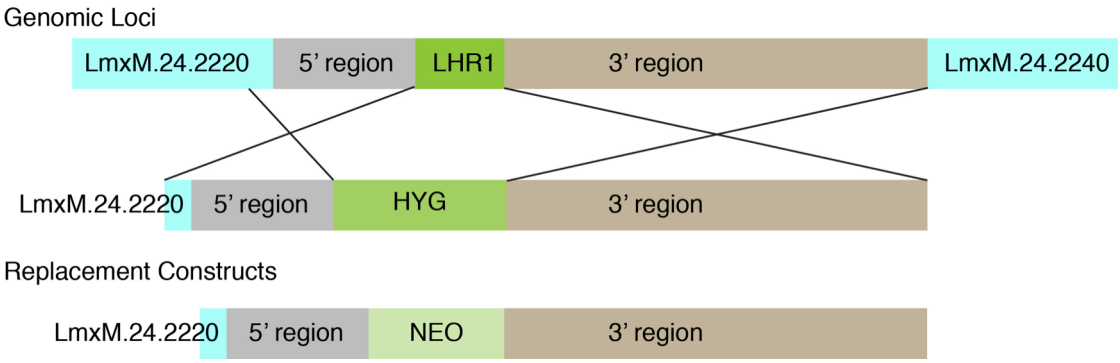

Figure 8 – Illustration of Gene Replacement Constructs to Generate *L. amazonensis* Δ*lhr1*/Δ*lhr1*. Constructs generated to replace *LHR1* via homologous recombination with the *HYG* and *NEO* resistance genes.

generate a homozygous knockout of *LHR1* using the *neomycin phosphotransferase* (*NEO*) gene deletion construct described in Figure 8, we were unable to recover viable parasites. Ultimately we attempted to replace the second endogenous copy of *LHR1* by first episomally expressing *LHR1-3xFLAG* in the SKO and then using the *NEO* gene replacement construct to replace the final copy. Triple drug resistant parasites were recovered (hygromycin = first copy of *LHR1*; nourseothricin = episomal *LHR1-3xFLAG*; neomycin = second copy of *LHR1*) and genomic DNA was isolated and tested using a PCR assay to verify if the neomycin resistance gene had in fact replaced the second endogenous copy of *LHR1*. The primers used for the PCR were designed specifically to detect 1) the *HYG* gene (Hyg) in the *LHR1* genomic locus, 2) the episomally expressing *LHR1-3xFLAG* (Flag), 3) endogenous *LHR1* (LHR1) and 4) *NEO* gene (Neo) gene in the

LHR1 genetic locus. Two independent genomic isolations from recovered isolates were run in PCR reactions with the multiple primer sets, and the band pattern indicated that there was still an endogenous copy of *LHR1* present (Figure 9, lane 5).

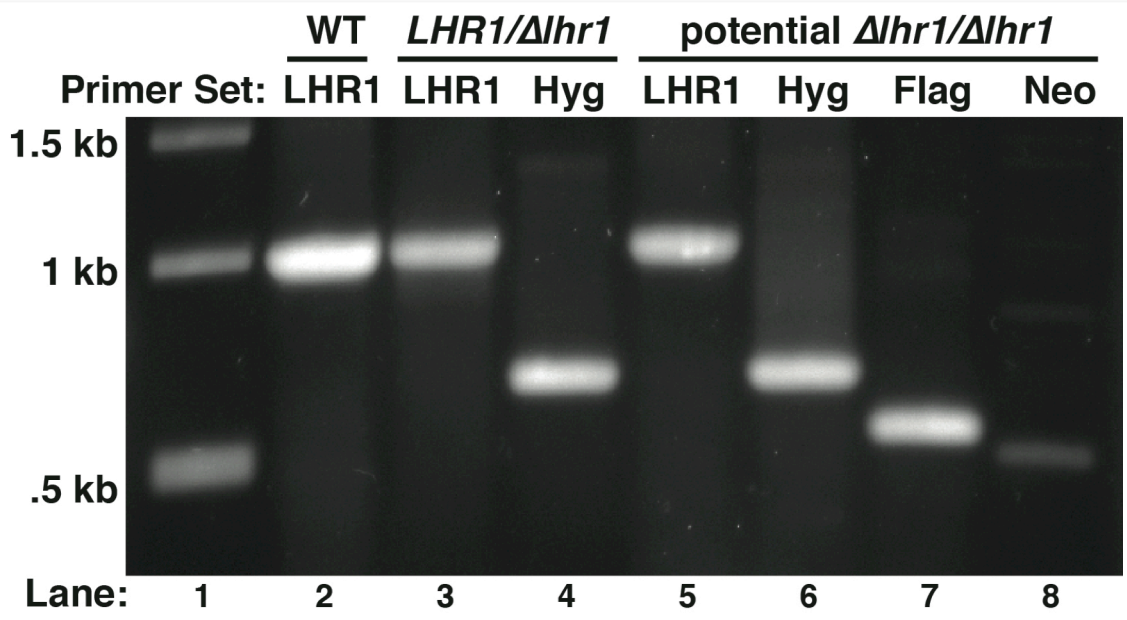

Figure 9 – Triple Drug Resistant Isolates Still Contain an Endogenous Copy of *LHR1*. Genomic DNA from potential Δ*lhr1*/Δ*lhr1* clones episomally expressing LHR1-3xFLAG that were resistant to hygromycin B (100 μg/ml), nourseothricin (50 μg/ml), and G418 (50 μg/ml) was subjected to PCR to detect the different copies of drug resistance cassettes or *LHR1* that could be present. Gel is representative of genomic DNA isolations from multiple clones.

Characterization of *L. amazonensis* Δ*lhr1/LHR1* (SKO) Using [^{55}Fe]-heme Uptake

In collaboration with Dr. Tamika Samuel, we performed further characterization of the SKO parasites using [^{55}Fe]-heme uptake assays in parasites grown under heme-depleted and regular conditions. As expected, mid-log promastigote forms of WT *L. amazonensis* and SKO showed increased heme uptake when grown in heme-depleted

conditions, with WT *L. amazonensis* showing a 8.5-fold increase and SKO a 2.5-fold increase over basal uptake (Figure 10). Interestingly, in this assay the SKO showed a 2.8-fold higher heme uptake under basal conditions when compared to WT *L. amazonensis,* and only slightly lower levels than WT under heme-depleted conditions. The difference in heme uptake between WT and SKO *L. amazonensis* when grown under heme-depleted conditions is not as large as what was observed previously when uptake was measured using ZnMP (35). This disparity is potentially due to the differences in the time point at which uptake was measured. The radioactive heme uptake assay measured uptake after 60 minutes, whereas ZnMP uptake was measured after 3 hours; it is possible that a larger difference between WT *L. amazonensis* and the SKO grown in heme-depleted conditions would be observed at later time points in the radioactive heme uptake assay.

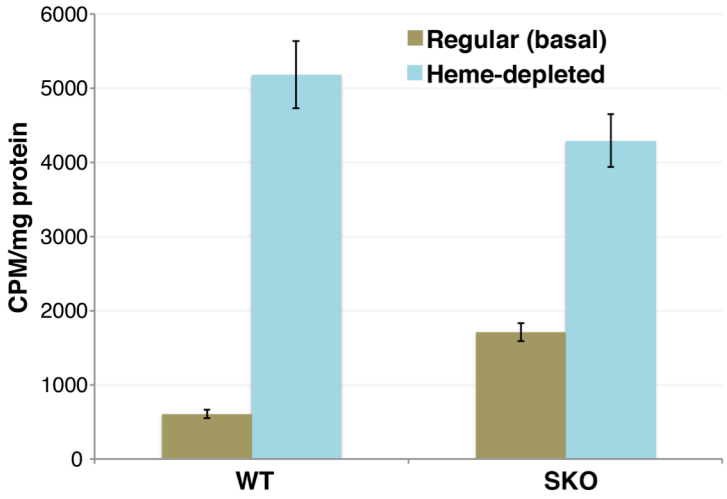

Figure 10 – WT *L. amazonensis* and SKO Show Increased Heme Uptake When Grown in Heme-depleted Conditions. Parasites were grown in heme-depleted or regular media O/N and [^{55}Fe]-heme uptake was performed for 60 min. CPM of 0° C was subtracted from CPM of 26° C and then normalized to mg protein. Assay was performed in triplicate and data is representative of 2-3 independent experiments. Data represents the mean +/- SD of assay triplicates. (T. Samuel, unpublished data).

LHR1 Heme Binding is pH Independent and Heme Transport is pH Dependent

In *L. amazonensis*, GFP-LHR1 localizes to acidic intracellular compartments that accumulate lysotracker and to the plasma membrane (35), and LHR1-3xFLAG localizes mostly to acidic intracellular compartments (D. Miguel, unpublished results). These localization patterns raised the question as to whether LHR1-mediated heme transport across membranes occurs at the plasma membrane, or after endocytosis into the parasite's endosomal/lysosomal pathway. To investigate this we tested the binding affinity of LHR1 for heme over a range of pH values from 5-8. We used LHR1-3xFLAG overexpressing *L. amazonensis* to generate cell lysates buffered at varying pH values to test the ability of LHR1 to bind heme over a range of pH values using hemin-agarose.

We found that LHR1 binding to hemin-agarose was independent of pH (Figure 11 A). To provide further evidence, we grew the Δ*hem1* (6D) yeast strain, which has a non-functional heme biosynthesis pathway and utilizes exogenous heme poorly, transformed with vector alone, *C. elegans* HRG-4-HA, or *L. amazonensis* LHR1-HA in 1 μM hemin at pH 5 and 6 (this strain is unable to grow at pH 7 or 8) and observed no differential growth pattern (Figure 11 B), indicating that LHR1 is capable of rescuing heme uptake under these two different levels of acidity. These findings are consistent with previous observations showing that *C. elegans* HRG-4, the heme transporter most closely related to LHR1, binds to hemin-agarose over a broad pH range (61).

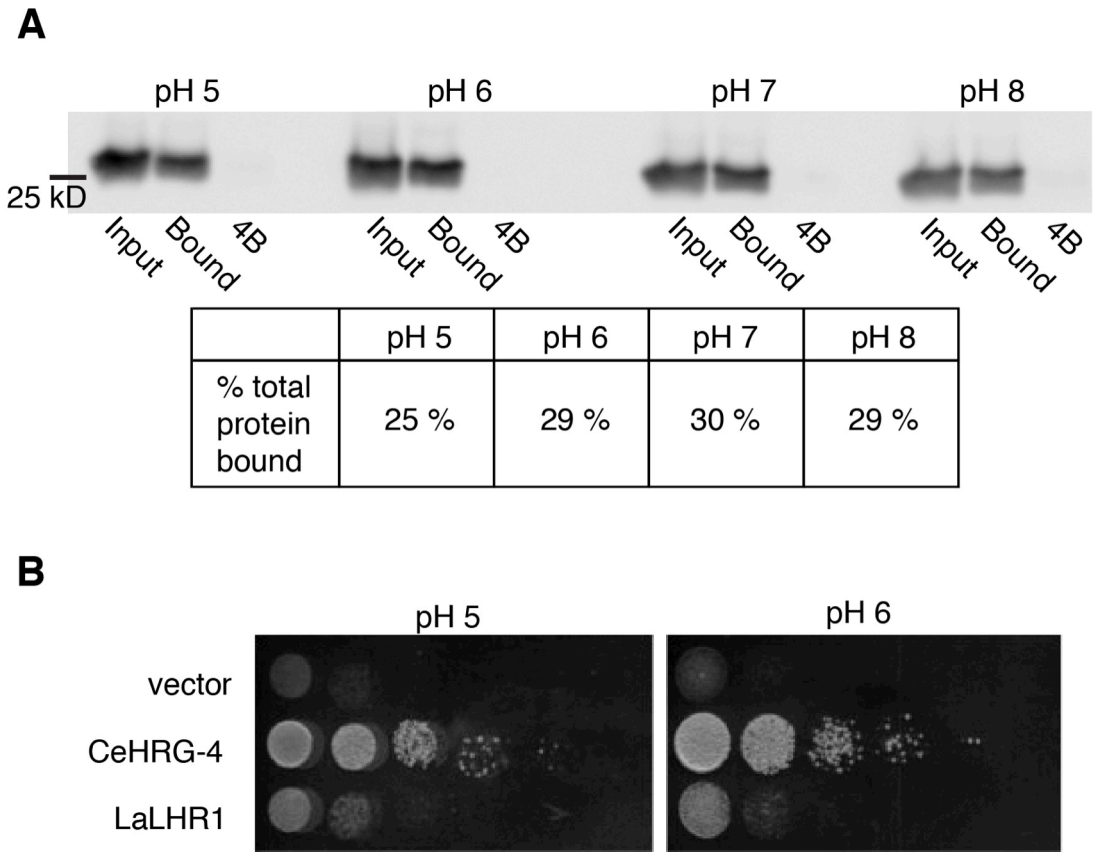

	pH 5	pH 6	pH 7	pH 8
% total protein bound	25 %	29 %	30 %	29 %

Figure 11 – Heme Binding to LHR1 is Independent of pH. **A**) LHR1-3xFLAG binding to hemin-agarose at different pH values. Input represents 20% of total input protein. Bound is total protein eluted from beads. 4B is sepharose 4B beads alone as a control for nonspecific binding. Western blot is representative of three independent experiments. The table shows the % of total protein that was bound to hemin-agarose and was calculated using densitometry in ImageJ software from the western blot pictured and is representative of three experiments. **B**) Growth Spot Assay of Δ*hem1* (6D) transformed with vector alone (vector), *C. elegans* HRG-4-HA (CeHRG-4) or *L. amazonensis* LHR1-HA (LaLHR1) grown in 1 μM hemin at the indicated pH values. Images were acquired on day 5 after spotting**.**

Working in collaboration with Dr. Tamika Samuel we performed radioactive heme binding and uptake assays at different pH values and temperatures as part of the optimization process to characterize kinetic heme uptake in *L. amazonensis*. We

incubated *L. amazonensis* promastigotes with [^{55}Fe]-heme at 0° C in pH 5.5 and pH 7.4 buffer to assay heme binding, and at 26° C in pH 5.5 and pH 7.4 buffer to assay heme transport for 60 minutes, followed by quantitation of the [^{55}Fe]-heme in lysates. When parasites were incubated at 0° C for 60 min, there was no difference in [^{55}Fe]-heme binding at the two pH values. In contrast, when the parasites were incubated at 26° C for 60 min, the parasites in pH 5.4 appeared to take up more [^{55}Fe]-heme than those at pH 7.4 (Figure 12). This suggests that binding of heme to LHR1 may be unaffected by pH but that transport might benefit from acidic conditions, consistent with the possibility that LHR1 translocates heme across the membrane into the cytosol from a parasite late endosomal/lysosomal compartment.

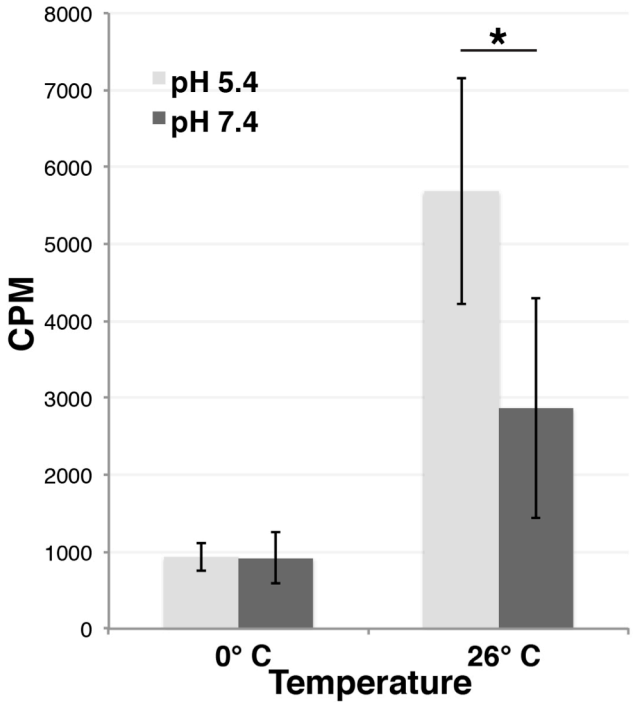

Figure 12 – [^{55}Fe]-Heme Binding and Uptake in *L. amazonensis*. *L. amazonensis* was incubated with [^{55}Fe]-heme for 60 min at either 0° C or 26° C and [^{55}Fe]-heme measured in cell lysates. Assay was performed in triplicate and experiment was performed once. Error bars represent standard deviation. * p = 0.07 Student's *t*-test. (T. Samuel, unpublished data).

Conclusions/Discussion

The dependence of *Leishmania* on exogenous heme was first characterized almost forty years ago (41), however it was not until recently that a protein, LHR1, responsible for direct heme acquisition in *L. amazonensis* was described (35). LHR1 is only ~15% identical and ~45% similar to the *bona fide* heme transporter CeHRG-4 that has been characterized in *C. elegans*. The studies done using CeHRG-4 provided a reference point for these *Leishmania* heme transport studies (35,61,62).

In this work we showed that episomal expression of tagged versions of *LHR1* were able to modulate the total intracellular heme pool of *L. amazonensis* (Figure 6). Additionally, LHR1 expression in yeast was able to promote uptake of a fluorescent heme analog ZnMP that was not observed with vector alone and ZnMP uptake could be reduced when incubated with 10-fold excess hemin (Figure 7). *LHR1* null strains could not be generated despite all our efforts, suggesting that LHR1 is essential for survival of the promastigote forms.

Using radioactive heme uptake, we further characterized *L. amazonensis* WT and SKO parasites grown in regular and heme-depleted conditions. We expected that SKO parasites would have less [^{55}Fe]-heme uptake than WT, but surprisingly under basal conditions the SKO parasites seem to import more or equal amounts of heme compared to WT cells. Under heme-depleted conditions uptake is markedly increased, but there is no statistical difference between WT and SKO (Figure 10). Given the genetic plasticity of *Leishmania*, (94) and since heme is essential for survival, it is not too surprising that the SKO parasites appear to have compensated for the lack of one LHR1 allele in order to acquire sufficient heme in the promastigote form (84).

Finally, we provide evidence that the binding of heme to LHR1 is independent of pH and some data suggesting that the LHR1-mediated transport of heme across the membrane is dependent upon pH (Figures 11 & 12). It is entirely possible that binding of heme and the transport across the membrane are distinct in their pH dependencies. One can envision a scenario for promastigotes, which replicate in the gut of the sand fly, where heme binds to LHR1 at the plasma membrane (where some transport could occur at neutral pH) and then the LHR1+heme complex is internalized and trafficked to acidic intracellular compartments of the parasite where heme is transported into the cytoplasm with greater efficiency.

Campos-Salinas and co workers have looked at heme/heme analog acquisition in *Leishmania* using a visceralizing strain, *L. donovani* (54). They showed that hemoglobin and free heme appear to follow different routes of entry, and that uptake of the heme analog MgPP followed faster kinetics than what we have described here for LHR1 from *L. amazonensis*. The differences in the systems and heme analogs employed in the assays could account for the differences observed in kinetic acquisition (our assays were performed with ZnMP in yeast and theirs were performed with MgPP in *L. donovani*). There are only minor differences between the LHR1 proteins from *L. amazonensis* and *L. donovani* (93% identical, 98% similar) and these differences are not thought to play a role in the observed kinetic difference between our assays and the ones performed with *L. donovani*.

The findings presented here are significant because they further characterize LHR1 as a bona fide heme transporter, thereby adding to our understanding of heme transporters and heme acquisition in *Leishmania*. A blastp search of the human genome

(http://blast.ncbi.nlm.nih.gov) using LHR1 showed no significant homology to any known human proteins, which is supported by the fact that *L. amazonensis* LHR1 is most closely related to *C. elegans* HRG-4, which also does not have a human homologue (61). Consequently, small molecules designed to inhibit LHR1 may have less off target effects because there are no LHR1 homologues in humans. LHR1 is essential for parasite survival within macrophages, providing additional evidence that LHR1 is an attractive drug target (84).

Chapter 3: Differential Heme Acquisition in *L. chagasi (L. infantum)* and *L. amazonensis*

Partially adapted from Flannery et al. Curr Opin Microbiol 2013 (31)

Introduction

The markedly distinct clinical disease manifestations that occur after infection with different species of *Leishmania* are dependent upon the infecting species of *Leishmania* and the host (Figure 13). The underlying mechanism(s) of the parasites that are responsible for these differences in clinical disease manifestations are not understood. Studies have been performed looking for species-specific genes that could potentially explain some trends in disease association, but so far there have been relatively few species-specific genes identified that could account for the varying disease manifestations (95-98). Visceral leishmaniasis is characterized by parasite replication within macrophages of the spleen, liver, and bone marrow; whereas cutaneous leishmaniasis is characterized by replication within macrophages at the skin near the site of the initial sand fly bite (99). Based on the location where infected macrophages reside in the two

***Leishmania* species reported to cause clinical symptoms in humans**

Species	Major disease manifestation			
	Cutaneous	Diffuse cutaneous	Mucocutaneous	Visceral
L. tropica				✓
L. major	✓			
L. aethiopica	✓	✓		
L. donovani				✓
L. infantum (*L. chagasi*)	✓			✓
L. mexicana	✓	✓		
L. amazonensis	✓	✓	✓	
L. pifanoi	✓			
L. braziliensis	✓	✓	✓	
L. panamensis	✓		✓	
L. peruviana	✓			
L. guyanensis	✓		✓	
L. siamensis				✓

Figure 13 – Table of Clinical Disease Manifestations and the Associated *Leishmania* species.

Leishmaniasis disease manifestation is dependent upon the infecting species and the host.

forms of leishmaniasis, the heme availability at those sites has the potential to be quite different. Macrophages in the spleen are involved in extensive phagocytosis of senescent red blood cells, a rich source of heme, whereas macrophages present in the skin are not likely to perform this role. Given the potential differences in heme availability at the different sites where infected macrophages reside, it is possible that the acquisition of heme is differentially regulated between the two species, and examining this aspect could provide insights into the mechanism connecting disease outcome with the parasite species.

Regulation of gene expression in trypanosomatid parasites is not controlled by classical transcriptional promoters present in other eukaryotic cells (100). Protein coding genes are arranged in polycistronic units with variable numbers of genes on the chromosomes (101-104), and RNA Polymerase II transcribes these arrays as polycistronic transcripts (105-108). These polycistronic messages are subsequently processed via trans-splicing with a 39 nucleotide splice leader (SL) from the SL-RNA at the 5′ end and polyadenylation at the 3′ end to form mature monocistronic mRNAs (109-112). The 3′ polyadenylation of an upstream gene is coupled to SL 5′ trans-splicing of the downstream gene and the polyadenylation site of the upstream gene is selected based on the position of the downstream gene's SL-acceptor site; consequently there is the potential for multiple polyadenylation sites and SL-acceptor sites within a given transcript (112,113). There is little control over the initiation of transcription, and therefore trypanosomatids utilize extensive post-transcriptional regulation strategies such as mRNA stability, translation initiation, and post-translational protein modifications (100,114,115). Elements in the UTRs, both 5′ and 3′, have been found to be involved in

post-transcriptional gene regulation and there are many different mechanisms by which these elements could control gene expression (i.e. RNA binding protein sites, tertiary RNA structures, etc.) (116,117). As part of the investigation into how trypanosomatids regulate gene expression, alternative splicing (100,118-121), mRNA stability (96,122-133), differential translation (134-136), post-translational protein modifications (137-141), and protein stability (142) have all been described as strategies employed to control gene expression.

Herein we investigate whether *L. amazonensis* and *L. chagasi* differ in their response to heme deprivation, their ability to acquire heme from the environment, and we focus on mechanism(s) of gene regulation that could be involved in regulating LHR1. This is significant because it could provide insight into the biological differences between cutaneous and visceral strains, which are poorly understood, and could influence future therapies and drug development. We hypothesized that *L. chagasi* and *L. amazonensis* differ in their responses to heme deprivation and their ability to acquire heme from the environment by differentially regulating LHR1 mRNA.

Results

Higher *LHR1* Transcript Levels in *L. chagasi* than *L. amazonensis* Under Heme Deplete Conditions

To ascertain potential differences in LHR1 regulation in *L. chagasi* and *L. amazonensis*, we used Reverse Transcription Quantitative Polymerase Chain Reaction (RT-qPCR) to examine transcript levels under different growth conditions. It was already known that *L. amazonensis* has higher LHR1 transcript levels when grown in heme-depleted promastigote growth media (PGM) vs. regular PGM (35). Both species

were grown in either regular or heme-depleted PGM for 24 h and RNA was isolated for use in RT-qPCR analysis. *L. chagasi* had 11-fold higher and *L. amazonensis* had 4-fold higher amounts of *LHR1* transcripts in heme-depleted conditions, compared to regular growth conditions (Figure 14).

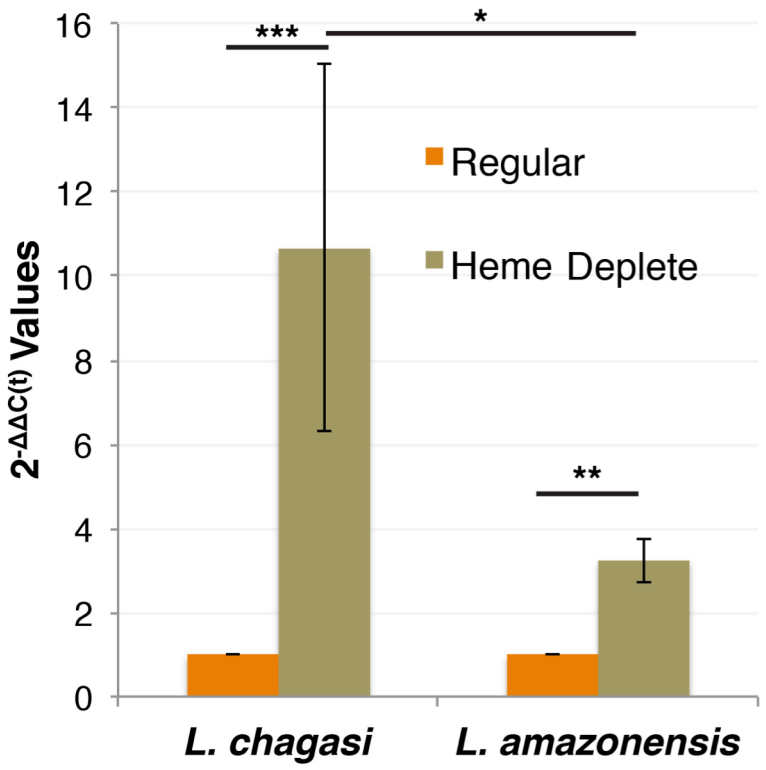

Figure 14 – *LHR1* Transcripts Levels are Higher in *L. chagasi* than *L. amazonensis* After Heme Deprivation. *L. amazonensis* and *L. chagasi* were grown for 24 h in regular or heme-depleted media and RNA isolated for use in RT-qPCR. Each sample was normalized to ubiquitin hydrolase transcript levels and regular media growth was considered 1.0. Experiments were repeated three to five times. Errors shown are standard deviations. Student's *t*-test: *L. chagasi* Regular vs. Heme Deplete = 0.001; *L. amazonensis* Regular vs. Heme Deplete = 0.002; *L. chagasi* Heme Deplete vs. *L. amazonensis* Heme Deplete = 0.03.

Differential Uptake of ZnMP by *L. chagasi* and *L. amazonensis*

Transcript levels do not always correlate well with proteins levels in trypanosomatids (132); consequently we examined if the differences in transcript levels observed under heme-depleted conditions reflected an increase in heme uptake, consistent with an increase in LHR1 protein levels. To do this we used the fluorescent heme analog ZnMP that can be detected using a fluorescence microscope upon accumulation within parasites. *L. chagasi* and *L. amazonensis* were incubated in heme-depleted medium for 16 h, ZnMP was added, and uptake was quantified over time using fluorescence microscopy images and Volocity image analysis software (Improvision). *L. chagasi* acquired detectable intracellular fluorescence earlier than *L. amazonensis,* and had higher mean fluorescence intensities per parasite at identical time points (Figure 15). This observation correlates directly with the higher transcript levels in *L. chagasi* upon growth in heme-depleted medium.

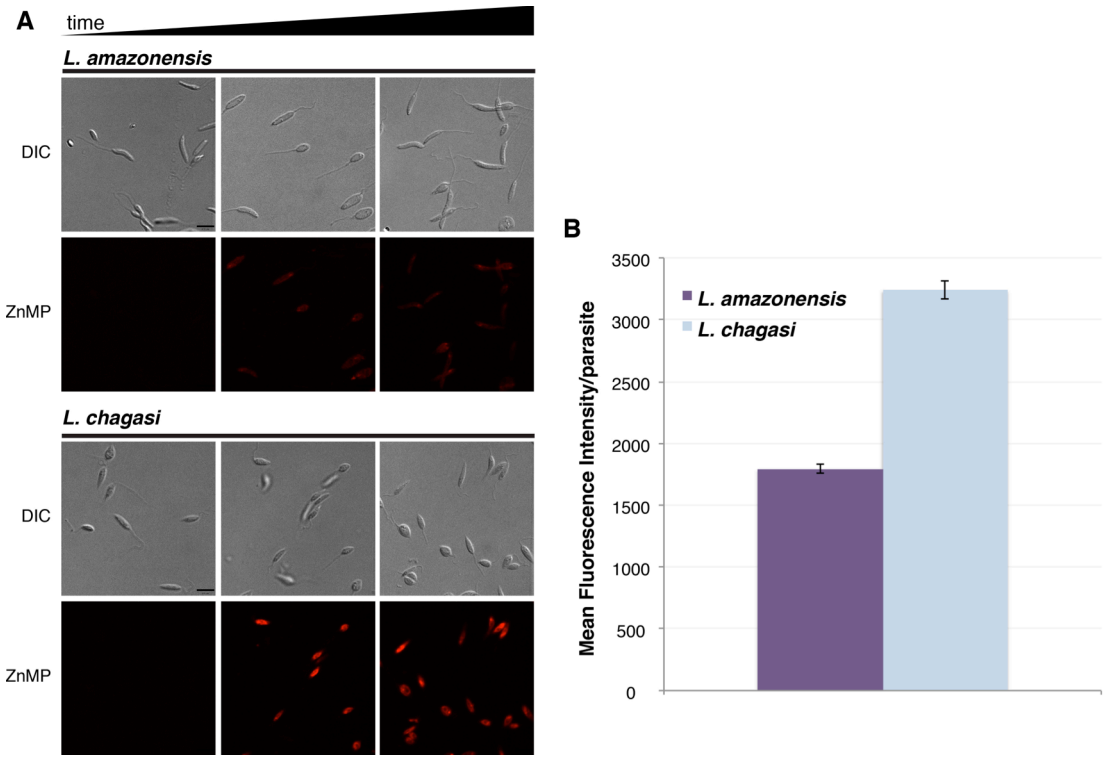

Figure 15 – *L. chagasi* uptake ZnMP faster than *L. amazonensis* upon heme deprivation. **A**) Mid-log phase *L. amazonensis* and *L. chagasi* were grown for 16 h in heme-depleted medium. 10 µM ZnMP was added and cells were incubated at 26°C and imaged at 0, 1 and 3 h on a spinning disk confocal microscope using identical acquisition settings. Scale bar is 9 µm. **B**) Relative Mean Fluorescence per parasite was quantified at the 3 h time point using Volocity (PerkinElmer). Graph is representative of two independent experiments.

Examination of the *LHR1* Genomic Regions of *L. chagasi* and *L. amazonensis*

The extensive use of post-transcriptional regulation in trypanosomes led us to investigate the untranslated regions (UTRs) of *LHR1* because of the role that UTRs have been shown to play in regulating gene expression via elements present in these regions of the mRNAs. We examined the UTRs in each species in order to identify regions of interest that could potentially provide insight into our previously observed differential modulation of transcript levels and ZnMP uptake. Using TriTrypDB

(www.tritrypdb.org), we examined the *LHR1* genomic regions for *L. infantum* (LinJ.24.2320) and *L. mexicana* (LmxM.24.2230), two closely related species to *L. chagasi* and *L. amazonensis* respectively. We found that this region encompasses approximately 4,000 base pairs (distance from the end of the upstream gene to the start of the downstream gene) and that *LHR1* is syntenic across a range of trypanosomatid species (most of the *Leishmania* and *Trypanosoma* species in the database) (Figure 16).

A

Gene	Organism	Product	is syntenic	has comments
LbrM.24.2310	Leishmania braziliensis MHOM/BR/75/M2904	hypothetical predicted multi-pass transmembrane protein	yes	no
LdBPK_242320.1	Leishmania donovani BPK282A1	hypothetical predicted multi-pass transmembrane protein	yes	no
LinJ.24.2320	Leishmania infantum JPCM5	hypothetical predicted multi-pass transmembrane protein	yes	no
LmjF.24.2230	Leishmania major strain Friedlin	hypothetical predicted multi-pass transmembrane protein	yes	yes
LtaP24.2390	Leishmania tarentolae Parrot-TarII	Hypothetical predicted multi-pass transmembrane protein	yes	no
Tb427.08.6010	Trypanosoma brucei Lister strain 427	hypothetical predicted multi-pass transmembrane protein	yes	no
Tb927.8.6010	Trypanosoma brucei TREU927	hypothetical predicted multi-pass transmembrane protein	yes	yes
Tbg972.8.6030	Trypanosoma brucei gambiense DAL972	T. brucei spp.-specific protein	yes	no
TcIL3000_8_5780	Trypanosoma congolense IL3000	unspecified product	yes	no
TcCLB.511071.190	Trypanosoma cruzi CL Brener Esmeraldo-like	hypothetical protein, conserved	yes	no
TcCLB.504037.10	Trypanosoma cruzi CL Brener Non-Esmeraldo-like	hypothetical protein, conserved	no	no
TevSTIB805.8.6270	Trypanosoma evansi strain STIB 805	hypothetical predicted multi-pass transmembrane protein	yes	no

B

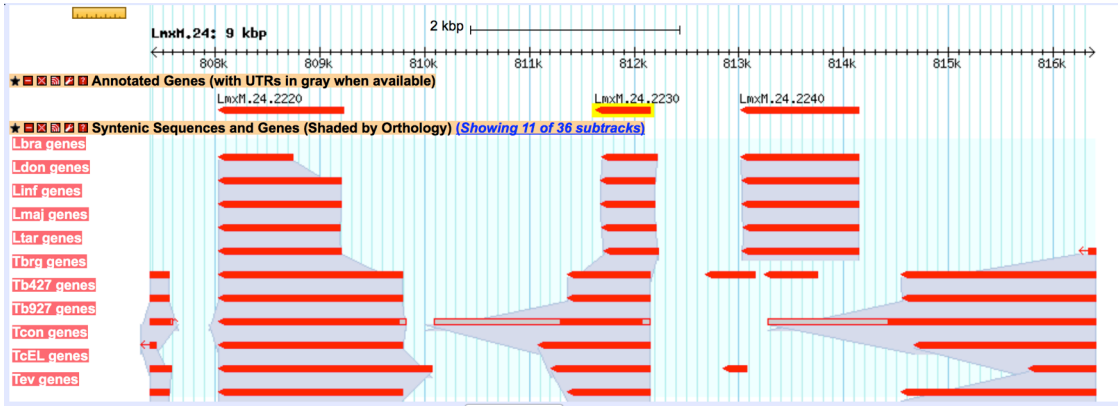

Figure 16 – *LHR1* Genomic Region and Synteny Across a Range of Trypanosomatid Parasites.

A) Table of *LHR1* orthologs and paralogs within TriTryp DB. **B**) Genome Browser from TriTrypDB showing the location of *LHR1* on the *L. mexicana* genome and the synteny between species of the Trypanosomatidae family. Lbra = *L. braziliensis*, Ldon = *L. donovani*, Linf = *L. infantum*, Lmaj = *L. major*, Ltar = *L. tarentolae*, Tbrg = *T. brucei* 927, Tb427 = *T. brucei* 427, Tb927 = *T. brucei* TREU927, Tcon = *T. congolense*, TcEL = *T. cruzi* Esmeraldo-like, & Tev = *T. evansi*. Images generated using www.tritrypdb.org.

The genomic regions (including the upstream gene, downstream gene, and intergenic regions) for *L. mexicana* and *L. infantum* were downloaded from TriTrypDB and aligned using Clustal Omega (https://www.ebi.ac.uk/Tools/msa/clustalo/) in order to

identify any species-specific genomic sequences present. The upstream and downstream genes were included in the alignment so that the intergenic regions would align in such a manner as to identify major differences between the two species. Figure 17 is an illustration of the alignment showing that there was 87% identity between the two species with no major difference in the 5′UTRs or the ORFs, but with differences present in the 3′UTRs. *L. mexicana* is missing three sections of the 3′UTR that are present in *L. infantum*, gaps of 35, 39, and 44 bp.

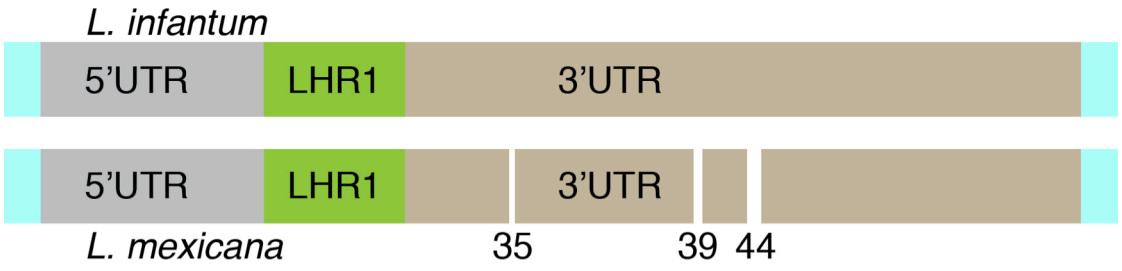

Figure 17 - Illustration of Alignment of *LHR1* Genomic Regions of *L. infantum* and *L. mexicana*. Genomic regions downloaded from TriTrypDB were aligned using Clustal Omega. There was 87% identity between the two species, with three segments of the 3′UTR missing from *L. mexicana* that are present in *L. infantum*. Light blue = upstream and downstream genes, gray = 5′UTR, green = ORF, tan = 3′UTR.

Identification of 3′ Polyadenylation Addition Sites in *L. chagasi* and *L. amazonensis*

The *LHR1* genomic region alignments revealed differences in the 3′UTR regions of these two genes, but it was unclear if these regions were within the mRNA for each species because the mRNA boundaries for *LHR1* and its homologues in TriTrypDB were not annotated (only exception is the *T. brucei* TREU927 strain). In order to confirm the sequence and define the 3′UTR boundaries for *L. chagasi* and *L. amazonensis*, mRNA from both species was isolated and used to amplify and sequence the *LHR1* mRNA. The

LHR1 mRNA from the *L. chagasi* strain that we sequenced shared 99% identity with the *L. infantum* sequence from TriTrypDB, and the *LHR1* mRNA from the *L. amazonensis* strain we sequenced shared 96% identity with the *L. mexicana* sequence from TriTrypDB. *LHR1* 3′UTRs from *L. chagasi* and *L. amazonensis* were found to share 83% identity and were 1.7 kb and 1.8 kb respectively (Figure 18). The portions of the 3′UTR (gaps of 35, 39, and 44 bp) found to be different in the genomic analysis, were absent from *L. amazonensis* 3′UTR but present in *L. chagasi*. *L. chagasi LHR1* mRNA utilizes two polyadenylation sites within a 10 nucleotide region and, *L. amazonensis LHR1* utilizes three polyadenylation sites within a 30 nucleotide region. When mRNAs were collected from these two species grown in heme-depleted conditions, there were no major differences in the polyadenylation sites used or the ratios between the sites used by either species. An alignment of the two mRNAs showed that the regions containing the polyadenylation sites aligned at exactly the same location. Since trypanosomatids utilize multiple polyadenylation sites (143), it is conceivable that this could include or exclude elements in the 3′UTR responsible for stability, but this does not appear to be the manner in which *LHR1* is regulated. There is also the possibility of alternative SL-acceptor site usage in controlling gene expression. It was previously shown that alternative SL-acceptor sites were not used by LHR1 in *L. amazonensis* when parasites were grown under normal conditions and under iron deplete conditions (144), so we focused our efforts on characterizing the 3′UTRs from both species.

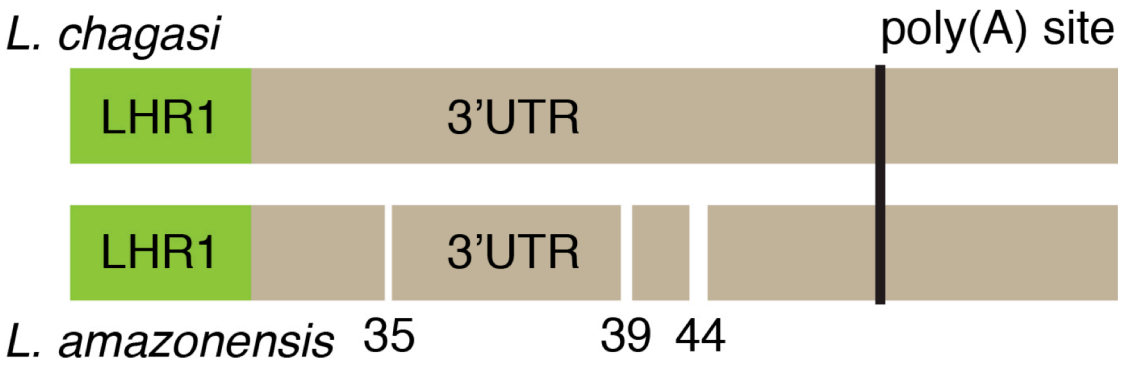

Figure 18 – LHR1 ORF and 3′UTR Alignments of *L. amazonensis* and *L. chagasi*. Alignment showed 83% identity between the transcripts with polyadenylation (poly(A)) sites at approximately the same location in both species. green = ORF, tan = 3′UTR.

Luciferase Reporter Gene Assays

Given the differences in the 3′UTRs of the two mRNAs, we asked if these differences were involved in the differential regulation of *LHR1* mRNA levels that we had observed. We generated luciferase reporter constructs that had the luciferase gene flanked by the 5′UTR and 3′UTR regions from either *L. amazonensis* or *L. chagasi LHR1* (Figure 19 A). These constructs were transfected into *L. amazonensis* and luciferase activity was measured upon heme depletion. We hypothesized that the luciferase gene would respond in the same manner as *LHR1* upon heme deprivation due to the presence of the *LHR1* UTRs flanking the luciferase gene. As a pilot experiment, we tested *L. amazonensis* transfected with the construct that had the luciferase gene under the control of the UTRs from *L. amazonensis* ([LamUTRs-luc]). We grew these isolates under regular or heme-depleted conditions for 24 h and then measured luciferase activity (Figure 19 B). Even though the luciferase activity was slightly higher under the heme-depleted conditions, it was not significant. This is not what we would expect to see upon

heme deprivation since we know that LHR1 transcripts are 4-fold higher when these parasites are grown in heme-depleted media and they take up ZnMP faster than parasites grown in regular media (35). Consequently we ran a RT-qPCR on the RNA isolated from the parasites that were grown under the same conditions to verify what was occurring at the transcript level. We found that the luciferase mRNA was higher in heme-depleted conditions, as would be expected, but the nourseothricin resistance gene (Sat) mRNA increased to the same extent as the luciferase mRNA (Figure 19 C). This luciferase reporter construct was episomally expressed in theses parasites and this data suggests that the stress of heme deprivation caused the entire plasmid to be transcribed more and not specifically just the luciferase gene, so the increase in luciferase transcripts was probably not due to the presence of the *LHR1* UTRs on the transcript. Consequently, it would be difficult to use this experimental set-up to verify if the UTRs are involved in gene regulation. Recently tools were constructed that would allow for the integration of this luciferase construct into the LHR1 loci, which could potentially overcome the overall transcription increase of the episome that we observed and allow us to clarify if the 3′UTRs are involved in the gene regulation of LHR1 (145). Using this new approach, we can integrate the *L. chagasi* and *L. amazonensis* UTR-Luc constructs into the genomes of *L. chagasi* and *L. amazonensis* and then measure luciferase activity and luciferase mRNA levels upon heme deprivation. If the differences in the UTRs are involved in gene regulation, we would expect to see higher luciferase activity when the luciferase gene is controlled by the *L. chagasi* UTRs than when it is controlled by the *L. amazonensis* UTRs.

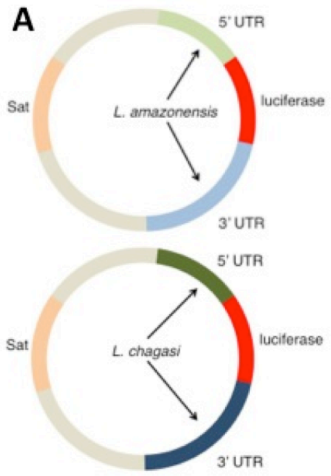

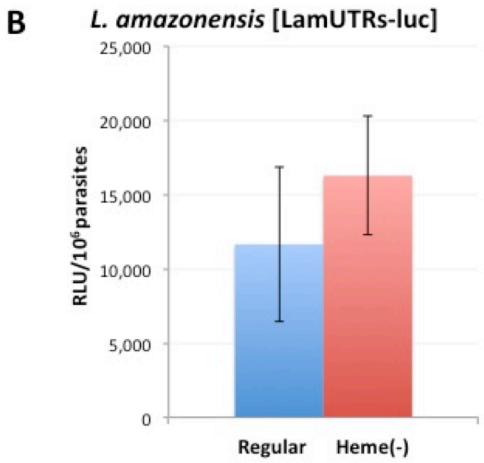

C ***L. amazonensis* [LamUTRs-luc]**

qPCR Target	Sample	C(t) Mean	C(t) SD	Normalized to Sat Δ Ct	Normalized to Sat ΔΔ Ct	Normalized to Sat 2-ΔΔCt	Normalized to UbH Δ Ct	Normalized to UbH ΔΔ Ct	Normalized to UbH 2-ΔΔCt
Luc	Reg	16.18	0.02	-3.27	1.27	0.42	-6.23	-1.33	2.52
Luc	HemeDep	15.23	0.02	-2.00			-7.57		
Sat	Reg	19.45	0.05	0.00	0.00	1.00	-2.97	-2.60	6.07
Sat	HemeDep	17.23	0.04	0.00			-5.57		
LHR1	Reg	18.50	0.03				-3.92	-1.66	3.15
LHR1	HemeDep	17.22	0.04				-5.57		
UbH	Reg	22.42	0.01				0.00	0.00	1.00
UbH	HemeDep	22.80	0.12				0.00		

Figure 19 – Luciferase Reporter Assays using *LHR1* UTRs from *L. amazonensis* and *L. chagasi*. **A**) Schematic of the plasmids constructed. **B**) Luciferase activity detected in *L. amazonensis* + [LamUTRs-luc] after growth for 24 h in heme-depleted medium. Assay was done in duplicate and experiment was repeated 4 times. Errors shown are standard deviations. **C**) qPCR data generated using mRNA isolated after growth in heme-depleted medium for 24 h. Fold changes in light blue are when C(t) values were normalized to Sat (on plasmid) and those in light green are when normalized to UbH (in genome). Experiment was repeated twice with similar outcomes.

Conclusions/Discussion

We showed that *L. chagasi* has higher *LHR1* transcript levels than *L. amazonensis* when grown under heme-depleted conditions, and that these higher transcript levels

correlate with ZnMP uptake over time, with *L. chagasi* showing higher fluorescence at earlier time points than *L. amazonensis*. Examination of the *LHR1* genomic locus of these two closely related species showed that the ORF is well conserved as are the UTRs, although there are some detectable differences in the 3′UTRs.. 3′UTRs have been shown to be involved in gene regulation in a number of genes in *Leishmania* including heat shock proteins, amastin surface proteins, and paraflagellar rod proteins via tertiary structure of the mRNA or conserved motifs that can bind regulatory proteins (117,125,146). The differences observed in the 3′UTRs at the LHR1 genomic locus led to the characterization of the polyadenylation addition sites for the LHR1 genes from *L. chagasi* and *L. amazonensis*. There were no significant differences in polyadenylation addition sites between the two species and neither the sites nor their usage ratios changed upon growth in heme-depleted conditions. Attempts to verify whether the differences in the 3′UTRs were responsible for the modulation of *LHR1* transcript levels upon heme depletion using luciferase reporter constructs failed to reveal any differences in luciferase activity under the conditions examined.

These data suggest that there are fundamental differences in the manner in which *L. chagasi* and *L. amazonensis* regulate heme acquisition and LHR1. Given the high degree of similarity between the LHR1 proteins from these two species, the observed differences are probably not due to intrinsic characteristics of the proteins themselves, but could be related to differential post-transcriptional regulation. We showed that there were no major differences in polyadenylation sites between the two species in regular or heme-depleted conditions, indicating that differential mRNA processing is not likely to play a major role in LHR1 regulation. Thus, one of the many other forms of post-

transcriptional regulation present in trypanosomatid parasites is likely to be responsible for the differences we observed.

To our knowledge, this is the only study that has been performed investigating the differential heme acquisition in *L. chagasi* and *L. amazonensis*. Heme acquisition in *L. amazonensis* (35), as well as some other trypanosomatids (90,91) has been described, but other species of *Leishmania* have not been examined. A kinetic analysis of heme uptake in multiple *Leishmania spp*. still needs to be performed in order to compare heme acquisition between species that are associated with cutaneous leishmaniasis and species that are associated with visceral leishmaniasis.

The underlying mechanisms behind the differences observed between visceral and cutaneous strains remain elusive. An understanding of the mechanisms and traits that cause or allow one species and not another to visceralize might allow us to design better treatments for individuals already infected and potentially intervene with preventative measures before infection occurs. In order to characterize the potential heme acquisition differences between visceral and cutaneous strains further, a study of additional visceralizing (*L. donovani*, *L. tropica*, *L. siamensis,* etc.) and cutaneous (*L. major, L. pifanoi, L. peruviana*, etc.) species needs to be done. It would also be of great interest to identify the mechanism by which heme acquisition is regulated in these different species, and if modulation of the heme acquisition pathway could alter the outcome of disease. It would be particularly interesting, as suggested by our initial results with *L. chagasi*, if *Leishmania* species that can leave the skin to invade deep organs during visceralization have an enhanced ability to upregulate LHR1 expression. If heme acquisition regulation

is a major difference between visceral and cutaneous species it would provide a new direction for future treatments and drug development.

Chapter 4: Mutagenesis Analysis of LHR1

Adapted from Renberg et al. Manuscript in preparation.

Introduction

Iron and heme are both essential nutrients for growth of *Leishmania*. *Leishmania* parasites have two life cycles stages that grow in two different hosts and occupy two vastly different environments, the gut of sand fly and the PV within macrophages, that have different pH values, temperatures, nutrient availability, etc. (147-150). These two environments potentially contain different concentrations of available heme and iron. It is logical then, that these parasites have evolved many different mechanisms for acquiring these essential nutrients. The availability of iron is known to have a profound effect on the outcome of infection, and it has been demonstrated that parasites alter macrophage iron import and export pathways and that infected macrophages bind more hemoglobin via CD163 than non-infected macrophages, thus allowing the parasites to acquire these two important nutrients (22,23,34,151-153). Gaining an understanding of heme acquisition pathways of this medically important parasite will provide insight into its biology and possibly provide targets for new drug development (154).

Heme binding proteins have been described in bacteria and in metazoans. In bacteria many proteins of the cytochrome c maturation pathway have been characterized that transport heme via interactions with histidine residues (155-163). Three metazoan heme transporters have been characterized in order to identify the amino acid residues that are involved in heme transport. Two heme transporters from *C. elegans*, CeHRG-1 and CeHRG-4, were shown to utilize histidines, tyrosines and the FARKY motif for

heme transport, and the human homologue of CeHRG-1, hHRG-1, utilizes a histidine residue in a transmembrane domain for heme transport (62). None of the heme transporters that have been identified in trypanosomatid parasites have been characterized to identify the amino acid residues involved in heme transport. Here we present a mutagenesis analysis of LHR1 and show for the first time that key tyrosine residues but not histidine residues are important for heme transport.

Results

Selection of Amino Acid Residues for Mutagenesis Analysis in LHR1

LHR1 was originally identified by its homology with CeHRG-4, small size, and predicted structure of four transmembrane domains (35). The Hamza group, which discovered and characterized CeHRG-4 and CeHRG-1 (61), also identified the amino acid residues that are important for heme transport (62). They found that in CeHRG-4 a histidine in extracellular loop 2 (His-108) and the c-terminal FARKY motif, the potential heme interacting cluster of basic and aromatic amino acids, were important for heme transport, and in CeHRG-1 a histidine in transmembrane domain 2 (His-90) and the c-terminal FARKY motif were important for heme transport (62). LHR1 has a homologous histidine (His-105) to CeHRG-4 His-108, but the FARKY motif is not present in LHR1 so it is probable that LHR1 utilizes different amino acids in the C-terminus to mediate transport. Based on the mutagenesis analysis of CeHRG-4, research done on bacterial heme binding proteins (164,165), and residues that could participate in disulfide bonds, we selected nine LHR1 amino acids for mutation analysis: Tyr-18, His-36, Tyr-64, Tyr-80, His-105, Arg-106, Tyr-129, Tyr-136, and Cys-174 (Figure 20 A, B). We selected His-105 and Arg-106 because they aligned well with His-108 from CeHRG-4, which was

shown to participate in heme transport (62). Next we selected various histidines and tyrosines throughout the protein (Tyr-18, His-36, Tyr-64, Tyr-80, Try-129, Tyr-136) based on findings showing that these amino acids can be involved in heme coordination (164). Finally we selected the only cysteine residue (Cys-174) because of its potential involvement in disulfide bond formation and intermolecular interactions. All amino acid residues were mutated to alanine and mutant proteins were examined for phenotypes.

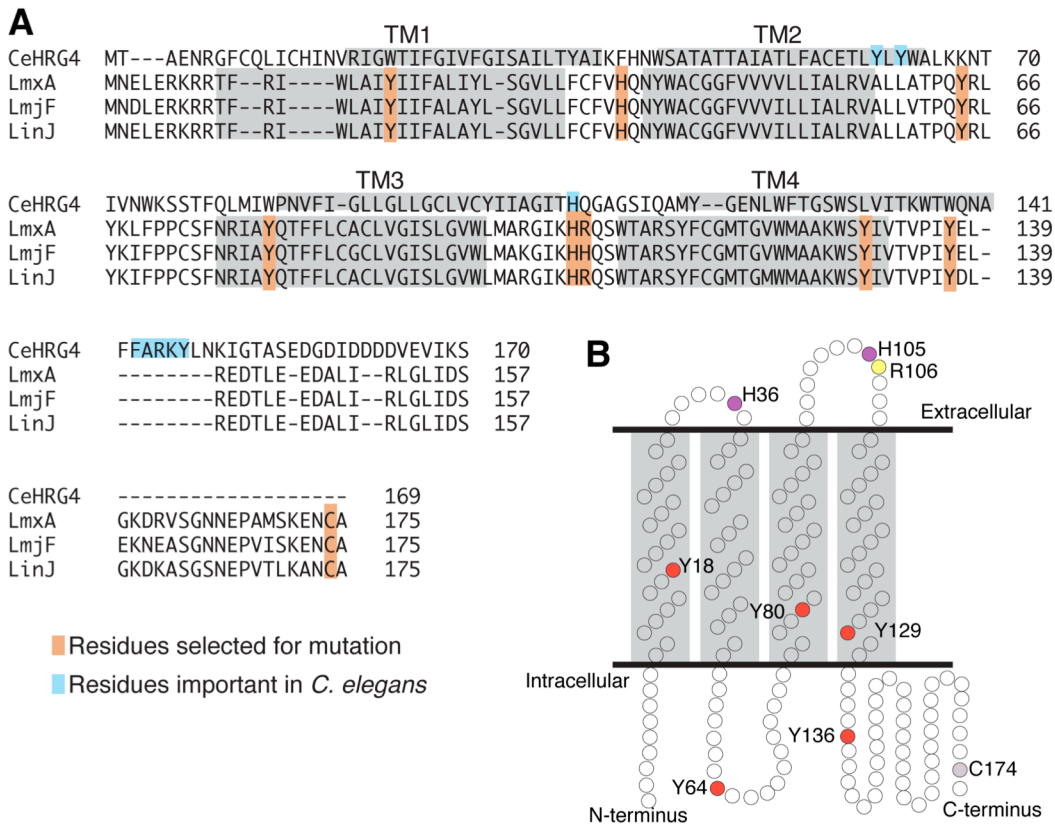

Figure 20 – Selection of Amino Acid Residues for Mutagenesis Analysis in LHR1. A) Alignment of CeHRG-4 with *L. amazonensis* (LmxA) LHR1 and LHR1 homologues from *L. major* (LmjF) and *L. infantum* (LinJ) highlighting the residues selected for mutation analysis; light blue indicates residues found to be important in *C. elegans* HRG-4; orange indicates residues selected for mutagenesis in *L. amazonensis*; light gray boxes indicate transmembrane domains. **B**) Predicted structure of LHR1 with amino acids selected for mutation highlighted to show their location in the predicted structure of LHR1; red are tyrosines; purple are histidines; yellow is arginine; light purple is cysteine.

Tyrosines 18, 80, & 129 are Important for LHR1 Function

Despite extensive efforts, we were unable to generate a homozygous *LHR1* knockout in *L. amazonensis*, which made the use of *L. amazonensis* unsuitable for a fast and efficient screen of the mutant proteins for phenotypes (35). Consequently we used a heterologous system that would allow us to characterize the ability of the mutant proteins to transport heme without interference from endogenous heme transporters. We took advantage of *S. cerevisiae* because it utilizes exogenous heme poorly (even when it lacks an essential enzyme in the heme biosynthetic pathway), doesn't contain LHR1 homologs, and there are many mutant strains available. We used the *S. cerevisiae* Δ*hem1* (6D) strain, which lacks the *HEM1* gene that encodes the first enzyme in the heme biosynthesis pathway, δ-aminolevulinic acid synthase (ALAS) (62,166). The Δ*hem1* (6D) strain needs to be supplemented with the product of ALAS, δ-aminolevulinic acid (ALA), or excess hemin (≥ 10 μM) in order to grow. LHR1 WT and mutant proteins tagged at the C-terminus with an HA epitope were expressed in the Δ*hem1* (6D) strain under the inducible *GAL1* promoter. We used two independent assays already well established in the Δ*hem1* (6D) strain to assess the ability of the LHR1 WT and mutant proteins to transport heme (166). First, we assessed the rescue of growth of the Δ*hem1* (6D) strain transformed with plasmids expressing LHR1 or the lhr1 mutants on agar plates containing varying heme concentrations (Figure 21 A). Cells transformed with pYES-DEST52 alone were only able to grow on agar plates when supplemented with ALA or ≥1 μM heme. In contrast, cells transformed with WT LHR1 were able to grow at 0.25 μM heme. At 0.25 μM heme, cells transformed with Y18A, Y80A, and Y129A showed decreased growth, cells transformed with H36A showed increased growth, and

all other mutants showed no significant difference in growth pattern when compared to cells expressing WT LHR1 (Figure 21 A). There were some variations in expression levels between the mutant proteins, but the majority expressed at levels comparable to WT, with H36A being the only one with significantly higher expression levels, which may account for the increased growth observed in the growth spot assay (Figure 21 A,B). Second, we measured changes in regulatory intracellular pools of heme using β-galactosidase activity from a *CYC*::*lacZ* promoter-reporter fusion. In this system, *lacZ* expression is dependent upon Hap1-5, a transcription complex that binds heme and activates the *CYC1* promoter; consequently the level of β-galactosidase activity directly correlates to the amount of intracellular heme that is available to activate the *CYC1* promoter (62). Cells transformed with pYES-DEST52 alone had negligible cytoplasmic heme levels, but cells transformed with WT LHR1 had increased cytoplasmic heme levels. Cells expressing Y18A, Y80A, R106A and Y129A mutants had significantly decreased cytoplasmic heme levels at both concentrations of heme tested when compared to cells expressing WT LHR1. Cell expressing H36A showed an increased level of cytoplasmic heme when compared to WT LHR1 only when grown in 10 μM heme. All other mutations assayed did not alter the cytoplasmic heme levels to a significant extent at either concentrations of heme tested (Figure 21 C).

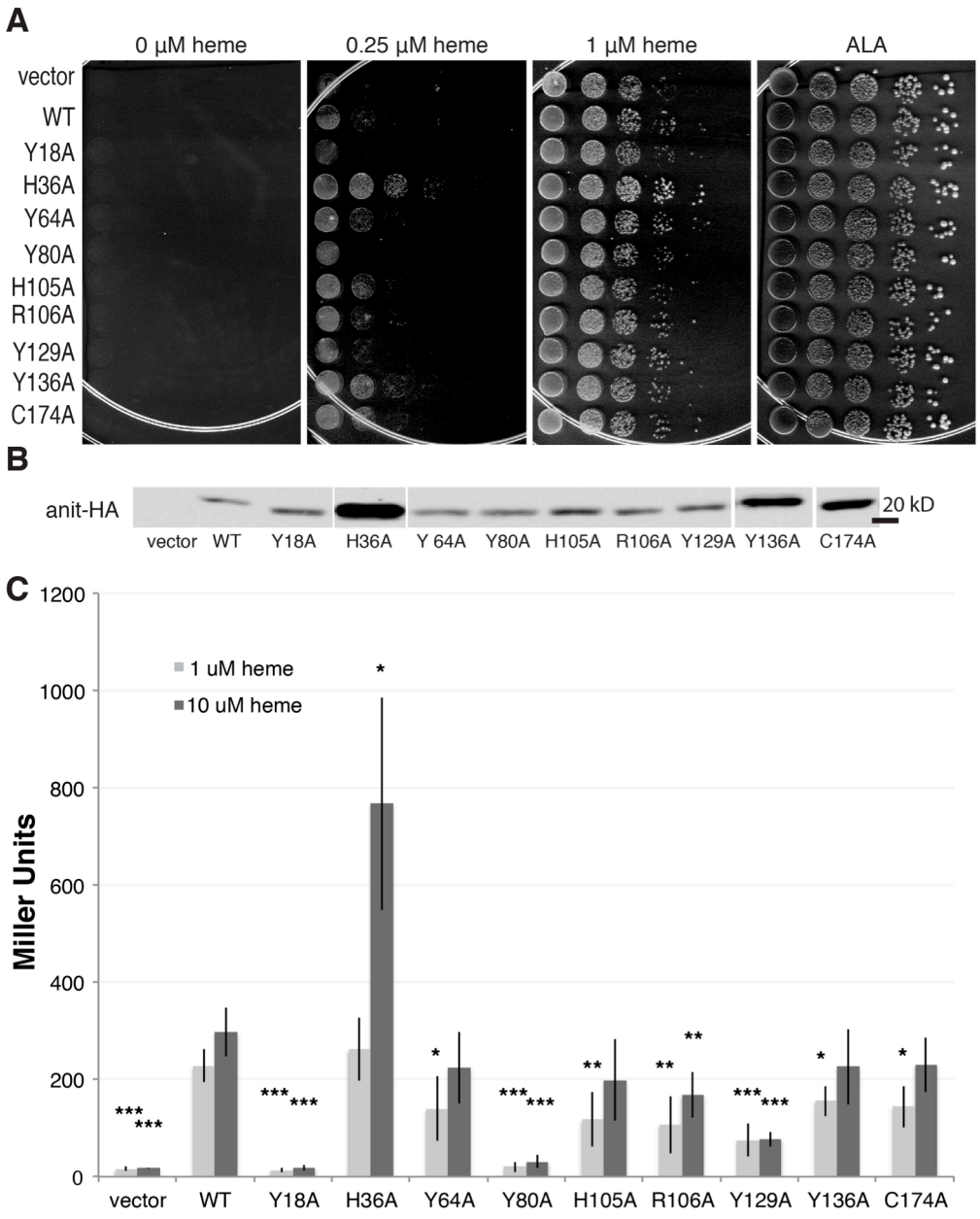

Figure 21 – Tyrosines 18, 80, & 129 are Important for LHR1 Function. **A**) Cells expressing LHR1, WT or mutant proteins, were serially diluted and spotted onto agar plates with varying concentrations of heme or 250 μM ALA and incubated at 30°C for 4 days and then imaged. Experiment was repeated 2-4 times with independent transformants. **B**) Western blot of *S. cerevisae* lysates transformed with LHR1, WT or mutant, grown in 10 μM heme. **C**) β-galactosidase reporter assay performed in yeast grown in either 1 or 10 μM hemin for 16 h. Experiment was repeated 5-8 times with independent transformants. *Student's *t*-test ** $p \leq 0.005$, ** $p \leq 0.01$, * $p \leq 0.05$ compared to WT.

Tyrosines 18, 80, & 129 are Not Required for Promastigote Growth in Complete Medium

Based on the results of the mutant screen performed in yeast, we selected four mutations, Y18A, H36A, Y80A, and Y129A, to characterize in *L. amazonensis*. Constructs contain WT *LHR1* and mutant *lhr1* were transformed into *L. amazonensis* Δ*lhr1/LHR1* (SKO) promastigotes and isolates were selected that had comparable expression levels (Figure 22 B). Multiple Y18A clonal isolates were tested, and all showed lower expression levels when compared to WT and the other mutants. SKO isolates expressing WT LHR1 or the mutant lhr1 proteins showed no growth defect in regular PGM (Figure 22 A).

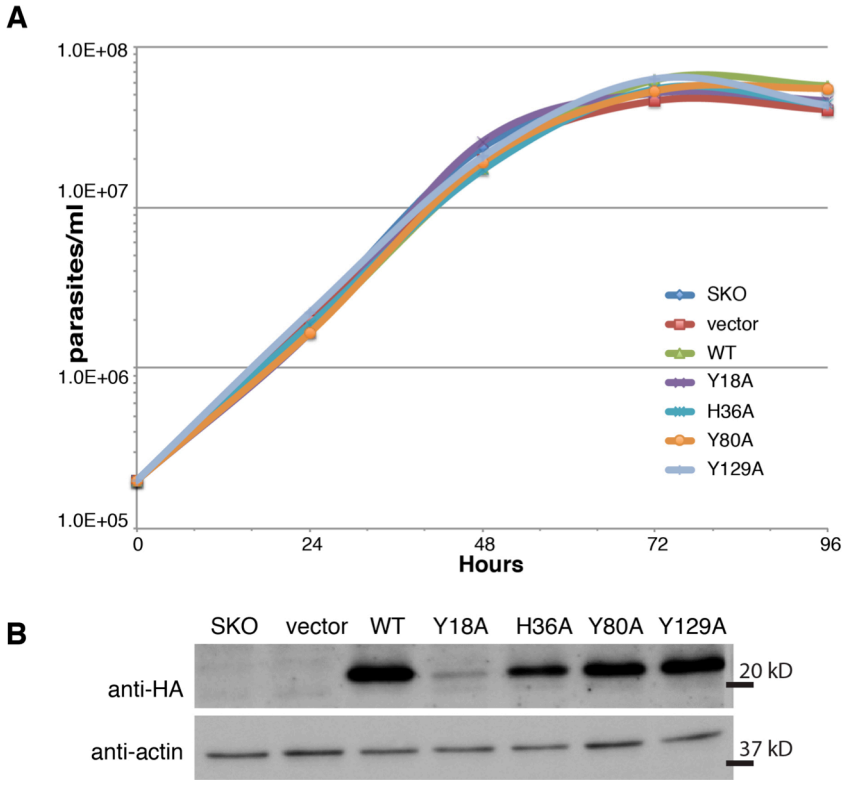

Figure 22 – Tyrosines 18, 80, & 129 are Not Required for Promastigote Growth but are Important for Heme Transport in *L. amazonensis*. **A**) Isolates were grown in regular PGM and growth followed over time. Experiment was repeated twice with consistent results. **B**) Western Blot showing expression levels of WT and mutant proteins in SKO background.

Tyrosines 18, 80, & 129 are Necessary for Virulence in Macrophage Infections

To this point we had investigated the role of the mutant LHR1 proteins in the promastigote form. To determine whether these mutations were important for growth of the intracellular amastigote form, bone marrow-derived macrophages (BMM) were infected with axenic amastigotes of heterozygous Δ*lhr1/LHR1* (SKO) *L. amazonensis* and SKO complemented with WT, Y18A, H36A, Y80A, or Y129A *lhr1* and intracellular parasites were quantified after 1, 36, and 72 hours post infection (Figure 23 A). Consistent with previous observations (84), SKO parasites fail to grow in BMMs but growth can be partially restored in parasites that episomally express LHR1, which undergoes two replication cycles by 72 h post infection. SKO parasites expressing Y18A, Y80A, and Y129A failed to rescue intracellular growth and don't complete one full replication cycle by 72 hours post infection. SKO parasites expressing H36A had growth comparable to the of SKO expressing WT and undergo one full replication cycle by 72 hours post infection (Figure 23 A,B). The growth defect in parasites expressing the Y18A mutant was comparable to the growth defect of SKO parasites without complementation, indicating that Y18A might be a non-functional protein or might not be expressed at levels high enough in order to observe its contribution over the background of the endogenous LHR1 in the SKO strain. On the other hand, Y80A and Y129A did not rescue growth to the same extent as WT but grew better than SKO, suggesting that Y80A and Y129A have decreased function when compared to WT LHR1, but are still functional proteins.

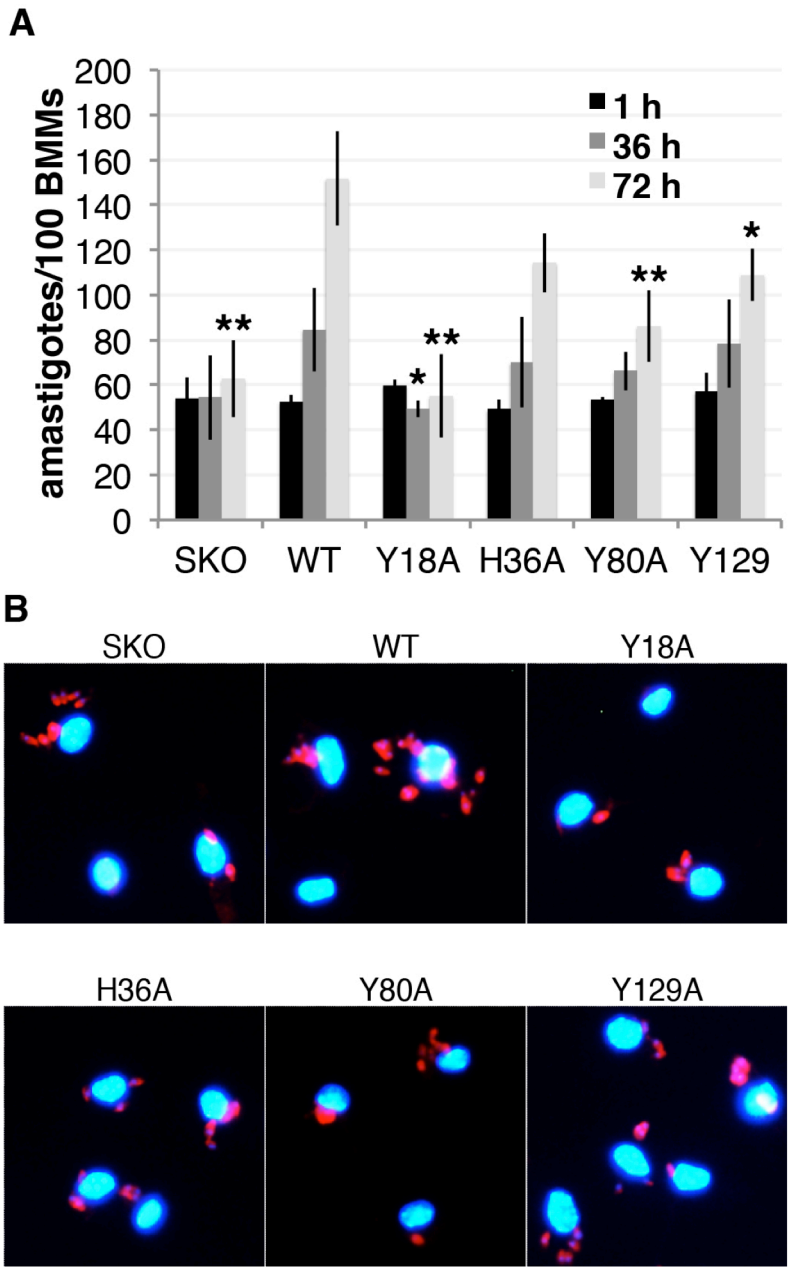

Figure 23 – Tyrosines 18, 80, & 129 are Necessary for Virulence in Macrophage Infections. A) SKO and SKO + WT/Y18A/H36A/Y80A/Y129A *LHR1*-HA were transformed into axenic amastigotes and used to infect BMMs from C57BL/6 mice; growth was followed over time. Assay was performed in triplicate and graph is representative of three experiments; * $p \leq 0.05$, ** $p \leq 0.01$; Student's *t*-test at 72 h: WT vs. SKO = 0.005, WT vs. Y18A = 0.004, WT vs. H36A = 0.06, WT vs. Y80A = 0.01, WT vs. Y129A = 0.04; at 36 h: WT vs. Y18A = 0.03 **B)** Immunofluorescence images of infected macrophages at 72 h; blue = DAPI, red = anti-*Leishmania (2)*.

Tyrosines 18, 80, & 129 are Essential for Virulence *in vivo*

To determine the effect of these mutations on *in vivo* infectivity, axenic amastigotes were injected in the left hind footpad of C57BL/6 mice and lesion development was followed over a 10-week period with parasites loads calculated at week 10. Consistent with previous observations (84), SKO parasites fail to form a lesion and have low parasite loads. SKO parasites complemented with WT LHR1 or H36A lhr1 were able to restore lesion development but not to wild type *L. amazonensis* levels (Figure 24 A,B) consistent with earlier findings (84). In agreement with the growth profiles observed in the macrophage infections, Y18A, Y80A, and Y129A all showed smaller lesion development and lower parasite loads when compared to WT LHR1 (Figure 24 A,B). Interestingly, Y18A had an even lower parasite load than SKO without complementation, suggesting that even at low expression levels this mutant is severely impacting the acquisition of heme, to an extent greater than would be expected if it was a non-functional protein.

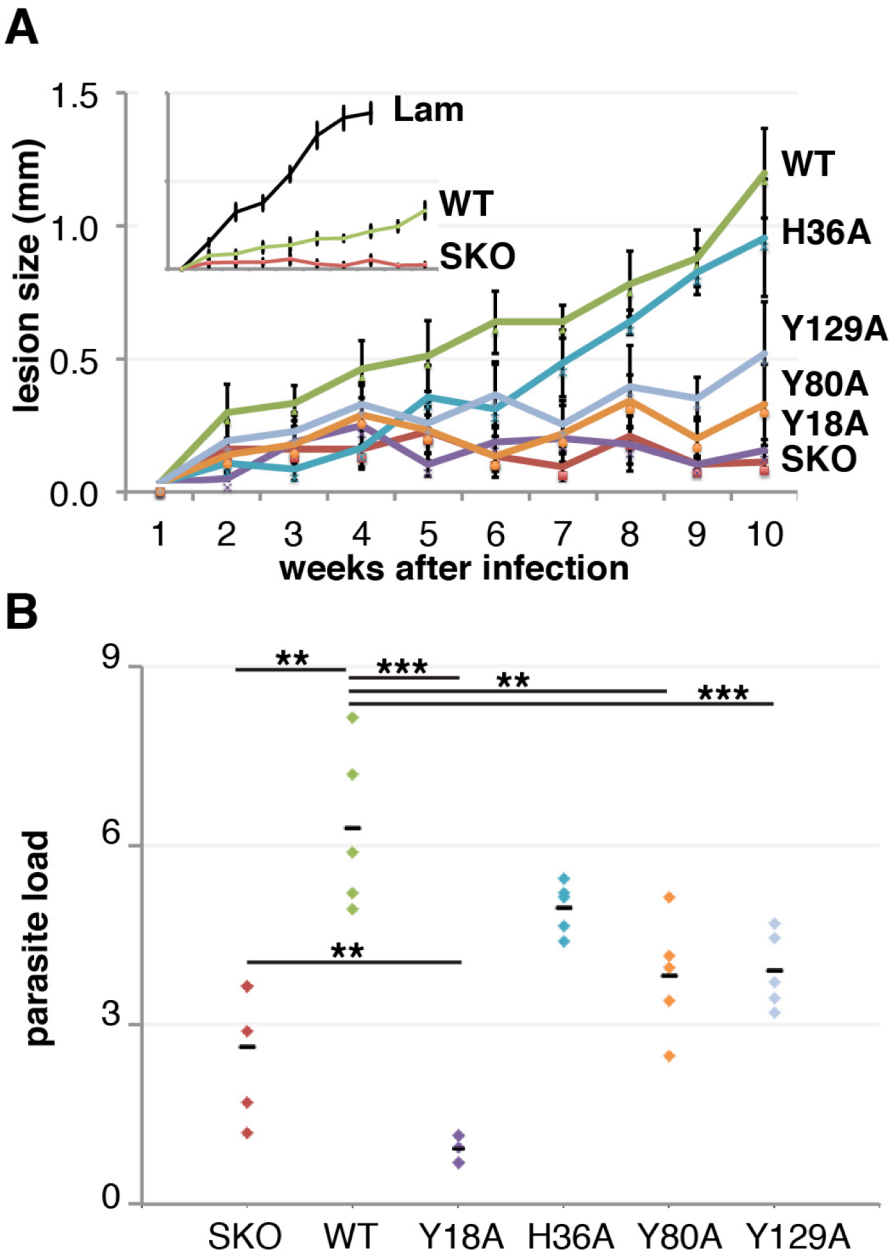

Figure 24 – Tyrosines 18, 80, & 129 are Essential for Virulence *in vivo*. **A**) Lesion growth over time of C57BL/6 mice infected with *L. amazonensis* (Lam), SKO, SKO+LHR1 (WT), SKO+Y18A (Y18A), SKO+H36A (H36A), SKO+Y80A (Y80A), or SKO+Y129A (Y129A). Inset shows the growth of Lam compared to SKO and WT; axes are the same as the large graph. Each group had 5 mice and experiment was performed once. **B**) Total parasite load isolated from lesions after 10 weeks of infection. Each group had five mice. Student's *t*-test values: WT vs. SKO = 0.002; WT vs. Y18A = 0.0005; WT vs. H36A = 0.07; WT vs. Y80A = 0.01; WT vs. Y129A = 0.008; SKO vs. Y18A = 0.01.

Conclusions/Discussion

A mutagenesis analysis of *L. amazonensis* LHR1 was performed in order to gain an understanding of the molecular mechanisms responsible for heme transport due to LHR1 in these parasites. Amino acid residues were selected for mutagenesis based on their alignment to residues known to be important for protein function in CeHRG-4 (62), their predicted interaction with heme, or their potential to form disulfide bonds. Four mutants of interest emerged from the yeast screen: three reduced heme transport function, Y18A, Y80A, and Y129A, and one appeared to increase heme uptake function, H36A (Figure 21). The expression level of H36A in the yeast assays was always consistently higher than all of the other mutant proteins, so we cannot rule out the possibility that the increase in function observed is due to more protein being present, and not an inherent change in the transporter caused by the mutation. These four mutant proteins were then expressed in *L. amazonensis* to verify the importance of these amino acids for LHR1 function in its native environment. None of the mutant proteins showed a phenotype in promastigote forms, but Y18A, Y80A, and Y129A all failed to rescue intracellular growth in BMM infections (Figure 23), and were important for *in vivo* footpad infection in mice with all three unable to rescue lesion growth or parasite loads to a comparable level to that of wild type LHR1 protein (Figure 24).

Histidines are known to be important in other heme transporters (62), and even though H36A had an interesting phenotype in the yeast screen, it failed to show a phenotype in *L. amazonensis* when its expression level was comparable to the other mutant proteins. Therefore, the apparent gain of function phenotype that was observed in the yeast assay was likely the result of the presence of more protein, and not an alteration

of LHR1 function. The histidine in LHR1 (His-105) homologous to the histidine known to be involved in CeHRG-4 function (His-108), showed no phenotype in the yeast screen (Figure 21). We mutated the other histidine in LHR1 (His-36) and it also did not show decreased function in the yeast. This result suggests that LHR1 does not employ histidines to form a complex with heme during transport, but instead utilizes alternative amino acids.

Tyrosines have been shown to coordinate with heme as well (167,168). Y18A consistently showed decreased function in yeast and *Leishmania* experiments; even though the expression levels were lower than the other mutant proteins examined in *Leishmania*, these low levels of expression were sufficient to give an intriguing result in the parasite load calculations in mouse infection experiments. Not only did Y18A fail to develop a lesion in mouse footpad infections, the parasite loads were lower than SKO; suggesting that Y18A may do more than render LHR1 non-functional because if Y18A was just non-functional it would be expected to have parasite loads similar to that of SKO. One interesting possibility, to be tested in future studies, is that the Y18A may have a dominant-negative effect, perhaps interfering with proper LHR1 oligomerization. Y80A and Y129A consistently decreased LHR1 function in both yeast and *Leishmania* assays. These tyrosine residues are located in transmembrane domains at positions where they could potentially coordinate with heme as it is transported across the membrane.

These findings are important because an understanding of heme acquisition in *Leishmania* is essential if therapeutics targeting this pathway are to be developed. New therapeutic drugs are urgently needed in order to combat these serious global human diseases. As stated earlier, *LHR1* is well conserved across the Trypanosomatidae family,

and acquisition of heme from the environment is essential for *Leishmania* survival. There are no known homologues of *LHR1* in humans, which decreases the possibility of off target effects if small molecule inhibitors to LHR1 can be developed.

With this study we have added to our understanding of the mechanisms involved in heme transport by the parasite *Leishmania*, but there is much that remains unknown. LHR1 is a small protein of only 175 amino acids with four predicted transmembrane domains that probably does not have the necessary size to form a transmembrane channel large enough to accommodate heme. We still do not know if LHR1 functions as a monomer or an oligomer and what the implications of that would be on our understanding of heme acquisition in these parasites. It would also be important to understand how LHR1 obtains the energy to transport heme against a concentration gradient. LHR1 doesn't contain any ATP-binding cassettes, but this doesn't rule out the possibility that heme transport by LHR1 could be ATP dependent, as heme transport may be coupled to an ATP-dependent process. There is some initial evidence that heme uptake in *T. cruzi* is dependent upon ATP (90), but whether this uptake observed in *T. cruzi* is due to the LHR1 homologue or to an alternative heme acquisition pathway via hemoglobin breakdown is unknown (91). Further research is necessary to have a comprehensive understanding of the role of LHR1 in heme acquisition in *Leishmania* and the other Trypanosomatidae family members, and how this protein might be exploited for generation of new treatments.

Chapter 5: Conclusions and Future Directions

The aim of this dissertation was to characterize *Leishmania* Heme Response 1 (LHR1) as a heme transporter and to gain an understanding of the molecular mechanisms responsible for heme transport. LHR1 is responsible for heme uptake in *L. amazonensis* and appears to bind heme in a pH independent manner, but transport heme more effectively in acidic pH (Chapter 2). *L. amazonensis* and *L. chagasi* differentially regulate *LHR1* and have different kinetics of ZnMP uptake after heme deprivation, which could be due to the differences in the 3′UTRs between the two species (Chapter 3). Three tyrosine residues, Tyr-18, Tyr-80, & Tyr-129, were found to be important in LHR1 function and due to their proximity to the cytoplasmic leaflet of the plasma membrane may play a direct role in heme binding and transport (Chapter 4).

There is a critical need for new therapeutics in the treatment of leishmaniasis, and a greater understanding of the basic biology of *Leishmania* is needed in order to develop safe and effective drugs. This dissertation provides evidence about how the heme transporter LHR1 functions, and adds to our understanding of *Leishmania* biology by providing insight into how these parasites acquire an essential nutrient, heme. This understanding of the molecular mechanisms involved in heme transport could provide a blueprint for development of novel therapies.

Even though there has been extensive research conducted on heme acquisition in *Leishmania*, many questions remain. We do not understand how LHR1 obtains the energy needed to transport heme across the membrane, as it is probably necessary to transport heme against a heme concentration gradient. The energy for heme transport could be provided by ATP or by an electrochemical gradient (169-171). There is

evidence that addition of ATP inhibitors reduces the total intracellular heme concentration in *T. cruzi* (90), but whether this reduction in intracellular heme is due to the inhibition of the LHR1 homologue is not known because *T. cruzi* can use hemoglobin as a heme source, and this pathway may be the one that is ATP-dependent (90,91,172). Since *Leishmania* appear to have two known pathways for acquiring heme, direct heme transport by LHR1 and hemoglobin breakdown followed by heme transport via LABCG5, it is necessary to develop a highly sensitive kinetic uptake assay to distinguish between these two pathways, to identify which is the major pathway for heme acquisition utilized by *Leishmania* promastigotes and amastigotes, and to identify the energy source(s) necessary for each pathway (54). Some evidence that LHR1 may be independent of ATP is that hHRG-1 has been shown to associate with the vacuolar H^+-ATPase (V-ATPase) proton pump, suggesting that a proton gradient generated via V-ATPases may drive heme transport for HRG-1-related proteins (62,63).

Another important aspect that needs to be clarified is if LHR1 is functioning as an oligomer and how oligomerization is mediated, in order to provide understanding on how heme transporters function at the molecular level and provide direction for drug development. Disruption of the potential oligomerization of LHR1 could interfere with heme transport, thus providing an additional target for drug development.

Our understanding of differences between visceral and cutaneous *Leishmania* species continues to be limited. It would be of interest to expand the investigation of the difference in heme acquisition between visceral and cutaneous species with a focus on how that differential acquisition is mediated. If heme acquisition is an important determinant in the ability of a species to visceralize, then it might be reflected in the

optimal heme concentration for growth of a visceral or cutaneous species, which has not been experimentally determined. An understanding of how LHR1 expression is regulated would also aid this avenue of investigation, and provide much needed understanding in the parasitology field of mechanisms of gene regulation in *Leishmania*.

LHR1 is essential for virulence and appears to be most important in intracellular amastigote forms, because that is where the most severe growth phenotype is observed (35,84). It would be useful to measure the total intracellular heme concentrations and the expression levels of LHR1 in intracellular and axenic amastigotes, for comparisons with what we know about the promastigote forms. It is also of interest to understand what role the tyrosine residues are playing in the function of LHR1. Based on their predicted position in the transmembrane domains near the cytoplasmic leaflet of the plasma membrane, we hypothesize that these tyrosines would be involved in coordinating with heme during the transport process and would not be directly involved in the initial binding of heme to LHR1. The evidence for the involvement of tyrosines in this process argues against the possibility that the tyrosine mutations interfered with proper folding and targeting of LHR1. There are other tyrosines in LHR1 that are located within transmembrane domains closer to the extracellular leaflet of the plasma membrane that could act as the initial coordinators of heme and then pass the heme through the transmembrane domain to the next set of coordinating tyrosines. There are two computer programs available for predicting if amino acid residues can interact with heme, HemeBIND and PSSMPP (173,174). We used HemeBIND (173), freely available on line at http://mleg.cse.sc.edu/hemeBIND, to predict which amino acid residues could interact with heme. The program predicted that 36% of the amino acid residues located

throughout LHR1 could interact with heme. Tyr-18 and Tyr-80 were predicted to interact with heme while His-36 and Tyr-129 were not likely to interact with heme. These programs could be useful in guiding future investigations to help identify the amino acids important for binding of heme and those important for transport.

This dissertation has provided evidence about the molecular mechanisms involved in heme acquisition via LHR1 in *L. amazonensis* and has presented data concerning differential heme acquisition in representative visceral and cutaneous species. Although further research is needed in order to understand the role of LHR1 in heme acquisition and parasite survival, these data establish a basis for further studies. There are LHR1 homologues present in many *Leishmania* and *Trypanosoma* species and a broad-spectrum therapeutic drug could have a large impact on global health and quality of life.

Materials & Methods

Parasite Cultures – L. amazonensis IFLA/BR/67/PH8 strain was provided by Dr. David Sacks (Laboratory of Parasitic Diseases, NIAID, NIH). *L. amazonensis* Δ*lhr1/LHR1* (SKO) was generated by Dr. Chau Huynh as described (35). *L. chagasi* Sau Paulo was provided by Dr. David Sacks. *L. amazonensis* parasites were cultured at 26°C in promastigote growth medium (PGM): M199 (Gibco BRL; Cat. #11825-015) pH 7.4 supplemented with 40 mM HEPES, 0.1 mM adenine, 0.00001% biotin, 0.0005% hemin (7.6 μM), 20 % heat-inactivated FBS, 5 mM L-Glutamine, and 5% penicillin-streptomycin. *L. chagasi* parasites were culture at 26°C in promastigote growth medium (LcPGM): M199 pH 6.8 supplemented with 25 mM HEPES, 4.2 mM sodium bicarbonate, 1X RPMI Vitamin Mix (Sigma; R7256), 23 μM folic acid, 100 μM adenosine, 10% heat-inactivated FBS, and 5% penicillin-streptomycin as described elsewhere (175).

Heme Depleted FBS - Heat-inactivated FBS was treated with 10 mM (+)-Sodium L-ascorbate (Sigma; Cat. # A-7631) overnight at room temperature, followed by three rounds of dialysis with PBS+/+ and filter-sterilization. Heme depletion was verified by measuring the optical absorbance at 405 nm (176).

Yeast Strains and Growth Media - The *Saccharomyces cerevisiae* strain Δ*hem1* (6D) strain was constructed as described elsewhere (92). Cells were maintained in YPD (yeast extract-peptone-dextrose) or appropriate synthetic complete (SC) media supplemented

with 250 μM δ-aminolevulinic acid hydrochloride (ALA) (Frontier Scientific; Cat. #A167).

Chapter 1

Radioactive Heme Uptake – Mid log promastigotes of *L. amazonensis* WT were grown O/N in regular of heme-depleted PGM. Parasites were washed and resuspended in binding buffer (HBSS without $Ca^{2+/}Mg^{2+}$, pH 5.5, 1% BSA) at 1.25 x 10^8 parasites/ml. 5 x 10^7 parasites were used for each time point in triplicate. ~200 pmol of ^{55}[Fe]-heme was added to the samples. Samples were incubated at 26 °C for the indicated time. Reaction was stopped by adding an equal volume of cold quench/wash buffer (HBSS pH 7.4, 5% BSA, 1 μM cold hemin chloride). Cells were washed twice with wash buffer and once with HBSS. Cells were hydrolyzed with 1 N NaOH at 50 °C, then placed into scintillation vials with scintillation fluid for counting. Samples were read on a Beckman LS 6500 Multipurpose Scintillation Counter. Counts were normalized to paired samples at 0 °C.

Chapter 2

Total Intracellular Heme Concentrations – Concentrations of heme were determined using the pyridine hemochrome method (177). 4 x 10^9 promastigotes growing in mid-log phase in regular promastigote growth medium were collected via centrifugation, counted, washed once with PBS, and resuspended in 1 ml 1 mM Tris-HCl pH 8.0 and sonicated twice for 2 min in an ice water bath with a Branson digital sonifier at 30% amplitude, in pulses of 2 sec interspaced with 2 sec of cooling. Aliquots of 840 μl were transferred to

13x100 mm glass tubes and 100 µl of 1 N NaOH was added followed by vortexing. After 2 min, 200 µl of pyridine (Sigma-Aldrich; Cat. # P57506) was added followed by vortexing. Samples were transferred to a 1 ml cuvette and a baseline absorbance spectrum between 500 and 600 nm was acquired. A few crystals of sodium hydrosulfite (2-3 mg) (Sigma-Aldrich; Cat. # 71699) were added to the samples and after 1 min the reduced hemochrome absorbance spectrum between 500 and 600 nm was acquired. Heme concentrations were then calculated based on the millimolar extinction coefficient of 20.7 using the difference in the absorption spectra at 557 nm (peak) and 541 nm (valley); [heme] mM = $(OD_{557nm} - OD_{541nm})/20.7$

ZnMP Uptake Assay in Yeast - pYes-DEST52-LHR1-HA and pYes-DEST52 (vector control) were transformed into the Δ*hem1* (6D) strain using the lithium acetate method (178). Transformants were selected on 2% w/v glucose SC (-Ura) plates supplemented with 250 µM ALA. Eight to ten colonies were picked and grown over night in YPD supplemented with 250 µM ALA and 40 mg/l adenine. The cells were resuspended in 2% w/v glucose SC (-Ura) supplemented with 250 µM ALA and 40 mg/l adenine and incubated at 30°C for 24 h. Cells were resuspended in 2% w/v raffinose SC (-Ura) supplemented with 250 µM ALA and 40 mg/l adenine and incubated at 30°C for 18 h to deplete of glucose. Cells were washed once with PBS and resuspended in 2% w/v galactose SC (-Ura) supplemented with 40 mg/l adenine and incubated over night at 30°C to deplete of heme and induce LHR1 expression. Cells were washed once with PBS+BSA (1 g/l), resuspended in PBS+BSA and placed at 30°C or 4°C for 20 min to equilibrate the temperature. ZnMP (Frontier Scientific; Cat. # M40628) was then added

from a stock of 10 mM in DMSO to a final concentration of 100 μM. Hemin (Frontier Scientific; Cat. # H651-9) was added to appropriate tubes from a stock of 10 mM in 0.3M ammonium hydroxide to a final concentration of 1000 μM. Cells were maintained at the respective temperatures with rotation until aliquots were taken at 20, 40, 60, and 90 min. Cells were washed twice with PBS+BSA at 4°C and placed in pre-chilled 5 ml BD Falcon FACS tubes on ice. 1 X 10^6 cells per sample were examined using a flow cytometer (BD FACSCanto, excitation at 488 nm and emission equal or greater than 670 nm) and data for 10,000 events were collected. Samples were gated at $10^{2.2}$ with left of the line considered negative and right of the line positive. Baseline fluorescence was considered to be the empty vector at 30°C with ZnMP and this baseline fluorescence value was subtracted from total values for each sample and plotted as % fluorescence vs. time. Experiment was repeated twice with consistent trends.

Potential Δlhr1/Δlhr1 PCR - Genomic DNA from potential Δ*lhr1*/Δ*lhr1* clones expressing [pXGSAT-*LHR1*-3xFLAG] that were resistant to hygromycin B (100 μg/ml), nourseothricin (50 μg/ml), and G418 (50 μg/ml) was isolated in TELT lysis buffer as previously described (179). PCR reactions were performed in a BioRad Thermocycler using OneTaq Hot Start DNA Polymerase (New England BioLabs) according to the manufacturer's instructions. PCR reactions were run on a 1% agarose gel using GelRed (Biotium) to detect presence of bands.

Primer Set	Forward Primer (5′ to 3′)	Reverse Primer (5′ to 3′)
Endogenous LHR1 (**LHR1**)	GGCGATCTACATAATATT CGCCCTGATC	CACCGCCTCTACCCAACT CACCTC
Hygromycin B phosphotransferase (**Hyg**)	GCCGATAGTGGAAACCGA CGCC	CACCGCCTCTACCCAACT CACCTC
Neomycin phosphotransferase (**Neo**)	CGCTCCCGATTCGCAGCG C	CACCGCCTCTACCCAACT CACCTC
Episomal LHR1-3xFLAG (**Flag**)	GGCGATCTACATAATATT CGCCCTGATC	CGATGTCATGATCTTTAT AATCACCGTCATGG

Radioactive Heme Uptake – Mid-log promastigotes of *L. amazonensis* WT or SKO were grown O/N in regular of heme-depleted PGM. Parasites were washed and resuspended in binding buffer (HBSS without $Ca^{2+/}Mg^{2+,}$ pH 5.5, 1% BSA) at 1.25 x 10^8 parasites/ml. 5 x 10^7 parasites were used for each time point in triplicate. ~200 pmol of ^{55}[Fe]-heme was added to each sample. Samples were incubated at 26 °C or 0 °C for 60 min. Reaction was stopped by adding an equal volume of cold quench/wash buffer (HBSS pH 7.4, 5% BSA, 1 μM cold hemin chloride). Cells were washed twice with wash buffer and once with HBSS. Cells were hydrolyzed with 1 N NaOH at 50 °C, then placed into scintillation vials with scintillation fluid for counting. Samples were read on a Beckman LS 6500 Multipurpose Scintillation Counter. Counts were normalized to paired samples at 0 °C.

Hemin Agarose Binding – Mid-log phase *L. amazonensis* [pXGSAT-*LHR1*-3XFLAG] grown in PGM were lysed with modified MS Buffer (210 mM mannitol, 70 mM sucrose, 0.5% NP-40, 25 mM MES/MOPS pH 5, 6, 7, or 8, 1X cOmplete protease inhibitor cocktail (Roche Cat. # 04693159001) at indicated pH values and passed through a 25 gauge needle. 50 µg of total protein was added to 120 µl (300 nmol) hemin-agarose (Sigma; Cat. # H6390) or Sepharose 4B (Sigma; Cat. # 4B200). Samples were incubated at room temperature with rotation for 30 min then washed well with wash buffer (150 mM NaCl, 1% NP-40, 25 mM MES/MOPS pH 5, 6, 7, or 8). Proteins were eluted from the beads with Thorner Sample Buffer and run on a 12% SDS-PAGE gel. Proteins were transferred to nitrocellulose membrane (BioRad; Cat. # 162-0115). Membranes were blocked with 5% milk, probed with anti-FLAG M2-HRP (Sigma; Cat. # A8592), developed with ECL (BioRad) and imaged on a FujiFilm LAS-3000 Imager. Densitometry analysis of bands was preformed using ImageJ. Percentage total protein bound was calculated by dividing the intensity of bound band by the input band (adjusted based on total protein loaded on gel).

Growth Spot Assay – Assay was performed as described previously (62) with some adaptation. Briefly, Δ*hem1* (6D) were transfected with pYES-DEST52-LHR1-HA, pYES-DEST52-CeHRG-4 or vector alone using the lithium acetate method. Transformants were selected on 2% glucose SC (-Ura) plates supplemented with 250 µM ALA. Five to seven colonies were picked and inoculated into 2% raffinose SC (-Ura) supplemented with 250 µM ALA and grown for 24 h at 30°C to deplete glucose and expand the culture. The glucose depleted cultures was sub-cultured in 2% raffinose SC (-

Ura) and grown O/N to deplete heme. Prior to spotting, cultures were resuspended in water to OD_{600} of 0.2 and ten-fold serial dilutions were performed and10 ul of each dilution was spotted onto 2% raffinose SC (-Ura) plates buffed with 50 mM MES/MOPS at pH 5 or 6 supplemented with either 0.4% glucose with 250 μM ALA (positive control) or 0.4% galactose with 1 μM hemin or no hemin as negative control. Plates were incubated at 30°C and imaged every day for five days.

^{55}[Fe]-Heme Binding and Uptake - Mid-log promastigotes of *L. amazonensis* WT were grown O/N in heme-depleted PGM. Parasites were washed and resuspended in binding buffer (HBSS without $Ca^{2+/}Mg^{2+}$, pH 5.4 or pH 7.4, 1% BSA) at 1.25 x 10^8 parasites/ml. 5 x 10^7 parasites were used for each condition in triplicate. ~200 pmol of ^{55}[Fe]-heme was added to each sample. Samples were incubated at 26 °C or 0 °C for 60 min. Reaction was stopped by adding an equal volume of cold quench/wash buffer (HBSS pH 7.4, 5% BSA, 1 μM cold hemin chloride). Cells were washed twice with wash buffer and once with HBSS. Cells were hydrolyzed with 1 N NaOH at 50 °C, then placed into scintillation vials with scintillation fluid for counting. Samples were read on a Beckman LS 6500 Multipurpose Scintillation Counter.

Chapter 3

RT-qPCR – Mid-log phase *L. chagasi* and *L. amazonensis* were grown for 24 h in regular or heme-depleted PGM. RNA was isolated from 1x10^8 parasites for each condition using Macherey-Nagel NucleoSpin RNA kit (ClonTech Cat. # 740955) according to the

manufacturer's instructions. 5 μg of RNA was used to generate cDNA using SuperScript III Reverse Transcriptase (Invitrogen; Cat. # 18080) according to the manufacturer's instructions. *LHR1* transcript levels were quantified using 1 μl of cDNA per reaction in triplicate with specific primer sets for *LHR1* and Ubiquitin Hydrolase (*UbH*) as the reference gene (see table below). Primer sets were validated to find the optimal annealing temperature and PCR Efficiency. Quantitative real time PCR was performed using PerfeCTa SYBR Green FastMix for iQ (Quanta Biosciences; Cat. # 95071) and the BioRad CFX96 Real-Time System C1000 Thermal Cycler (BioRad Laboratories) according to the manufacturer's instructions. The cycle threshold (Ct) values were determined and the $2^{-\Delta\Delta Ct}$ was determined for each condition (180).

Gene	Sense (5′ to 3′)	Antisense (5′ to 3′)
LHR1	GCATTAAGCATCGCCAGTCTTGGA	TTCCCTGAATCAATGAGGCCAAGC
UbH	AACGTGAACAACTGGATGTGCGTC	ATGGTACCAAGCTTGACACATGCC

ZnMP Uptake Assay in Leishmania – Mid-log cultures of *L. chagasi* and *L. amazonensis* were grown O/N in heme-depleted PGM. 10 μM ZnMP was added to each culture and cells were incubated at 26 °C. Aliquots from each culture were taken at 0, 1, and 3 h and imaged live on an UltraVIEW VoX Spinning Disk Confocal Imaging System (Perkin Elmer) equipped with an Electron Multiplier CCD Camera (C9100-50; Hamamatsu). Images were acquired under identical acquisition settings and processed using the Volocity software suite (PerkinElmer). Fluorescence intensity was measured for more than 160 individual parasites in each condition and time point and the Mean Fluorescence

Intensity was calculated per parasite. Experiment was repeated twice with consistent results.

Genomic Alignments – Genomic sequences for LmxM.24.2230 and LinJ.24.2320 plus the upstream and downstream genes (LmxM.24.2240 & LmxM.24.2220 for LmxM.24.2230 and LinJ.24.2330 & LinJ.24.2310 for LinJ.24.2320) were downloaded from TriTrypDB (http://tritrypdb.org). Sequences were aligned using Clustal Omega (http://www.ebi.ac.uk/Tools/msa/clustalo/).

Polyadenylation Site Identification - mRNA was isolated from $1x10^8$ parasites of mid-log *L. chagasi* and *L. amazonensis* using Macherey-Nagel NucleoSpin RNA kit (ClonTech Cat. # 740955) according to the manufacturer's instructions. The 3′ portion of *LHR1* mRNA was cloned following the 3′ RACE System for Rapid Amplification of cDNA Ends protocol (Invitrogen; Cat. # 18373-019) with an *LHR1* specific primer 5′ – AACCGCATTGCATACCAGAC – 3′. Fragments were cloned into pCR2.1-TOPO using the TOPO TA Cloning Kit (Invitrogen; Cat. # 45-0046). Plasmids were verified for insert and then sequenced.

Luciferase Reporter Assays – [pF4X1.4-SAT-LamUTRs-luc] was generated using the In-Fusion HD Cloning System (Clontech; Cat. # 639645). [pCR2.1-TOPO-LamLHR1r] (LamLHR1 5′UTR = from the end of the upstream gene to the start of LHR1 and the LamLHR1 3′UTR = from the end codon of LHR1 to the start of the downstream gene) was used as a template to amplify the plasmid backbone with the UTRs but without the

LHR1 gene using Platinum Taq DNA Polymerase High Fidelity (Invitrogen; Cat. # 11304) = linearize vector. The luciferase insert was amplified from pCR2.1-TOPO-luciferase using the primers below. [pCR2.1-TOPO-LamLHR1-luc] was then generated

Luciferase Insert primers	Linearized Vector Primers
TCCCTTTGACACTTCTCCATGGAAG ATGCC	GAAGTGTCAAAGGGAAAAGAAA
GTACACGAAGGTGCTCGGGCTACA ATTTGGAC	GAGCACCTTCGTGTACTCAC

using In-Fusion. pCR2.2-TOPO-LamUTRs-luc was digested with BglII and NotI and the insert gel purified and ligated into [pF4X1.4-SAT] that has been digested with BglII and NotI using T4 DNA Ligase (NEB; Cat. # M0202) according to the manufacturer's instructions. [pF4X1.4-SAT-LamUTRs-luc] was then transformed into *L. amazonensis* and clones resistant to 50 μg/ml nourseothricin were selected. *L. amazonensis* [pF4X1.4-SAT-LamUTRS-luc] was grown for 24h in either regular or heme-depleted PGM. $1x10^8$ parasites were washed with PBS and then luciferase activity was detected using Promega Luciferase Assay System (Promega; Cat. # E1500) according to the manufacturer's instructions. Luciferase activity was read using a SpectraMax $M5^e$ (Molecular Devices) plate reader.

RT-qPCR – Mid-log phase *L. amazonensis* [pF4X1.4-SAT-LamUTRs-luc] was grown in regular or heme-depleted PGM for 24 h. RNA was isolated from $1x10^8$ parasites for each condition using Macherey-Nagel NucleoSpin RNA kit (ClonTech Cat. # 740955) according to the manufacturer's instructions. 5 μg of RNA was used to generate cDNA using SuperScript III Reverse Transcriptase (Invitrogen; Cat. # 18080) according to the

manufacturer's instructions. Luciferase, *SAT1, LHR1,* and Ubiquitin Hydrolase (*UbH*) transcript levels were quantified using 1 µl of cDNA per reaction in triplicate with specific primer sets (see table below). Primer sets were validated to find the optimal annealing temperature and PCR efficiency. Quantitative real time PCR was performed using PerfeCTa SYBR Green FastMix for iQ (Quanta Biosciences; Cat. # 95071) and the BioRad CFX96 Real-Time System C1000 Thermal Cycler (BioRad Laboratories) according to the manufacturer's instructions. The cycle threshold (Ct) values were determined and the $2^{-\Delta\Delta Ct}$ was determined for each condition (180).

Gene	Sense (5′ to 3′)	Antisense (5′ to 3′)
Luc	ATTTATCGGAGTTGCAGTTGCGCC	AACAAACACTACGGTAGGCTGCGA
SAT1	TTCGATGTGCACCTATCCGACCAA	ATGAATGCGCCATAGCAAGCAGAG
LHR1	GCATTAAGCATCGCCAGTCTTGGA	TTCCCTGAATCAATGAGGCCAAGC
UbH	AACGTGAACAACTGGATGTGCGTC	ATGGTACCAAGCTTGACACATGCC

Chapter 4

Alignment – C. elegans HRG-4 was provided by Dr. Iqbal Hamza (University of Maryland, Animal Sciences), *L. amazonensis LHR1* sequence was performed in the Andrews' lab, *L. major* and *L. infantum LHR1* sequences were downloaded from TriTrypDB. Sequences were aligned using Clustal Omega (http://www.ebi.ac.uk/Tools/msa/clustalo/). Transmembrane domain predictions were performed using TMHMM (http://www.cbs.dtu.dk/services/TMHMM-2.0/).

Plasmid Constructs and Site-Directed Mutagenesis In Yeast – pYes-DEST52-LHR1-HA was constructed as described elsewhere (35). Site-directed mutagenesis was performed on pYes-DEST52-LHR1-HA using the QuikChange Site-Directed Mutagenesis protocol (Agilent Technologies; Cat. # 200518); see table below for the list of primers used.

Mutation	Forward Primer	Reverse Primer

Y18A	CCGCATTTGGTTGGCGATCG CCATAATATTCGCCCTGATC	GATCAGGGCGAATATTATGG CGATCGCCAACCAAATGCGG
H36A	TATTACTTTTTTGCTTTGTGG CCCAGAACTACTGGGCCTGTG	CACAGGCCCAGTAGTTCTGGG CCACAAAGCAAAAAAGTAATA
Y64A	GGCGACGCCGCAGG CCCGCCTGTACAAG	CTTGTACAGGCGGG CCTGCGGCGTCGCC
H80A	TGCAGCTTCAACCGCATTGCA GCCCAGACGTTCTTTCTTTG	CAAAGAAAGAACGTCTGGGCT GCAATGCGGTTGAAGCTGCA
H105A	GGCGAGGGGCATTAA GGCTCGCCAGTCTTGG	CCAAGACTGGCGACG CTTAATGCCCCTCGCC
R106A	GCGAGGGGCATTAAGCA TGCCCAGTCTTGGACAG	CTGTCCAAGACTGGGCA TGCTTAATGCCCCTCGC
Y129A	CGGCGAAGTGGAGCG CCATCGTGACGGTGC	GCACCGTCACGATGG CGCTCCACTTCGCCG
Y136A	TGACGGTGCCCATCG CCGAGCTCCGAGAGG	CCTCTCGGAGCTCGG CGATGGGCACCGTCA
C174A	GCGATGTCAAAGGAGAACG CTGCATACCCATACGACGT	ACGTCGTATGGGTATGCAG CGTTCTCCTTTGACATCGC

Growth Spot Assay – pYES-DEST52-LHR1-HA and pYES-DEST52-LHR1-HA-Y18A/H36A/Y64A/Y80A/H105A/R106A/Y129A/Y136A/C174A were transfected into Δ*hem1* (6D) using the lithium acetate method. Spotting of cultures was performed as described previously (62) with some adaptation. Briefly, transformants were selected on

2% glucose SC(-Ura) plates supplemented with 250 μM ALA. Five to seven colonies were picked and inoculated into 2% raffinose SC(-Ura) supplemented with 250 μM ALA and grown for 24 h at 30°C to deplete glucose and expand the culture. The glucose depleted culture was subcultured in 2% raffinose SC(-Ura) and grown O/N to deplete heme. Prior to spotting, cultures were resuspended in water to OD_{600} of 0.2 and ten-fold serial dilutions were performed. 10 ul of each dilution was spotted onto a 2% raffinose SC(-Ura) plate supplemented with either 0.4% glucose plus 250 μM ALA (positive control) or 0.4% galactose plus varying concentrations of hemin (no hemin added as negative control). Plates were incubated at 30°C and imaged every day for five days.

Immunoblotting – For yeast protein extractions, the cells were resuspended in breaking buffer (100 mM Tris-HCl pH 8, 1 mM dithiothreitol (DTT), 20 % glycerol) with 1X cOmplete protease inhibitor cocktail (Roche Cat. # 04693159001) and equal volume of 0.5 mm glass beads (Sigma Cat. # G8772). The cells were disrupted using a bead beater for 1 min, 3 times at 4°C. Cell lysates were collected and protein concentration measured using Bradford reagent (BioRad; Cat. # 500-0006). Equal amounts of protein were run on a 12% SDS-PAGE gel and then transferred to a nitrocellulose membrane (BioRad; Cat. #162-0115). Membranes were blocked with 5% milk, incubated with mouse anti-HA (Covance; Cat. # MMS-101P) at a 1:2,000 dilution for 2 h at room temperature, followed by HRP-conjugated donkey anti-mouse IgG (Jackson ImmunoResearch Labs; Cat. # 715-035-151) at a 1:10,000 dilution for 1 h at room temperature. Membranes were developed using ImmunoStar ECL (BioRad) and imaged using a FujiFilm LAS-3000.

For *L. amazonensis* protein extracts, cells were lysed in Thorner buffer and lysates were cleared by centrifugation at 15,000 rpm, 15 min, at 4°C. Total protein was quantified using a Pierce Modified Lowry Protein Assay Kit (ThermoScientific; Cat. # 23240) and equal amounts of protein were run on a 12% SDS-PAGE gel. Proteins were transferred to a nitrocellulose membrane (BioRad; Cat. #162-0115), blocked with 5% milk, and probed with mouse anti-HA (Covance; Cat. # MMS-101P) at 1:1,000 dilution for 2 h at room temperature followed by HRP-conjugated goat anti-mouse (BioRad; Cat. # 170-5047) at 1:20,000 dilution for 1 h at room temperature. Membranes were developed and imaged as described above.

β-Galactosidase Reporter Assay – pYES-DEST52-LHR1-HA was constructed as described elsewhere (35). pRS314m-CYC1-LacZ was constructed as described elsewhere (62). This assay was performed as described previously (35,62). Briefly, the plasmids for expression of LHR1 wild type or mutant proteins (pYES-DEST52-LHR1-HA or mutants) was co-transformed with the β-galactosidase reporter construct (pRS314m-CYC1-LacZ) into Δ*hem1* (6D) strain using the lithium acetate method and transformants were selected on 2% glucose SC(-Ura-Trp) supplemented with 250 μM ALA. Five to seven colonies were picked from the selection plates and inoculated into 2% raffinose SC(-Ura-Trp) supplemented with 250 μM ALA and grown for 24 h at 30°C to deplete glucose and expand the culture. The glucose depleted culture was subcultured in 2% raffinose SC(-Ura-Trp) and incubated O/N at 30°C to deplete heme. Heme depleted cultures were then used to inoculate 2% raffinose SC(-Ura-Trp) supplemented with either 0.4% glucose plus 250 μM ALA (positive control) or 0.4% galactose plus

varying concentrations of hemin (no hemin added for negative control) at an OD_{600} of 0.1 and incubated at 30°C, 250 rpm for 20 h. Cultures were then evaluated with the β-galactosidase assay as described elsewhere (181). β-galactosidase activities were normalized to protein concentration for direct comparison.

Leishmania Expression Plasmids – Cloning of *LHR1-HA* WT/Y18A/H36A/Y80A/ Y129A into *Leishmania* expression vector pXG-SAT (courtesy of Dr. S. Beverley, Washington University) was done using the In-Fusion HD Cloning System (Clontech; Cat. # 639645) following the manufacturer's instructions. Briefly pYES-DEST52-*LHR1-HA* (WT, Y18A, H36A, Y80A, & Y129A) plasmids were used to amplify the ORF using primers designed for In-Fusion Cloning. The PCR fragment was then sub-cloned into pXG-SAT that had been linearized by BamHI digestion using the In-Fusion system.

In-Fusion Cloning Forward	In-Fusion Cloning Reverse
TGTCCCCGGGGGATCCATG AACGAGTTGGAGCGCAA	ATCTGCTAGTGGATCCTTA AGCGTAGTCTGGGACGT

Leishmania Transfections – pXGSAT-LHR1-HA WT/Y18A/H36A/Y80A/Y129A were transfected into *L. amazonensis* Δ*lhr1/LHR1* as previously described (182). Parasites resistant to 50 μg/ml nourseothricin were selected and screened for expression using immunoblotting.

Leishmania Growth Curves – L. amazonensis Δ*lhr1/LHR1* (SKO), Δ*lhr1/LHR1 + LHR1,* Δ*lhr1/LHR1 + LHR1*-Y18A*,* Δ*lhr1/LHR1 + LHR1*-H36A*,* Δ*lhr1/LHR1 + LHR1-*

Y80A,and Δ*lhr1/LHR1* + *LHR1*-Y129A were seeded at $2x10^5$ parasites/ml in PGM and growth was monitored by counting using a hemocytometer over a 96h time period.

Macrophage Infections - C57BL/6 mouse bone marrow macrophages (BMM) were obtained as previously described (183). Approximately $1x10^6$ BMM were plated on glass coverslips that had been placed in a 6-well plate using RPMI medium (Invitrogen/Gibco; Cat. # 11875-119) supplemented with 20% endotoxin-free FBS, 1% penicillin/streptomycin, 2 mM L-glutamine, 50 ng/ml human recombinant human macrophage colony-stimulating factor (M-CSF) (PeproTech; Cat. # 300-25) and incubated for 24 h at 37°C, 5% CO_2. BMMs were infected using axenic amastigotes at a ratio of 2 parasites per BMM for 4 h at 34°C. The cells were washed 3 times with PBS and incubated for 1, 36, and 72 h at 34°C. Coverslips were then fixed in 4% paraformaldehyde and permeabilized with 0.1% Triton X-100 for 10 min. BMM and *Leishmania* DNA were stained with 10 mg/ml DAPI (4',6-diamidino-2-phenylindole) for 1 h, then coverslips washed with PBS and mounted using ProLong Gold Antifade Mountant (LifeTechnologies; Cat. # P36934). The number of intracellular parasites was determined by counting the total macrophages and the total intracellular parasites per microscopic field using a Nikon E200 epifluorescence microscope. Counts were performed in triplicate for each period of infection. The number of amastigotes was divided by the number of macrophages and multiplied by 100 to obtain number of amastigotes per 100 BMM.

Immunofluorescence – Infected BMM were fixed with 4% paraformaldehyde, quenched with 15 mM NH_4Cl, and permeabilized with 0.1% Triton X-100. Coverslips were washed with PBS and blocked with 3% Bovine Serum Albumin (BSA). For parasite staining, coverslips were incubated with mouse polyclonal antibodies prepared using *L. amazonensis* axenic amastigotes (2), followed by Alexa Fluor 546 goat anti-mouse IgG (H+L) (Molecular Probes; Cat. # A-11003) at 1:1000 dilution. Coverslips were washed with PBS and stained with 10mg/ml DAPI and then mounted with ProLong Gold Antifade Mountant (LifeTechnologies; Cat. # P36934). Images were acquired using a Nikon E200 epifluorescence microscope equipped with a Nikon Digital Sight-Fi1 camera using a 100X objective. Images were processed using Volocity software suite (PerkinElmer).

Mouse Infections - Six-week-old female C57BL/6 mice (n = 5 per group) were inoculated with $1x10^6$ axenic amastigotes of wild-type (Lam), Δ*lhr1/LHR1* (SKO), Δ*lhr1/LHR1 + LHR1-HA,* Δ*lhr1/LHR1 + LHR1-HA-Y18A,* Δ*lhr1/LHR1 + LHR1-HA-H36A,* Δ*lhr1/LHR1 + LHR1-HA-Y80A,* Δ*lhr1/LHR1 + LHR1-HA-Y129A L. amazonensis* in the left hind footpad in a volume of 50 µl sterile PBS. Lesion progression was monitored once a week by measuring the left and right hind footpads with a caliper (Mitutoyo Corp., Japan). The parasite burden recovered from the infected tissue was determined after 10 weeks by limiting dilution (184). The Institutional Animal Care and Use Committee at the University of Maryland approved the animal study protocol.

References

1. Kaye, P., and Scott, P. (2011) Leishmaniasis: complexity at the host-pathogen interface. *Nat Rev Microbiol* **9**, 604-615

2. Cortez, M., Huynh, C., Fernandes, M. C., Kennedy, K. A., Aderem, A., and Andrews, N. W. (2011) Leishmania promotes its own virulence by inducing expression of the host immune inhibitory ligand CD200. *Cell Host Microbe* **9**, 463-471

3. Cunningham, D. (1903) On the Presence of Peculiar Parasitic Organisms in the Tissue of a Specimen of Delhi Boil. *Scientific Memoirs by Medical Officers of the Army of India* **1**, 21-31

4. Wright, J. H. (1903) Protozoa in a Case of Tropical Ulcer ("Delhi Sore"). *J Med Res* **10**, 472-482.477

5. Hoare, C. A. (1938) Early Discoveries Regarding the Parasites of Oriental Sore. *Transactions of the Royal Society of Tropical Medicine and Hygiene* **32**, 66-92

6. Leishman, W. B. (1903) On The Possibility of the Occurrence of Trypanosomiasis in India. *British Medical Journal*, 1252-1254

7. Donovan, C. (1903) The Etiology of one of the Heterogeneous Fevers of India. *British Medical Journal*, 1903

8. Cox, F. E. (2002) History of human parasitology. *Clin Microbiol Rev* **15**, 595-612

9. Ueno, N., and Wilson, M. E. (2012) Receptor-mediated phagocytosis of Leishmania: implications for intracellular survival. *Trends Parasitol* **28**, 335-344

10. Alvar, J., Vélez, I. D., Bern, C., Herrero, M., Desjeux, P., Cano, J., Jannin, J., den Boer, M., and Team, W. L. C. (2012) Leishmaniasis worldwide and global estimates of its incidence. *PLoS One* **7**, e35671

11. WHO. (2014) Leishmaniasis.

12. WHO. (2014) Global Health Observatory Data Repository, Neglected Tropical Diseases: Leishmaniasis.

13. Freitas-Junior, L. H., Chatelain, E., Kim, H. A., and Siqueira-Neto, J. L. (2012) Visceral leishmaniasis treatment: What do we have, what do we need and how to deliver it? *Int J Parasitol Drugs Drug Resist* **2**, 11-19

14. Croft, S. L., and Olliaro, P. (2011) Leishmaniasis chemotherapy--challenges and opportunities. *Clin Microbiol Infect* **17**, 1478-1483

15. Mohapatra, S. (2014) Drug resistance in leishmaniasis: Newer developments. *Trop Parasitol* **4**, 4-9

16. Naderer, T., and McConville, M. J. (2011) Intracellular growth and pathogenesis of Leishmania parasites. *Essays Biochem* **51**, 81-95

17. Taylor, M. C., and Kelly, J. M. (2010) Iron metabolism in trypanosomatids, and its crucial role in infection. *Parasitology* **137**, 899-917

18. Cassat, J. E., and Skaar, E. P. (2013) Iron in infection and immunity. *Cell Host Microbe* **13**, 509-519

19. Blackwell, J. M., Goswami, T., Evans, C. A., Sibthorpe, D., Papo, N., White, J. K., Searle, S., Miller, E. N., Peacock, C. S., Mohammed, H., and Ibrahim, M. (2001) SLC11A1 (formerly NRAMP1) and disease resistance. *Cell Microbiol* **3**, 773-784

20. Roach, T. I., Kiderlen, A. F., and Blackwell, J. M. (1991) Role of Inorganic Nitrogen Oxides and Tumor Necrosis Factor Alpha in Killing *Leishmania donovani* Amastigotes in Gamma Interferon-Lipopolysaccharide-Activated Macrophages from Lsh^S and Lsh^r Congenic Mouse Strains. *Infection and Immunity* **59**, 3935-3944

21. Cellier, M., Courville, P., and Campion, C. (2007) Nramp1 phagocyte intracellular metal withdrawal defense. *Microbes and Infection* **9**, 1662-1670

22. Das, N. K., Biswas, S., Solanki, S., and Mukhopadhyay, C. K. (2009) Leishmania donovani depletes labile iron pool to exploit iron uptake capacity of macrophage for its intracellular growth. *Cell Microbiol* **11**, 83-94

23. Ben-Othman, R., Flannery, A. R., Miguel, D. C., Ward, D. M., Kaplan, J., and Andrews, N. W. (2014) Leishmania-mediated inhibition of iron export promotes parasite replication in macrophages. *PLoS Pathog* **10**, e1003901

24. Knutson, M., and Wessling-Resnick, M. (2003) Iron metabolism in the reticuloendothelial system. *Crit Rev Biochem Mol Biol* **38**, 61-88

25. White, C., Yuan, X., Schmidt, P. J., Bresciani, E., Samuel, T. K., Campagna, D., Hall, C., Bishop, K., Calicchio, M. L., Lapierre, A., Ward, D. M., Liu, P., Fleming, M. D., and Hamza, I. (2013) HRG1 is essential for heme transport from the phagolysosome of macrophages during erythrophagocytosis. *Cell Metab* **17**, 261-270

26. Donovan, A., Lima, C. A., Pinkus, J. L., Pinkus, G. S., Zon, L. I., Robine, S., and Andrews, N. C. (2005) The iron exporter ferroportin/Slc40a1 is essential for iron homeostasis. *Cell Metab* **1**, 191-200

27. Hentze, M. W., Muckenthaler, M. U., Galy, B., and Camaschella, C. (2010) Two to tango: regulation of Mammalian iron metabolism. *Cell* **142**, 24-38

28. Huynh, C., Sacks, D. L., and Andrews, N. W. (2006) A Leishmania amazonensis ZIP family iron transporter is essential for parasite replication within macrophage phagolysosomes. *The Journal of experimental medicine* **203**, 2363-2375

29. Flannery, A. R., Huynh, C., Mittra, B., Mortara, R. A., and Andrews, N. W. (2011) LFR1 ferric iron reductase of Leishmania amazonensis is essential for the generation of infective parasite forms. *J Biol Chem* **286**, 23266-23279

30. Jacques, I., Andrews, N. W., and Huynh, C. (2010) Functional characterization of LIT1, the Leishmania amazonensis ferrous iron transporter. *Mol Biochem Parasitol* **170**, 28-36

31. Flannery, A. R., Renberg, R. L., and Andrews, N. W. (2013) Pathways of iron acquisition and utilization in Leishmania. *Curr Opin Microbiol* **16**, 716-721

32. Chang, C. S., and Chang, K. P. (1985) Heme requirement and acquisition by extracellular and intracellular stages of Leishmania mexicana amazonensis. *Molecular and biochemical parasitology* **16**, 267-276

33. Campos-Salinas, J., Cabello-Donayre, M., García-Hernández, R., Pérez-Victoria, I., Castanys, S., Gamarro, F., and Pérez-Victoria, J. M. (2011) A new ATP-binding cassette protein is involved in intracellular haem trafficking in Leishmania. *Mol Microbiol* **79**, 1430-1444

34. Carvalho, S., Cruz, T., Santarém, N., Castro, H., Costa, V., and Tomás, A. M. (2009) Heme as a source of iron to Leishmania infantum amastigotes. *Acta Trop* **109**, 131-135

35. Huynh, C., Yuan, X., Miguel, D. C., Renberg, R. L., Protchenko, O., Philpott, C. C., Hamza, I., and Andrews, N. W. (2012) Heme uptake by Leishmania amazonensis is mediated by the transmembrane protein LHR1. *PLoS Pathog* **8**, e1002795

36. Severance, S., and Hamza, I. (2009) Trafficking of heme and porphyrins in metazoa. *Chem Rev* **109**, 4596-4616

37. Ajioka, R. S., Phillips, J. D., and Kushner, J. P. (2006) Biosynthesis of heme in mammals. *Biochim Biophys Acta* **1763**, 723-736

38. Yuan, X., Fleming, M. D., and Hamza, I. (2013) Heme transport and erythropoiesis. *Curr Opin Chem Biol* **17**, 204-211

39. Chiabrando, D., Vinchi, F., Fiorito, V., Mercurio, S., and Tolosano, E. (2014) Heme in pathophysiology: a matter of scavenging, metabolism and trafficking across cell membranes. *Front Pharmacol* **5**, 61

40. Kumar, S., and Bandyopadhyay, U. (2005) Free heme toxicity and its detoxification systems in human. *Toxicol Lett* **157**, 175-188

41. Chang, K. P., Chang, C. S., and Sassa, S. (1975) Heme biosynthesis in bacterium-protozoon symbioses: enzymic defects in host hemoflagellates and complemental role of their intracellular symbiotes. *Proc Natl Acad Sci U S A* **72**, 2979-2983

42. Ivens, A. C., Peacock, C. S., Worthey, E. A., Murphy, L., Aggarwal, G., Berriman, M., Sisk, E., Rajandream, M. A., Adlem, E., Aert, R., Anupama, A., Apostolou, Z., Attipoe, P., Bason, N., Bauser, C., Beck, A., Beverley, S. M., Bianchettin, G., Borzym, K., Bothe, G., Bruschi, C. V., Collins, M., Cadag, E., Ciarloni, L., Clayton, C., Coulson, R. M., Cronin, A., Cruz, A. K., Davies, R. M., De Gaudenzi, J., Dobson, D. E., Duesterhoeft, A., Fazelina, G., Fosker, N., Frasch, A. C., Fraser, A., Fuchs, M., Gabel, C., Goble, A., Goffeau, A., Harris, D., Hertz-Fowler, C., Hilbert, H., Horn, D., Huang, Y., Klages, S., Knights, A., Kube, M., Larke, N., Litvin, L., Lord, A., Louie, T., Marra, M., Masuy, D., Matthews, K., Michaeli, S., Mottram, J. C., Müller-Auer, S., Munden, H., Nelson, S., Norbertczak, H., Oliver, K., O'neil, S., Pentony, M., Pohl, T. M., Price, C., Purnelle, B., Quail, M. A., Rabbinowitsch, E., Reinhardt, R., Rieger, M., Rinta, J., Robben, J., Robertson, L., Ruiz, J. C., Rutter, S., Saunders, D., Schäfer, M., Schein, J., Schwartz, D. C., Seeger, K., Seyler, A., Sharp, S., Shin, H., Sivam, D., Squares, R., Squares, S., Tosato, V., Vogt, C., Volckaert, G., Wambutt, R., Warren, T., Wedler, H., Woodward, J., Zhou, S., Zimmermann, W., Smith, D. F., Blackwell, J. M., Stuart, K. D., Barrell, B., and Myler, P. J. (2005) The genome of the kinetoplastid parasite, Leishmania major. *Science* **309**, 436-442

43. Rastrojo, A., Carrasco-Ramiro, F., Martín, D., Crespillo, A., Reguera, R. M., Aguado, B., and Requena, J. M. (2013) The transcriptome of Leishmania major in the axenic promastigote stage: transcript annotation and relative expression levels by RNA-seq. *BMC Genomics* **14**, 223

44. Zwerschke, D., Karrie, S., Jahn, D., and Jahn, M. (2014) Leishmania major Possesses a Unique HemG-type Protoporphyrinogen IX Oxidase. *Biosci Rep*

45. Phillips, J. D., Whitby, F. G., Warby, C. A., Labbe, P., Yang, C., Pflugrath, J. W., Ferrara, J. D., Robinson, H., Kushner, J. P., and Hill, C. P. (2004) Crystal structure of the oxygen-dependant coproporphyrinogen oxidase (Hem13p) of Saccharomyces cerevisiae. *J Biol Chem* **279**, 38960-38968

46. Gaughan, P. L. Z., and Krassner, S. M. (1971) Hemin Deprivation in Culture Stages of the Hemoflagellate, *Leishmania tarentolae*. *Comparative Biochemistry and Physiology* **39**, 5-&

47. Alves, J. M., Voegtly, L., Matveyev, A. V., Lara, A. M., da Silva, F. M., Serrano, M. G., Buck, G. A., Teixeira, M. M., and Camargo, E. P. (2011) Identification and phylogenetic analysis of heme synthesis genes in trypanosomatids and their bacterial endosymbionts. *PLoS One* **6**, e23518

48. Opperdoes, F. R., and Coombs, G. H. (2007) Metabolism of Leishmania: proven and predicted. *Trends Parasitol* **23**, 149-158

49. Sah, J. F., Ito, H., Kolli, B. K., Peterson, D. A., Sassa, S., and Chang, K. P. (2002) Genetic rescue of Leishmania deficiency in porphyrin biosynthesis creates mutants suitable for analysis of cellular events in uroporphyria and for photodynamic therapy. *J Biol Chem* **277**, 14902-14909

50. Korený, L., Lukes, J., and Oborník, M. (2010) Evolution of the haem synthetic pathway in kinetoplastid flagellates: an essential pathway that is not essential after all? *Int J Parasitol* **40**, 149-156

51. Tripodi, K. E., Menendez Bravo, S. M., and Cricco, J. A. (2011) Role of heme and heme-proteins in trypanosomatid essential metabolic pathways. *Enzyme Res* **2011**, 873230

52. Hutner, S. H., Bacchi, C.J., and Baker, H. (1979) Nutrition of the kinetoplastida. in *Biology of the Kinetoplastida* (Lumsden, W. H. R. a. E., D.A. ed.), Academic Press, London. pp 664-691

53. Galbraith, R. A., and McElrath, M. J. (1988) Heme binding to Leishmania mexicana amazonensis. *Molecular and biochemical parasitology* **29**, 47-53

54. Campos-Salinas, J., Cabello-Donayre, M., García-Hernández, R., Pérez-Victoria, I., Castanys, S., Gamarro, F., and Pérez-Victoria, J. M. (2011) A new ATP-binding cassette protein is involved in intracellular haem trafficking in Leishmania. *Mol Microbiol*

55. Worthington, M., Cohn, S., Miller, S., Luo, R., and Berg, C. (2001) Characterization of a human plasma membrane heme transporter in intestinal and hepatocyte cell lines. *American Journal of Physiology-Gastrointestinal and Liver Physiology* **280**, G1172-G1177

56. Chiabrando, D., Mercurio, S., and Tolosano, E. (2014) Heme and erythropoieis: more than a structural role. *Haematologica* **99**, 973-983

57. Shayeghi, M., Latunde-Dada, G., Oakhill, J., Laftah, A., Takeuchi, K., Halliday, N., Khan, Y., Warley, A., McCann, F., Hider, R., Frazer, D., Anderson, G., Vulpe, C., Simpson, R., and McKie, A. (2005) Identification of an intestinal heme transporter. *Cell* **122**, 789-801

58. Qiu, A., Jansen, M., Sakaris, A., Min, S., Chattopadhyay, S., Tsai, E., Sandoval, C., Zhao, R., Akabas, M., and Goldman, I. (2006) Identification of an intestinal folate transporter and the molecular basis for hereditary folate malabsorption. *Cell* **127**, 917-928

59. Laftah, A., Latunde-Dada, G., Fakih, S., Hider, R., Simpson, R., and Mckie, A. (2009) Haem and folate transport by proton-coupled folate transporter/haem carrier protein 1 (SLC46A1). *British Journal of Nutrition* **101**, 1150-1156

60. Le Blanc, S., Garrick, M. D., and Arredondo, M. (2012) Heme carrier protein 1 transports heme and is involved in heme-Fe metabolism. *Am J Physiol Cell Physiol* **302**, C1780-1785

61. Rajagopal, A., Rao, A. U., Amigo, J., Tian, M., Upadhyay, S. K., Hall, C., Uhm, S., Mathew, M. K., Fleming, M. D., Paw, B. H., Krause, M., and Hamza, I. (2008) Haem homeostasis is regulated by the conserved and concerted functions of HRG-1 proteins. *Nature* **453**, 1127-1131

62. Yuan, X., Protchenko, O., Philpott, C. C., and Hamza, I. (2012) Topologically conserved residues direct heme transport in HRG-1-related proteins. *J Biol Chem* **287**, 4914-4924

63. O'Callaghan, K., Ayllon, V., O'Keeffe, J., Wang, Y., Cox, O., Loughran, G., Forgac, M., and O'Connor, R. (2010) Heme-binding Protein HRG-1 Is Induced by Insulin-like Growth Factor I and Associates with the Vacuolar H+-ATPase to Control Endosomal pH and Receptor Trafficking. *Journal of Biological Chemistry* **285**, 381-391

64. Yanatori, I., Tabuchi, M., Kawai, Y., Yasui, Y., Akagi, R., and Kishi, F. (2010) Heme and non-heme iron transporters in non-polarized and polarized cells. *BMC Cell Biol* **11**, 39

65. Delaby, C., Rondeau, C., Pouzet, C., Willemetz, A., Pilard, N., Desjardins, M., and Canonne-Hergaux, F. (2012) Subcellular localization of iron and heme metabolism related proteins at early stages of erythrophagocytosis. *PLoS One* **7**, e42199

66. Duffy, S., Shing, J., Saraon, P., Berger, L., Eiden, M., Wilde, A., and Tailor, C. (2010) The Fowler Syndrome-Associated Protein FLVCR2 Is an Importer of Heme. *Molecular and Cellular Biology* **30**, 5318-5324

67. Khan, A., and Quigley, J. (2013) Heme and FLVCR-related transporter families SLC48 and SLC49. *Molecular Aspects of Medicine* **34**, 669-682

68. Meyer, E., Ricketts, C., Morgan, N. V., Morris, M. R., Pasha, S., Tee, L. J., Rahman, F., Bazin, A., Bessières, B., Déchelotte, P., Yacoubi, M. T., Al-Adnani, M., Marton, T., Tannahill, D., Trembath, R. C., Fallet-Bianco, C., Cox, P., Williams, D., and Maher, E. R. (2010) Mutations in FLVCR2 are associated with proliferative vasculopathy and hydranencephaly-hydrocephaly syndrome (Fowler syndrome). *Am J Hum Genet* **86**, 471-478

69. Quigley, J., Yang, Z., Worthington, M., Phillips, J., Sabo, K., Sabath, D., Berg, C., Sassa, S., Wood, B., and Abkowitz, J. (2004) Identification of a human heme exporter that is essential for erythropoiesis. *Cell* **118**, 757-766

70. Yang, Z., Philips, J., Doty, R., Giraudi, P., Ostrow, J., Tiribelli, C., Smith, A., and Abkowitz, J. (2010) Kinetics and Specificity of Feline Leukemia Virus Subgroup C Receptor (FLVCR) Export Function and Its Dependence on Hemopexin. *Journal of Biological Chemistry* **285**, 28874-28882

71. Chiabrando, D., Marro, S., Mercurio, S., Giorgi, C., Petrillo, S., Vinchi, F., Fiorito, V., Fagoonee, S., Camporeale, A., Turco, E., Merlo, G. R., Silengo, L., Altruda, F., Pinton, P., and Tolosano, E. (2012) The mitochondrial heme exporter FLVCR1b mediates erythroid differentiation. *J Clin Invest* **122**, 4569-4579

72. Krishnamurthy, P., Ross, D., Nakanishi, T., Bailey-Dell, K., Zhou, S., Mercer, K., Sarkadi, B., Sorrentino, B., and Schuetz, J. (2004) The stem cell marker Bcrp/ABCG2 enhances hypoxic cell survival through interactions with heme. *Journal of Biological Chemistry* **279**, 24218-24225

73. Desuzinges-Mandon, E., Arnaud, O., Martinez, L., Huche, F., Di Pietro, A., and Falson, P. (2010) ABCG2 Transports and Transfers Heme to Albumin through Its Large Extracellular Loop. *Journal of Biological Chemistry* **285**, 33123-33133

74. Krishnamurthy, P. C., Du, G., Fukuda, Y., Sun, D., Sampath, J., Mercer, K. E., Wang, J., Sosa-Pineda, B., Murti, K. G., and Schuetz, J. D. (2006) Identification of a mammalian mitochondrial porphyrin transporter. *Nature* **443**, 586-589

75. Polireddy, K., Khan, M. M., Chavan, H., Young, S., Ma, X., Waller, A., Garcia, M., Perez, D., Chavez, S., Strouse, J. J., Haynes, M. K., Bologa, C. G., Oprea, T. I., Tegos, G. P., Sklar, L. A., and Krishnamurthy, P. (2012) A novel flow cytometric HTS assay reveals functional modulators of ATP binding cassette transporter ABCB6. *PLoS One* **7**, e40005

76. Wang, L., He, F., Bu, J., Zhen, Y., Liu, X., Du, W., Dong, J., Cooney, J. D., Dubey, S. K., Shi, Y., Gong, B., Li, J., McBride, P. F., Jia, Y., Lu, F., Soltis, K. A., Lin, Y., Namburi, P., Liang, C., Sundaresan, P., Paw, B. H., Li, W., Li, D. Y., Phillips, J. D., and Yang, Z. (2012) ABCB6 mutations cause ocular coloboma. *Am J Hum Genet* **90**, 40-48

77. Helias, V., Saison, C., Ballif, B. A., Peyrard, T., Takahashi, J., Takahashi, H., Tanaka, M., Deybach, J. C., Puy, H., Le Gall, M., Sureau, C., Pham, B. N., Le Pennec, P. Y., Tani, Y., Cartron, J. P., and Arnaud, L. (2012) ABCB6 is dispensable for erythropoiesis and specifies the new blood group system Langereis. *Nat Genet* **44**, 170-173

78. Kiss, K., Brozik, A., Kucsma, N., Toth, A., Gera, M., Berry, L., Vallentin, A., Vial, H., Vidal, M., and Szakacs, G. (2012) Shifting the paradigm: the putative

mitochondrial protein ABCB6 resides in the lysosomes of cells and in the plasma membrane of erythrocytes. *PLoS One* **7**, e37378

79. Chavan, H., Khan, M. M., Tegos, G., and Krishnamurthy, P. (2013) Efficient purification and reconstitution of ATP binding cassette transporter B6 (ABCB6) for functional and structural studies. *J Biol Chem* **288**, 22658-22669

80. Zhao, S. G., Chen, X. F., Wang, L. G., Yang, G., Han, D. Y., Teng, L., Yang, M. C., Wang, D. Y., Shi, C., Liu, Y. H., Zheng, B. J., Shi, C. B., Gao, X., and Rainov, N. G. (2013) Increased expression of ABCB6 enhances protoporphyrin IX accumulation and photodynamic effect in human glioma. *Ann Surg Oncol* **20**, 4379-4388

81. Liu, H., Li, Y., Hung, K. K., Wang, N., Wang, C., Chen, X., Sheng, D., Fu, X., See, K., Foo, J. N., Low, H., Liany, H., Irwan, I. D., Liu, J., Yang, B., Chen, M., Yu, Y., Yu, G., Niu, G., You, J., Zhou, Y., Ma, S., Wang, T., Yan, X., Goh, B. K., Common, J. E., Lane, B. E., Sun, Y., Zhou, G., Lu, X., Wang, Z., Tian, H., Cao, Y., Chen, S., Liu, Q., and Zhang, F. (2014) Genome-wide linkage, exome sequencing and functional analyses identify ABCB6 as the pathogenic gene of dyschromatosis universalis hereditaria. *PLoS One* **9**, e87250

82. Kořený, L., Oborník, M., and Lukeš, J. (2013) Make it, take it, or leave it: heme metabolism of parasites. *PLoS Pathog* **9**, e1003088

83. Dean, P., Major, P., Nakjang, S., Hirt, R. P., and Embley, T. M. (2014) Transport proteins of parasitic protists and their role in nutrient salvage. *Front Plant Sci* **5**, 153

84. Miguel, D. C., Flannery, A. R., Mittra, B., and Andrews, N. W. (2013) Heme uptake mediated by LHR1 is essential for Leishmania amazonensis virulence. *Infect Immun* **81**, 3620-3626

85. Krishnamurthy, G., Vikram, R., Singh, S. B., Patel, N., Agarwal, S., Mukhopadhyay, G., Basu, S. K., and Mukhopadhyay, A. (2005) Hemoglobin receptor in Leishmania is a hexokinase located in the flagellar pocket. *J Biol Chem* **280**, 5884-5891

86. Agarwal, S., Rastogi, R., Gupta, D., Patel, N., Raje, M., and Mukhopadhyay, A. (2013) Clathrin-mediated hemoglobin endocytosis is essential for survival of Leishmania. *Biochim Biophys Acta* **1833**, 1065-1077

87. Sengupta, S., Tripathi, J., Tandon, R., Raje, M., Roy, R. P., Basu, S. K., and Mukhopadhyay, A. (1999) Hemoglobin endocytosis in Leishmania is mediated through a 46-kDa protein located in the flagellar pocket. *The Journal of biological chemistry* **274**, 2758-2765

88. Singh, S. B., Tandon, R., Krishnamurthy, G., Vikram, R., Sharma, N., Basu, S. K., and Mukhopadhyay, A. (2003) Rab5-mediated endosome-endosome fusion

regulates hemoglobin endocytosis in Leishmania donovani. *EMBO J* **22**, 5712-5722

89. Patel, N., Singh, S. B., Basu, S. K., and Mukhopadhyay, A. (2008) Leishmania requires Rab7-mediated degradation of endocytosed hemoglobin for their growth. *Proceedings of the National Academy of Sciences of the United States of America* **105**, 3980-3985

90. Cupello, M. P., Souza, C. F., Buchensky, C., Soares, J. B., Laranja, G. A., Coelho, M. G., Cricco, J. A., and Paes, M. C. (2011) The heme uptake process in Trypanosoma cruzi epimastigotes is inhibited by heme analogues and by inhibitors of ABC transporters. *Acta Trop* **120**, 211-218

91. Lara, F. A., Sant'anna, C., Lemos, D., Laranja, G. A., Coelho, M. G., Reis Salles, I., Michel, A., Oliveira, P. L., Cunha-E-Silva, N., Salmon, D., and Paes, M. C. (2007) Heme requirement and intracellular trafficking in Trypanosoma cruzi epimastigotes. *Biochem Biophys Res Commun* **355**, 16-22

92. Crisp, R. J., Pollington, A., Galea, C., Jaron, S., Yamaguchi-Iwai, Y., and Kaplan, J. (2003) Inhibition of heme biosynthesis prevents transcription of iron uptake genes in yeast. *J Biol Chem* **278**, 45499-45506

93. Protchenko, O., Rodriguez-Suarez, R., Androphy, R., Bussey, H., and Philpott, C. C. (2006) A screen for genes of heme uptake identifies the FLC family required for import of FAD into the endoplasmic reticulum. *J Biol Chem* **281**, 21445-21457

94. Ubeda, J. M., Raymond, F., Mukherjee, A., Plourde, M., Gingras, H., Roy, G., Lapointe, A., Leprohon, P., Papadopoulou, B., Corbeil, J., and Ouellette, M. (2014) Genome-wide stochastic adaptive DNA amplification at direct and inverted DNA repeats in the parasite leishmania. *PLoS Biol* **12**, e1001868

95. Peacock, C. S., Seeger, K., Harris, D., Murphy, L., Ruiz, J. C., Quail, M. A., Peters, N., Adlem, E., Tivey, A., Aslett, M., Kerhornou, A., Ivens, A., Fraser, A., Rajandream, M. A., Carver, T., Norbertczak, H., Chillingworth, T., Hance, Z., Jagels, K., Moule, S., Ormond, D., Rutter, S., Squares, R., Whitehead, S., Rabbinowitsch, E., Arrowsmith, C., White, B., Thurston, S., Bringaud, F., Baldauf, S. L., Faulconbridge, A., Jeffares, D., Depledge, D. P., Oyola, S. O., Hilley, J. D., Brito, L. O., Tosi, L. R., Barrell, B., Cruz, A. K., Mottram, J. C., Smith, D. F., and Berriman, M. (2007) Comparative genomic analysis of three Leishmania species that cause diverse human disease. *Nat Genet* **39**, 839-847

96. Depledge, D. P., Evans, K. J., Ivens, A. C., Aziz, N., Maroof, A., Kaye, P. M., and Smith, D. F. (2009) Comparative expression profiling of Leishmania: modulation in gene expression between species and in different host genetic backgrounds. *PLoS Negl Trop Dis* **3**, e476

97. Smith, D. F., Peacock, C. S., and Cruz, A. K. (2007) Comparative genomics: from genotype to disease phenotype in the leishmaniases. *Int J Parasitol* **37**, 1173-1186

98. Real, F., Vidal, R. O., Carazzolle, M. F., Mondego, J. M., Costa, G. G., Herai, R. H., Würtele, M., de Carvalho, L. M., Carmona e Ferreira, R., Mortara, R. A., Barbiéri, C. L., Mieczkowski, P., da Silveira, J. F., Briones, M. R., Pereira, G. A., and Bahia, D. (2013) The genome sequence of Leishmania (Leishmania) amazonensis: functional annotation and extended analysis of gene models. *DNA Res* **20**, 567-581

99. McCall, L. I., Zhang, W. W., and Matlashewski, G. (2013) Determinants for the development of visceral leishmaniasis disease. *PLoS Pathog* **9**, e1003053

100. Kramer, S. (2012) Developmental regulation of gene expression in the absence of transcriptional control: the case of kinetoplastids. *Mol Biochem Parasitol* **181**, 61-72

101. Berriman, M., Ghedin, E., Hertz-Fowler, C., Blandin, G., Renauld, H., Bartholomeu, D. C., Lennard, N. J., Caler, E., Hamlin, N. E., Haas, B., Böhme, U., Hannick, L., Aslett, M. A., Shallom, J., Marcello, L., Hou, L., Wickstead, B., Alsmark, U. C., Arrowsmith, C., Atkin, R. J., Barron, A. J., Bringaud, F., Brooks, K., Carrington, M., Cherevach, I., Chillingworth, T. J., Churcher, C., Clark, L. N., Corton, C. H., Cronin, A., Davies, R. M., Doggett, J., Djikeng, A., Feldblyum, T., Field, M. C., Fraser, A., Goodhead, I., Hance, Z., Harper, D., Harris, B. R., Hauser, H., Hostetler, J., Ivens, A., Jagels, K., Johnson, D., Johnson, J., Jones, K., Kerhornou, A. X., Koo, H., Larke, N., Landfear, S., Larkin, C., Leech, V., Line, A., Lord, A., Macleod, A., Mooney, P. J., Moule, S., Martin, D. M., Morgan, G. W., Mungall, K., Norbertczak, H., Ormond, D., Pai, G., Peacock, C. S., Peterson, J., Quail, M. A., Rabbinowitsch, E., Rajandream, M. A., Reitter, C., Salzberg, S. L., Sanders, M., Schobel, S., Sharp, S., Simmonds, M., Simpson, A. J., Tallon, L., Turner, C. M., Tait, A., Tivey, A. R., Van Aken, S., Walker, D., Wanless, D., Wang, S., White, B., White, O., Whitehead, S., Woodward, J., Wortman, J., Adams, M. D., Embley, T. M., Gull, K., Ullu, E., Barry, J. D., Fairlamb, A. H., Opperdoes, F., Barrell, B. G., Donelson, J. E., Hall, N., Fraser, C. M., Melville, S. E., and El-Sayed, N. M. (2005) The genome of the African trypanosome Trypanosoma brucei. *Science* **309**, 416-422

102. El-Sayed, N. M., Ghedin, E., Song, J., MacLeod, A., Bringaud, F., Larkin, C., Wanless, D., Peterson, J., Hou, L., Taylor, S., Tweedie, A., Biteau, N., Khalak, H. G., Lin, X., Mason, T., Hannick, L., Caler, E., Blandin, G., Bartholomeu, D., Simpson, A. J., Kaul, S., Zhao, H., Pai, G., Van Aken, S., Utterback, T., Haas, B., Koo, H. L., Umayam, L., Suh, B., Gerrard, C., Leech, V., Qi, R., Zhou, S., Schwartz, D., Feldblyum, T., Salzberg, S., Tait, A., Turner, C. M., Ullu, E., White, O., Melville, S., Adams, M. D., Fraser, C. M., and Donelson, J. E. (2003) The sequence and analysis of Trypanosoma brucei chromosome II. *Nucleic Acids Res* **31**, 4856-4863

103. Hall, N., Berriman, M., Lennard, N. J., Harris, B. R., Hertz-Fowler, C., Bart-Delabesse, E. N., Gerrard, C. S., Atkin, R. J., Barron, A. J., Bowman, S., Bray-Allen, S. P., Bringaud, F., Clark, L. N., Corton, C. H., Cronin, A., Davies, R., Doggett, J., Fraser, A., Grüter, E., Hall, S., Harper, A. D., Kay, M. P., Leech, V., Mayes, R., Price, C., Quail, M. A., Rabbinowitsch, E., Reitter, C., Rutherford, K., Sasse, J., Sharp, S., Shownkeen, R., MacLeod, A., Taylor, S., Tweedie, A., Turner, C. M., Tait, A., Gull, K., Barrell, B., and Melville, S. E. (2003) The DNA sequence of chromosome I of an African trypanosome: gene content, chromosome organisation, recombination and polymorphism. *Nucleic Acids Res* **31**, 4864-4873

104. McDonagh, P. D., Myler, P. J., and Stuart, K. (2000) The unusual gene organization of Leishmania major chromosome 1 may reflect novel transcription processes. *Nucleic Acids Res* **28**, 2800-2803

105. Johnson, P. J., Kooter, J. M., and Borst, P. (1987) Inactivation of transcription by UV irradiation of T. brucei provides evidence for a multicistronic transcription unit including a VSG gene. *Cell* **51**, 273-281

106. Kooter, J. M., van der Spek, H. J., Wagter, R., d'Oliveira, C. E., van der Hoeven, F., Johnson, P. J., and Borst, P. (1987) The anatomy and transcription of a telomeric expression site for variant-specific surface antigens in T. brucei. *Cell* **51**, 261-272

107. Martínez-Calvillo, S., Yan, S., Nguyen, D., Fox, M., Stuart, K., and Myler, P. J. (2003) Transcription of Leishmania major Friedlin chromosome 1 initiates in both directions within a single region. *Mol Cell* **11**, 1291-1299

108. Martínez-Calvillo, S., Nguyen, D., Stuart, K., and Myler, P. J. (2004) Transcription initiation and termination on Leishmania major chromosome 3. *Eukaryot Cell* **3**, 506-517

109. LeBowitz, J. H., Smith, H. Q., Rusche, L., and Beverley, S. M. (1993) Coupling of poly(A) site selection and trans-splicing in Leishmania. *Genes Dev* **7**, 996-1007

110. Ullu, E., Matthews, K. R., and Tschudi, C. (1993) Temporal order of RNA-processing reactions in trypanosomes: rapid trans splicing precedes polyadenylation of newly synthesized tubulin transcripts. *Mol Cell Biol* **13**, 720-725

111. Matthews, K. R., Tschudi, C., and Ullu, E. (1994) A common pyrimidine-rich motif governs trans-splicing and polyadenylation of tubulin polycistronic pre-mRNA in trypanosomes. *Genes Dev* **8**, 491-501

112. Michaeli, S. (2011) Trans-splicing in trypanosomes: machinery and its impact on the parasite transcriptome. *Future Microbiol* **6**, 459-474

113. Clayton, C., and Michaeli, S. (2011) 3' processing in protists. *Wiley Interdiscip Rev RNA* **2**, 247-255

114. Clayton, C. E. (2002) Life without transcriptional control? From fly to man and back again. *The EMBO journal* **21**, 1881-1888

115. Clayton, C. (2013) The regulation of trypanosome gene expression by RNA-binding proteins. *PLoS Pathog* **9**, e1003680

116. Papadopoulou, B., Huang, X.-F., Boucher, N., and McNicoll, F. (2003) Stage-Specific Regulation of Gene Expression in *Leishmania ASM News* **69**, 282-288

117. McNicoll, F., Müller, M., Cloutier, S., Boilard, N., Rochette, A., Dubé, M., and Papadopoulou, B. (2005) Distinct 3'-untranslated region elements regulate stage-specific mRNA accumulation and translation in Leishmania. *J Biol Chem* **280**, 35238-35246

118. Manning-Cela, R., González, A., and Swindle, J. (2002) Alternative splicing of LYT1 transcripts in Trypanosoma cruzi. *Infect Immun* **70**, 4726-4728

119. Benabdellah, K., González-Rey, E., and González, A. (2007) Alternative trans-splicing of the Trypanosoma cruzi LYT1 gene transcript results in compartmental and functional switch for the encoded protein. *Mol Microbiol* **65**, 1559-1567

120. García-Estrada, C., Pérez-Pertejo, Y., Ordóñez, D., Balaña-Fouce, R., and Reguera, R. M. (2007) Analysis of genetic elements regulating the methionine adenosyltransferase gene in Leishmania infantum. *Gene* **389**, 163-173

121. Vasconcelos, E. J., Terrão, M. C., Ruiz, J. C., Vêncio, R. Z., and Cruz, A. K. (2012) In silico identification of conserved intercoding sequences in Leishmania genomes: unraveling putative cis-regulatory elements. *Mol Biochem Parasitol* **183**, 140-150

122. Akopyants, N. S., Matlib, R. S., Bukanova, E. N., Smeds, M. R., Brownstein, B. H., Stormo, G. D., and Beverley, S. M. (2004) Expression profiling using random genomic DNA microarrays identifies differentially expressed genes associated with three major developmental stages of the protozoan parasite Leishmania major. *Mol Biochem Parasitol* **136**, 71-86

123. Leifso, K., Cohen-Freue, G., Dogra, N., Murray, A., and McMaster, W. R. (2007) Genomic and proteomic expression analysis of Leishmania promastigote and amastigote life stages: the Leishmania genome is constitutively expressed. *Mol Biochem Parasitol* **152**, 35-46

124. Holzer, T. R., McMaster, W. R., and Forney, J. D. (2006) Expression profiling by whole-genome interspecies microarray hybridization reveals differential gene expression in procyclic promastigotes, lesion-derived amastigotes, and axenic amastigotes in Leishmania mexicana. *Mol Biochem Parasitol* **146**, 198-218

125. Holzer, T. R., Mishra, K. K., LeBowitz, J. H., and Forney, J. D. (2008) Coordinate regulation of a family of promastigote-enriched mRNAs by the 3'UTR PRE element in Leishmania mexicana. *Mol Biochem Parasitol* **157**, 54-64

126. Lahav, T., Sivam, D., Volpin, H., Ronen, M., Tsigankov, P., Green, A., Holland, N., Kuzyk, M., Borchers, C., Zilberstein, D., and Myler, P. J. (2011) Multiple levels of gene regulation mediate differentiation of the intracellular pathogen Leishmania. *FASEB J* **25**, 515-525

127. Saxena, A., Lahav, T., Holland, N., Aggarwal, G., Anupama, A., Huang, Y., Volpin, H., Myler, P. J., and Zilberstein, D. (2007) Analysis of the Leishmania donovani transcriptome reveals an ordered progression of transient and permanent changes in gene expression during differentiation. *Mol Biochem Parasitol* **152**, 53-65

128. Almeida, R., Gilmartin, B. J., McCann, S. H., Norrish, A., Ivens, A. C., Lawson, D., Levick, M. P., Smith, D. F., Dyall, S. D., Vetrie, D., Freeman, T. C., Coulson, R. M., Sampaio, I., Schneider, H., and Blackwell, J. M. (2004) Expression profiling of the Leishmania life cycle: cDNA arrays identify developmentally regulated genes present but not annotated in the genome. *Mol Biochem Parasitol* **136**, 87-100

129. Alcolea, P. J., Alonso, A., Gómez, M. J., Moreno, I., Domínguez, M., Parro, V., and Larraga, V. (2010) Transcriptomics throughout the life cycle of Leishmania infantum: high down-regulation rate in the amastigote stage. *Int J Parasitol* **40**, 1497-1516

130. Srividya, G., Duncan, R., Sharma, P., Raju, B. V., Nakhasi, H. L., and Salotra, P. (2007) Transcriptome analysis during the process of in vitro differentiation of Leishmania donovani using genomic microarrays. *Parasitology* **134**, 1527-1539

131. Rochette, A., Raymond, F., Corbeil, J., Ouellette, M., and Papadopoulou, B. (2009) Whole-genome comparative RNA expression profiling of axenic and intracellular amastigote forms of Leishmania infantum. *Mol Biochem Parasitol* **165**, 32-47

132. Cohen-Freue, G., Holzer, T. R., Forney, J. D., and McMaster, W. R. (2007) Global gene expression in Leishmania. *Int J Parasitol* **37**, 1077-1086

133. Erben, E., Chakraborty, C., and Clayton, C. (2014) The CAF1-NOT complex of trypanosomes. *Front Genet* **4**, 299

134. El Fakhry, Y., Ouellette, M., and Papadopoulou, B. (2002) A proteomic approach to identify developmentally regulated proteins in Leishmania infantum. *Proteomics* **2**, 1007-1017

135. Nugent, P. G., Karsani, S. A., Wait, R., Tempero, J., and Smith, D. F. (2004) Proteomic analysis of Leishmania mexicana differentiation. *Mol Biochem Parasitol* **136**, 51-62

136. McNicoll, F., Drummelsmith, J., Müller, M., Madore, E., Boilard, N., Ouellette, M., and Papadopoulou, B. (2006) A combined proteomic and transcriptomic approach to the study of stage differentiation in Leishmania infantum. *Proteomics* **6**, 3567-3581

137. Rosenzweig, D., Smith, D., Myler, P. J., Olafson, R. W., and Zilberstein, D. (2008) Post-translational modification of cellular proteins during Leishmania donovani differentiation. *Proteomics* **8**, 1843-1850

138. Morales, M. A., Watanabe, R., Dacher, M., Chafey, P., Osorio y Fortéa, J., Scott, D. A., Beverley, S. M., Ommen, G., Clos, J., Hem, S., Lenormand, P., Rousselle, J. C., Namane, A., and Späth, G. F. (2010) Phosphoproteome dynamics reveal heat-shock protein complexes specific to the Leishmania donovani infectious stage. *Proc Natl Acad Sci U S A* **107**, 8381-8386

139. Hem, S., Gherardini, P. F., Osorio y Fortéa, J., Hourdel, V., Morales, M. A., Watanabe, R., Pescher, P., Kuzyk, M. A., Smith, D., Borchers, C. H., Zilberstein, D., Helmer-Citterich, M., Namane, A., and Späth, G. F. (2010) Identification of Leishmania-specific protein phosphorylation sites by LC-ESI-MS/MS and comparative genomics analyses. *Proteomics* **10**, 3868-3883

140. Paape, D., Barrios-Llerena, M. E., Le Bihan, T., Mackay, L., and Aebischer, T. (2010) Gel free analysis of the proteome of intracellular Leishmania mexicana. *Mol Biochem Parasitol* **169**, 108-114

141. Paape, D., and Aebischer, T. (2011) Contribution of proteomics of Leishmania spp. to the understanding of differentiation, drug resistance mechanisms, vaccine and drug development. *J Proteomics* **74**, 1614-1624

142. Besteiro, S., Williams, R. A., Coombs, G. H., and Mottram, J. C. (2007) Protein turnover and differentiation in Leishmania. *Int J Parasitol* **37**, 1063-1075

143. Siegel, T. N., Hekstra, D. R., Wang, X., Dewell, S., and Cross, G. A. (2010) Genome-wide analysis of mRNA abundance in two life-cycle stages of Trypanosoma brucei and identification of splicing and polyadenylation sites. *Nucleic Acids Res* **38**, 4946-4957

144. Mittra, B., Cortez, M., Haydock, A., Ramasamy, G., Myler, P. J., and Andrews, N. W. (2013) Iron uptake controls the generation of Leishmania infective forms through regulation of ROS levels. *J Exp Med* **210**, 401-416

145. Soysa, R., Carter, N. S., and Yates, P. A. (2014) A dual luciferase system for analysis of post-transcriptional regulation of gene expression in Leishmania. *Mol Biochem Parasitol* **195**, 1-5

146. David, M., Gabdank, I., Ben-David, M., Zilka, A., Orr, I., Barash, D., and Shapira, M. (2010) Preferential translation of Hsp83 in Leishmania requires a thermosensitive polypyrimidine-rich element in the 3' UTR and involves scanning of the 5' UTR. *RNA* **16**, 364-374

147. Dostálová, A., and Volf, P. (2012) Leishmania development in sand flies: parasite-vector interactions overview. *Parasit Vectors* **5**, 276

148. Antoine, J. C., Prina, E., Lang, T., and Courret, N. (1998) The biogenesis and properties of the parasitophorous vacuoles that harbour Leishmania in murine macrophages. *Trends Microbiol* **6**, 392-401

149. Ndjamen, B., Kang, B. H., Hatsuzawa, K., and Kima, P. E. (2010) Leishmania parasitophorous vacuoles interact continuously with the host cell's endoplasmic reticulum; parasitophorous vacuoles are hybrid compartments. *Cell Microbiol* **12**, 1480-1494

150. Real, F., and Mortara, R. A. (2012) The diverse and dynamic nature of Leishmania parasitophorous vacuoles studied by multidimensional imaging. *PLoS Negl Trop Dis* **6**, e1518

151. Malafaia, G., Marcon, L. e. N., Pereira, L. e. F., Pedrosa, M. L., and Rezende, S. A. (2011) Leishmania chagasi: effect of the iron deficiency on the infection in BALB/c mice. *Exp Parasitol* **127**, 719-723

152. Thakur, A. K., Bimal, S., Singh, S. K., Gupta, A. K., Das, V. N., Das, P., and Narayan, S. (2013) Degree of anemia correlates with increased utilization of heme by Leishmania donovani parasites in visceral leishmaniasis. *Exp Parasitol* **135**, 595-598

153. Schaer, C. A., Vallelian, F., Imhof, A., Schoedon, G., and Schaer, D. J. (2008) Heme carrier protein (HCP-1) spatially interacts with the CD163 hemoglobin uptake pathway and is a target of inflammatory macrophage activation. *J Leukoc Biol* **83**, 325-333

154. Kelly, J. X., Ignatushchenko, M. V., Bouwer, H. G., Peyton, D. H., Hinrichs, D. J., Winter, R. W., and Riscoe, M. (2003) Antileishmanial drug development: exploitation of parasite heme dependency. *Molecular and biochemical parasitology* **126**, 43-49

155. Frawley, E. R., and Kranz, R. G. (2009) CcsBA is a cytochrome c synthetase that also functions in heme transport. *Proc Natl Acad Sci U S A* **106**, 10201-10206

156. Merchant, S. S. (2009) His protects heme as it crosses the membrane. *Proc Natl Acad Sci U S A* **106**, 10069-10070

157. Richard-Fogal, C., and Kranz, R. G. (2010) The CcmC:heme:CcmE complex in heme trafficking and cytochrome c biosynthesis. *J Mol Biol* **401**, 350-362

158. Kern, M., Scheithauer, J., Kranz, R. G., and Simon, J. (2010) Essential histidine pairs indicate conserved haem binding in epsilonproteobacterial cytochrome c haem lyases. *Microbiology* **156**, 3773-3781

159. San Francisco, B., Bretsnyder, E. C., Rodgers, K. R., and Kranz, R. G. (2011) Heme ligand identification and redox properties of the cytochrome c synthetase, CcmF. *Biochemistry* **50**, 10974-10985

160. Moriwaki, Y., Caaveiro, J. M., Tanaka, Y., Tsutsumi, H., Hamachi, I., and Tsumoto, K. (2011) Molecular basis of recognition of antibacterial porphyrins by heme-transporter IsdH-NEAT3 of Staphylococcus aureus. *Biochemistry* **50**, 7311-7320

161. Woo, J. S., Zeltina, A., Goetz, B. A., and Locher, K. P. (2012) X-ray structure of the Yersinia pestis heme transporter HmuUV. *Nat Struct Mol Biol* **19**, 1310-1315

162. San Francisco, B., Bretsnyder, E. C., and Kranz, R. G. (2013) Human mitochondrial holocytochrome c synthase's heme binding, maturation determinants, and complex formation with cytochrome c. *Proc Natl Acad Sci U S A* **110**, E788-797

163. San Francisco, B., and Kranz, R. G. (2014) Interaction of holoCcmE with CcmF in heme trafficking and cytochrome c biosynthesis. *J Mol Biol* **426**, 570-585

164. Wilks, A., and Burkhard, K. A. (2007) Heme and virulence: how bacterial pathogens regulate, transport and utilize heme. *Nat Prod Rep* **24**, 511-522

165. Tong, Y., and Guo, M. (2009) Bacterial heme-transport proteins and their heme-coordination modes. *Arch Biochem Biophys* **481**, 1-15

166. Protchenko, O., Shakoury-Elizeh, M., Keane, P., Storey, J., Androphy, R., and Philpott, C. C. (2008) Role of PUG1 in inducible porphyrin and heme transport in Saccharomyces cerevisiae. *Eukaryot Cell* **7**, 859-871

167. Grigg, J. C., Mao, C. X., and Murphy, M. E. (2011) Iron-coordinating tyrosine is a key determinant of NEAT domain heme transfer. *J Mol Biol* **413**, 684-698

168. Derbyshire, E. R., Deng, S., and Marletta, M. A. (2010) Incorporation of tyrosine and glutamine residues into the soluble guanylate cyclase heme distal pocket alters NO and O2 binding. *J Biol Chem* **285**, 17471-17478

169. Sauvage, V., Aubert, D., Escotte-Binet, S., and Villena, I. (2009) The role of ATP-binding cassette (ABC) proteins in protozoan parasites. *Mol Biochem Parasitol* **167**, 81-94

170. ter Kuile, B. H. (1994) Membrane-related processes and overall energy metabolism in Trypanosoma brucei and other kinetoplastid species. *J Bioenerg Biomembr* **26**, 167-172

171. Seyfang, A., and Landfear, S. M. (2000) Four conserved cytoplasmic sequence motifs are important for transport function of the Leishmania inositol/H(+) symporter. *J Biol Chem* **275**, 5687-5693

172. Paes, M. C., Cosentino-Gomes, D., de Souza, C. F., Nogueira, N. P., and Meyer-Fernandes, J. R. (2011) The Role of Heme and Reactive Oxygen Species in Proliferation and Survival of Trypanosoma cruzi. *J Parasitol Res* **2011**, 174614

173. Liu, R., and Hu, J. (2011) HemeBIND: a novel method for heme binding residue prediction by combining structural and sequence information. *BMC Bioinformatics* **12**, 207

174. Xiong, Y., Liu, J., Zhang, W., and Zeng, T. (2012) Prediction of heme binding residues from protein sequences with integrative sequence profiles. *Proteome Sci* **10 Suppl 1**, S20

175. Debrabant, A., Joshi, M. B., Pimenta, P. F., and Dwyer, D. M. (2004) Generation of Leishmania donovani axenic amastigotes: their growth and biological characteristics. *Int J Parasitol* **34**, 205-217

176. Zhu, Y., Hon, T., Ye, W., and Zhang, L. (2002) Heme deficiency interferes with the Ras-mitogen-activated protein kinase signaling pathway and expression of a subset of neuronal genes. *Cell Growth Differ* **13**, 431-439

177. Paul, K. G., Theorell, H., Akeson, A. (1953) The molar light absorption of pyridine ferroprotoporphyrin (pyridine haemochromogen). *Acta Chem Scand* **7**, 1284-1287

178. Ito, H., Fukuda, Y., Murata, K., and Kimura, A. (1983) Transformation of intact yeast cells treated with alkali cations. *J Bacteriol* **153**, 163-168

179. Medina-Acosta, E., and Cross, G. A. (1993) Rapid isolation of DNA from trypanosomatid protozoa using a simple 'mini-prep' procedure. *Mol Biochem Parasitol* **59**, 327-329

180. Livak, K. J., and Schmittgen, T. D. (2001) Analysis of relative gene expression data using real-time quantitative PCR and the 2(-Delta Delta C(T)) Method. *Methods* **25**, 402-408

181. Burke, D., Dawson, D., and Stearns, T. (2000) *Methods in Yeast Genetics*, Cold Spring Harbor Press

182. Kapler, G. M., Coburn, C. M., and Beverley, S. M. (1990) Stable transfection of the human parasite Leishmania major delineates a 30-kilobase region sufficient for extrachromosomal replication and expression. *Mol Cell Biol* **10**, 1084-1094

183. Rabhi, I., Rabhi, S., Ben-Othman, R., Rasche, A., Daskalaki, A., Trentin, B., Piquemal, D., Regnault, B., Descoteaux, A., Guizani-Tabbane, L., and

Consortium, S. (2012) Transcriptomic signature of Leishmania infected mice macrophages: a metabolic point of view. *PLoS Negl Trop Dis* **6**, e1763

184. Titus, R. G., Marchand, M., Boon, T., and Louis, J. A. (1985) A limiting dilution assay for quantifying Leishmania major in tissues of infected mice. *Parasite Immunol* **7**, 545-555